Imaging the Cochlear implant electrode position and related Performance
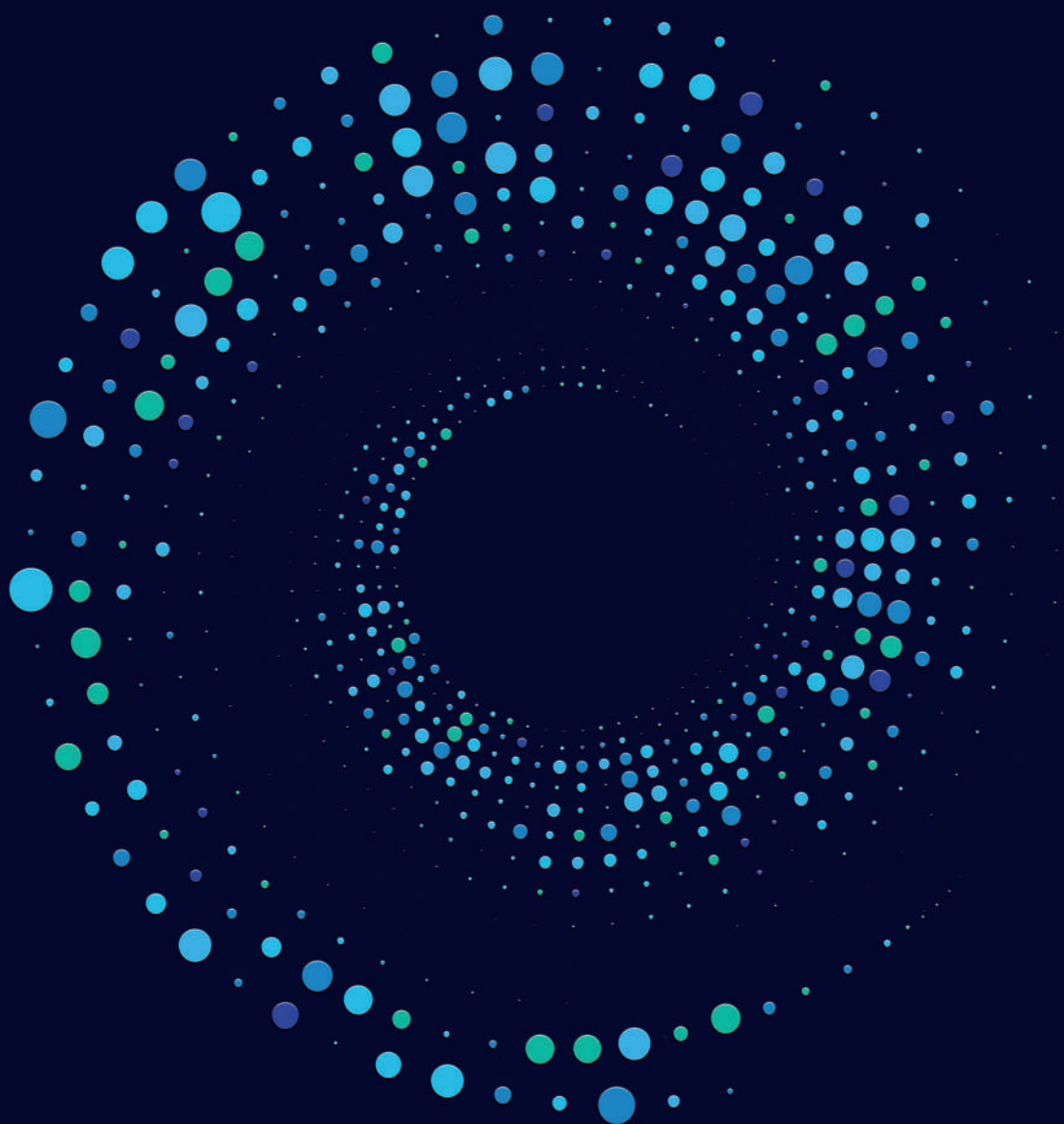
FLORIS HEUTINK

IMAGING THE COCHLEAR IMPLANT
ELECTRODE POSITION AND RELATED PERFORMANCE

Floris Heutink

IMAGING THE COCHLEAR IMPLANT
ELECTRODE POSITION AND RELATED PERFORMANCE

Floris Heutink

Thesis Radboud University Nijmegen

**Imaging the cochlear implant
electrode position and related performance**

Proefschrift

ter verkrijging van de graad van doctor

aan de Radboud Universiteit Nijmegen

op gezag van de rector magnificus prof. dr. J.H.J.M. van Krieken,

volgens besluit van het college voor promoties

in het openbaar te verdedigen op vrijdag 6 mei 2022

om 12:30 uur precies

door

Floris Heutink

geboren op 14 juli 1989

te Tilburg

Promotor

Prof. dr. H.A.M. Marres

Copromotoren

Dr. E.A.M. Mylanus

Dr. W.J. Huinck

Dr. B.M. Verbist

Manuscriptcommissie

Prof. dr. R.H.M.A. Bartels

Prof. dr. R.J. Stokroos (UMC Utrecht)

Prof. dr. P. Merkus (Amsterdam UMC)

Voor Doutse

Table of content

1

General introduction

Background

It was on September 10th, 2013, that Graeme M. Clark, Ingeborg Hochmair and Blake S. Wilson received the prestigious Lasker-DeBakey Clinical Medical Research Award for their pioneering work contributing to the invention of the cochlear implant (CI). Since 1945, this annual award is given to persons who have made major contributions to medical science, and, to date, 86 Lasker Award winners have later received the well-known Nobel Prize. The Lasker Award jury praised the invention of the CI because:

"The CI has, for the first time, substantially restored a human sense using a medical device."

Figure 1: Schematic drawing of modern cochlear implant. Used with permission of Mayo Foundation for Medical Education and Research, all rights reserved.

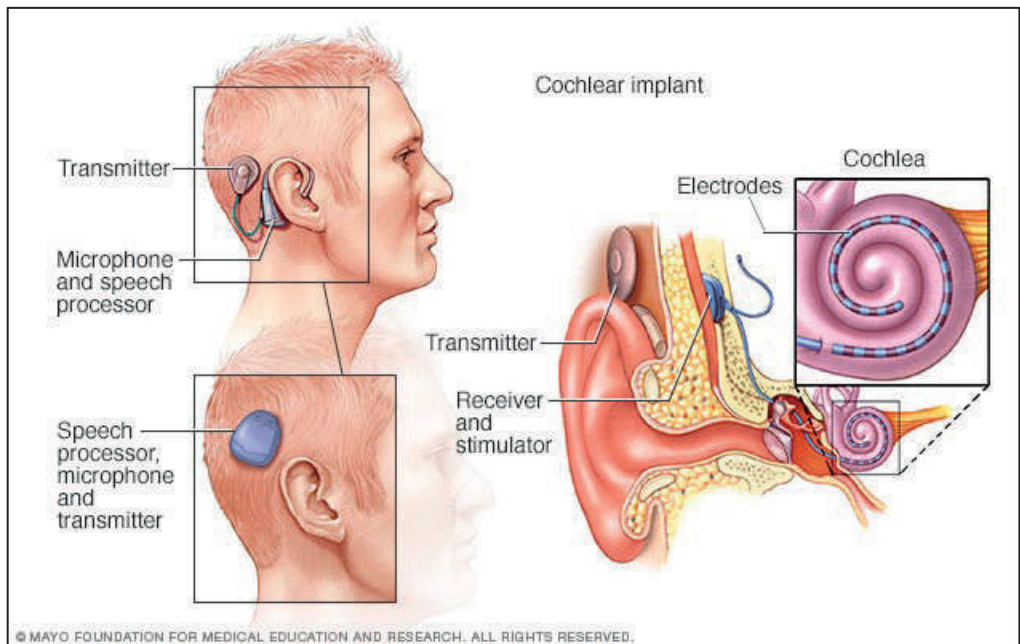Since the invention of CI around 600000 children and adults have (partially) regained hearing, improving their quality of life, due to this medical device [1]. A modern cochlear implant system (illustrated in Figure 1) contains three key elements: 1) the external processor that registers sound using multiple microphones and transforms this sound into an electric signal; 2) the internal receiver-stimulator, surgically positioned underneath the skin, that receives and transmits the electric signal through 3) a connected electrode array which is surgically positioned inside the cochlea of the patient. This electrode array forms the interface between the CI and the recipient and electrically stimulates the auditory nerve. A CI electrode array contains multiple leads connected to separate, sequentially placed electrode contacts, covering the most important area in the cochlea to understand speech namely the area containing the spiral ganglion cells of the auditory nerve. Each electrode contact stimulates a part of the spiral ganglion nerve cells with a considerable spread of excitation throughout the cochlea. The axons of the spiral ganglion nerve cells form small nerve bundles which eventually form the patients' auditory nerve connected to the brainstem. The success of this artificial stimulation mechanism is based on using the frequency tonotopy of the cochlea in such a manner that the cochlear implant manages to address various frequency domains and therefore manages to provide the percept of sound of different frequencies to the recipient.

Since the introduction, cochlear implant systems have continuously developed, resulting in improved sound quality and speech perception. As a result of the improved outcome, the CI indication criteria have gradually been broadened [2]. Today, not only profoundly deaf people are eligible for

CI but also children with congenital or unilateral hearing loss and even adults with some levels of residual hearing may profit from a CI. While on the whole cochlear implantation has been successful, a considerable variability in speech perception outcome between recipients is still observed. In a recent study in the Netherlands, the average speech perception in quiet at 1 year after implantation in 364 postlingual adults was 77.7% (Standard deviation (SD): 17.4), yet the range was 22% to 98% [3]. Outcome variation becomes even more apparent when measured in noisy conditions. Also, there is room for improvement in the appreciation of music, even for the best performing patients. The variability in performance and the drive for improving hearing results with a CI are hot topics since the introduction, and therefore a great deal of scientific studies are dedicated toward finding the mechanisms contributing to the performance with CI; obviously to potentially influence the speech perception in a beneficial way for the patient.

Dr. William F. House, a famous American otologist, also considered to have significantly contributed to the invention of the cochlear implant wrote in 1986:

"All of us in implant research have hoped that somehow we would hit upon an electrode configuration or external processing scheme that would suddenly give our patients normal hearing. This perfect device has eluded the many research teams that have formed around the world. Therefore, we have concentrated on determining whether one implant is a little better than another. However, differences in performance may be due as much to individual variation as to variations in the devices." —William F. House, MD, 1986 [4]

This quote in the early days of cochlear implant research covers the essence of the difficulty even in current day cochlear implant research. The physiological process of converting sound to electricity and stimulating the auditory nerve, leading to comprehensive speech perception is complex, and many patient-specific factors influence long-term speech perception. As a result of the improved knowledge, CI manufactures developed multiple electrode types with different technical characteristics that also potentially influence the performance with CI. Additionally, worldwide, there are differences in the clinical CI procedure, depending on the national reimbursement system, knowledge and the available resources, leading to different indication criteria and different choices with respect to CI systems, electrode types and surgical techniques. Therefore, the potential factors influencing the result with CI are extensive, which makes CI research both interesting and challenging.

The factors potentially affecting the variation in CI speech perception can be divided into three categories: biographical factors, audiometric factors, and electrode (positional) factors. Rapid developments in the CI field means that the influence of these factors on speech perception could be changing over time, as shown by Blamey et al. [5, 6]. Blamey and colleagues studied the influence of several biographic and audiologic factors on speech perception in two multicenter studies using the same study method (N=800 in 1996 and N=2251 in 2013). Compared to the results of the 1996 study, the authors showed less influence of the biographic and audiologic factors (i.e., age at implantation, age at onset of deafness, duration of deafness, etiology of hearing loss, and CI experience) on speech perception in the 2013 study, explaining 21% and 10% of the ariation in speech perception,

respectively. They attributed this to the less stringent CI patient selection criteria and the improved clinical management of hearing loss and cochlear implantation towards 2013 [6].

With the technical improvements of the device and the gained knowledge with respect to patient selection and counseling, CIs have evolved from devices that provide sound to patients with profound hearing loss only (average hearing loss ≥ 81dB) to devices that also improve speech perception in patients with moderate – to – severe hearing loss (average hearing loss of 41 – 80dB). In the last two decades, early implantation of patients with progressive hearing loss, when there still is some functional residual hearing, has been shown to positively affect the postoperative speech perception performance with CI [2, 3, 7-9]. The preservation of residual hearing became an important goal, both as an measuring tool in the strive towards intracochlear structure preservation but also because residual hearing can, in some CI recipients, be used in a combined electric–acoustic stimulation [10]. Following this development, post-operative imaging to evaluate the electrode position has become an important tool in terms of quality control. Several post-operative imaging studies have shown that translocation from the desired scala tympani (ST) to the scala vestibuli (SV) causes a higher loss of residual hearing and reduced speech perception [11-15]. Even more recently, the influence of electrode positional factors on speech perception has gained more interest, with studies exploring different electrode types and the effect of scalar location, insertion depth [11, 16, 17], and 'electrode-to-modiolus' distance [11,

18-20]. This thesis focusses on "imaging the cochlear implant electrode position and related performance".

Objective

The primary objective of this thesis is to investigate what influence cochlear implant electrode (position) related factors have on the CI performance. To evaluate these factors, advanced imaging technology, imaging evaluation and imaging interpretation have been used.

Outline of this thesis (PhD)

In the first part of this thesis, imaging is used as a clinical tool to evaluate the post-operative electrode position. The first part consists of three chapters. ***Chapter 2*** is a systematic review, summarizing the available literature on the influence of angular insertion depth on speech perception in CI patients. Angular insertion depth is the prime reported electrode positional factor. ***Chapter 3*** describes a study investigating four electrode positional factors: type of electrode, scalar location, depth of insertion and wrapping factor ("electrode to modiolus" distance) together with six other independent factors: 1. age at implantation; 2. level of education; 3. duration of hearing loss; 4. preoperative residual hearing; 5. preoperative speech perception and 6. postoperative residual hearing. The dependent variables are three speech perception outcomes: speech perception in quiet at 50dB and 65dB loudness, and speech perception in noise. This study is unique as it is conducted on a relatively large sample size within a single CI centre, evaluating CIs of one single manufacturer. By doing so, confounding bias is limited compared to previous studies. In ***Chapter 4*** the results of the first patients implanted with a slim perimodiolar CI electrode

1

in our clinic are described. This electrode was introduced in 2016 and developed to take a perimodiolar position and also be atraumatic in the cochlea, thereby addressing the main handicap – i.e. the higher rates of trauma, of earlier generation perimodiolar electrodes [12]. Results on electrode position and residual hearing preservation and performance in patients are reported and analyzed.

In the second part of this thesis we investigated additional imaging features in implanted ears on top of electrode position. The studies in this part of the thesis are more experimental and are the first step towards new diagnostic outcome measures that might be(come) useful to CI practice.

Implantation of a foreign body in the cochlea - i.e. a cochlear implant electrode, results in the formation of scar tissue around the cochlear implant electrode. In its most pronounced form the fibrous tissue progresses into neo-ossification. This new bone formation (NBF) has been observed in several animal and histopathological studies [21-26]. However, to date, in vivo detection of NBF has not yet been described. ***Chapter 5*** describes a postoperative imaging study which investigates in vivo presence of NBF around the cochlear implant.

Besides differences in postoperative electrode position and additional postoperative findings related to electrode design and surgical factors like NBF, also the variance in individual cochlear morphology should be considered for improving outcome. Driven by the desire to preserve of residual hearing a body of research is focused on individualized implant choice based on patient specific characteristics like cochlear size. If accurate image-based segmentation and measurements of the cochlea could be performed pre-operatively, this could potentially allow for the adaptation
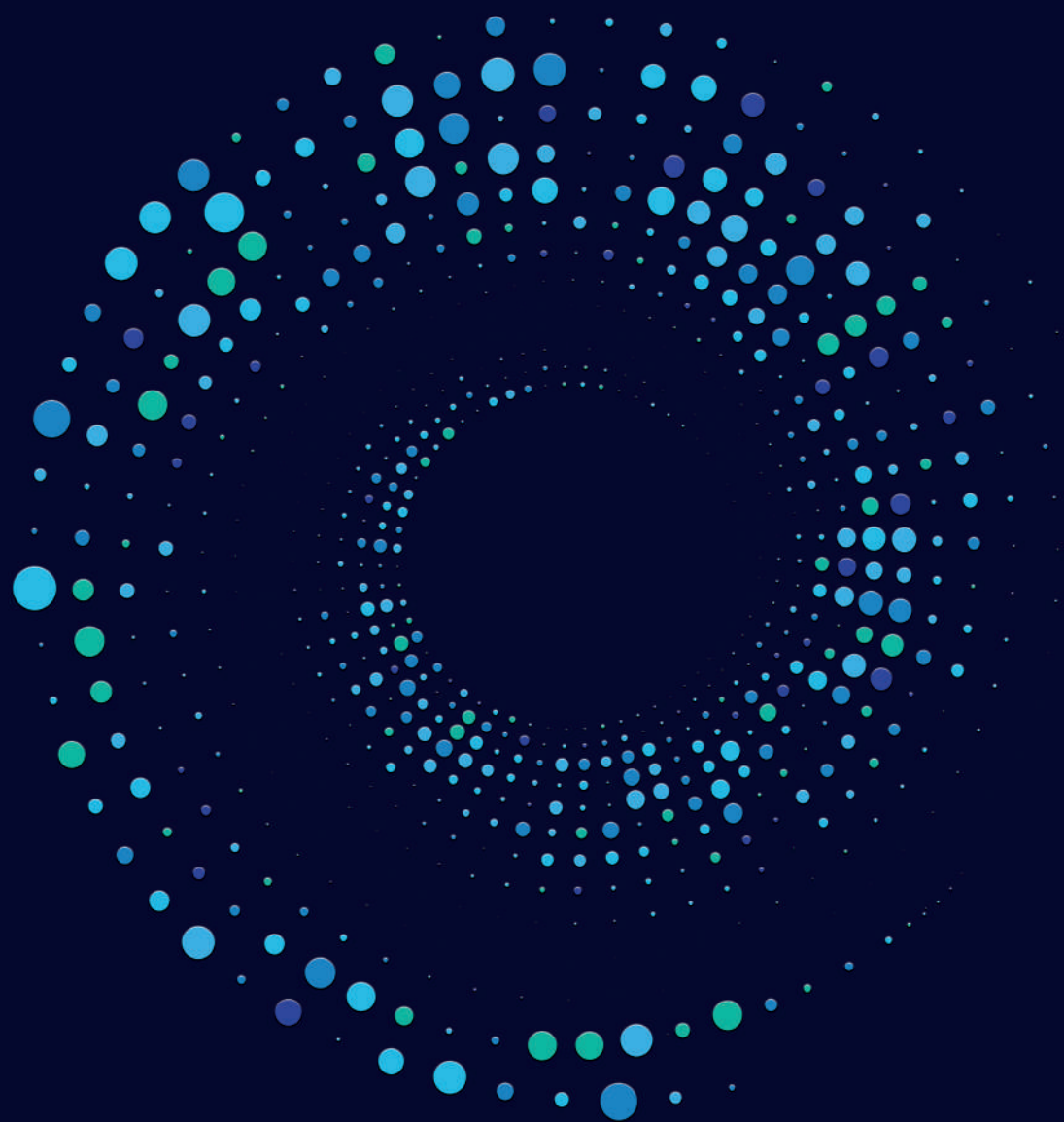
of electrode type size, shape and depth of insertion of the CI electrode to the anatomy of each single patient, possibly improving outcome. ***Chapter 6*** proposes a method to automatically segment and measure the human cochlea in clinical preoperative ultra-high-resolution (UHR) CT images, and investigate differences in cochlear size for possible personalized implant planning.

1

References

1.   McRackan, T.R., et al., *Meta-analysis of quality-of-life improvement after cochlear implantation and associations with speech recognition abilities.* Laryngoscope, 2018. **128**(4): p. 982-990.

2.   Huinck, W.J., E.A.M. Mylanus, and A.F.M. Snik, *Expanding unilateral cochlear implantation criteria for adults with bilateral acquired severe sensorineural hearing loss.* Eur Arch Otorhinolaryngol, 2019. **276**(5): p. 1313-1320.

3.   Snel-Bongers, J., et al., *Evidence-Based Inclusion Criteria for Cochlear Implantation in Patients With Postlingual Deafness.* Ear Hear, 2018. **39**(5): p. 1008-1014.

4.   House, W.F., *Cochlear implants. Present and future.* Otolaryngol Clin North Am, 1986. **19**(2): p. 217-8.

5.   Blamey, P., et al., *Factors affecting auditory performance of postlinguistically deaf adults using cochlear implants.* Audiol Neurootol, 1996. **1**(5): p. 293-306.

6.   Blamey, P., et al., *Factors affecting auditory performance of postlinguistically deaf adults using cochlear implants: an update with 2251 patients.* Audiol Neurootol, 2013. **18**(1): p. 36-47.

7.   Francis, H.W., et al., *Central effects of residual hearing: implications for choice of ear for cochlear implantation.* Laryngoscope, 2004. **114**(10): p. 1747-52.

8.   Friedland, D.R., H.S. Venick, and J.K. Niparko, *Choice of ear for cochlear implantation: the effect of history and residual hearing on predicted postoperative performance.* Otol Neurotol, 2003. **24**(4): p. 582-9.

9.   Gomaa, N.A., et al., *Residual speech perception and cochlear implant performance in postlingually deafened adults.* Ear Hear, 2003. **24**(6): p. 539-44.

10.   Buchner, A., et al., *Investigation of the effect of cochlear implant electrode length on speech comprehension in quiet and noise compared with the results with users of electro-acoustic-stimulation, a retrospective analysis.* PLoS One, 2017. **12**(5): p. e0174900.

11.   Holden, L.K., et al., *Factors affecting open-set word recognition in adults with cochlear implants.* Ear Hear, 2013. **34**(3): p. 342-60.

12.   Wanna, G.B., et al., *Impact of electrode design and surgical approach on scalar location and cochlear implant outcomes.* Laryngoscope, 2014. **124 Suppl 6**: p. S1-7.

13.   O'Connell, B.P., et al., *Electrode Location and Angular Insertion Depth Are Predictors of Audiologic Outcomes in Cochlear Implantation.* Otol Neurotol, 2016. **37**(8): p. 1016-23.

14.   O'Connell, B.P., J.B. Hunter, and G.B. Wanna, *The importance of electrode location in cochlear implantation.* Laryngoscope Investig Otolaryngol, 2016. **1**(6): p. 169-174.

15.   Chakravorti, S., et al., *Further Evidence of the Relationship Between Cochlear Implant Electrode Positioning and Hearing Outcomes.* Otol Neurotol, 2019. **40**(5): p. 617-624.

16.   Skinner, M.W., et al., *CT-derived estimation of cochlear morphology and electrode array position in relation to word recognition in Nucleus-22 recipients.* J Assoc Res Otolaryngol, 2002. **3**(3): p. 332-50.

17.   van der Marel, K.S., et al., *The influence of cochlear implant electrode position on performance.* Audiol Neurootol, 2015. **20**(3): p. 202-11.

18.   Frijns, J.H., J.J. Briaire, and J.J. Grote, *The importance of human cochlear anatomy for the results of modiolus-hugging multichannel cochlear implants.* Otol Neurotol, 2001. **22**(3): p. 340-9.

19.   Holden, L.K., et al., *Factors Affecting Outcomes in Cochlear Implant Recipients Implanted With a Perimodiolar Electrode Array Located in Scala Tympani.* Otol Neurotol, 2016. **37**(10): p. 1662-1668.

20.   van der Beek, F.B., et al., *Clinical evaluation of the Clarion CII HiFocus 1 with and without positioner.* Ear Hear, 2005. **26**(6): p. 577-92.

21.   Ishai, R., et al., *The pattern and degree of capsular fibrous sheaths surrounding cochlear electrode arrays.* Hear Res, 2017. **348**: p. 44-53.

22.   Kamakura, T. and J.B. Nadol, Jr., *Correlation between word recognition score and intracochlear new bone and fibrous tissue after cochlear implantation in the human.* Hear Res, 2016. **339**: p. 132-41.

23.   Sheikh, Z., et al., *Macrophages, Foreign Body Giant Cells and Their Response to Implantable Biomaterials.* Materials (Basel), 2015. **8**(9): p. 5671-5701.

24.   Fayad, J.N., A.O. Makarem, and F.H. Linthicum, Jr., *Histopathologic assessment of fibrosis and new bone formation in implanted human temporal bones using 3D reconstruction.* Otolaryngol Head Neck Surg, 2009. **141**(2): p. 247-52.

25.   Somdas, M.A., et al., *Quantitative evaluation of new bone and fibrous tissue in the cochlea following cochlear implantation in the human.* Audiol Neurootol, 2007. **12**(5): p. 277-84.

26.   O'Leary, S.J., et al., *Relations between cochlear histopathology and hearing loss in experimental cochlear implantation.* Hear Res, 2013. **298**: p. 27-35.

1

2

Angular electrode insertion depth and speech perception in adults with a cochlear implant: a systematic review.

Floris Heutink, Simone R. de Rijk, Berit M. Verbist, Wendy J. Huinck, Emmanuel A.M. Mylanus

Abstract

Objective: By discussing the design, findings, strengths, and weaknesses of available studies investigating the influence of angular insertion depth on speech perception, we intend to summarize the current status of evidence; and using evidence based conclusions, possibly contribute to the determination of the optimal cochlear implant (CI) electrode position.

Data Sources: Our search strategy yielded 10,877 papers. PubMed, Ovid EMBASE, Web of Science and the Cochrane Library were searched up to June 01, 2018. Both keywords and free-text terms, related to patient population, predictive factor and outcome measurements were used. There were no restrictions in languages or year of publication.

Study Selection: Seven articles were included in this systematic review. Articles eligible for inclusion: (a) investigated cochlear implantation of any CI system in adults with post-lingual onset of deafness and normal cochlear anatomy; (b) investigated the relationship between angular insertion depth and speech perception (c) measured angular insertion depth on imaging; and (d) measured speech perception at, or beyond 1 year post-activation.

Data Extraction and synthesis: In included studies; quality was judged low-to-moderate and risk of bias, evaluated using a Quality-in-Prognostic-Studies-tool (QUIPS), was high. Included studies were too heterogeneous to perform meta-analyses, therefore, effect estimates of the individual studies are presented. Six out of seven included studies found no effect of angular insertion depth on speech perception.

Conclusion: All included studies are characterized by methodological flaws, and therefore, evidence-based conclusions regarding the influence of angular insertion depth cannot be drawn to date.

Introduction

Rationale

At present, a large variability and unpredictability in hearing performance is seen in individuals following cochlear implantation. In addition to different biological and audiological factors - e.g. age at implantation, residual hearing and duration of hearing loss - position of the cochlear implant (CI) electrode array inside the cochlea is believed to contribute to variation in post-operative speech perception. The three seemingly most important electrode positional factors are; electrode scalar location, electrode–to–modiolus proximity and electrode insertion depth.

The suggested influence of electrode positional factors is used by manufactures for design and marketing of their CI electrodes. However, controversy exists as to whether the impact of various electrode position factors; in particular on electrode insertion depth. The range of CI electrode array lengths, that are currently in use by different manufactures, is: 15 to 31.5 millimetres. In theory, deep insertion of a CI electrode array into the apical region of the cochlea could enhance frequency alignment [1] and might give better experience of low-pitched sounds by stimulating the complete spiral ganglion covering deeper located areas [2]. Yet, other theories suggest that deep electrode insertion: a) causes apical frequency pitch confusion [3], b) has a higher risk of trauma to cochlear structures possibly causing loss of residual hearing [4, 5] and c) might reduce stimulation of the basal turn; due to potentially overly deep inserted electrodes [6].

2

Measurements of electrode insertion depth have been described in terms of linear distance in millimetres or insertion angle in degrees. In 2010, Verbist et al. [7] introduced an objective cochlear coordinate system to generate comparable measurements of cochlea dimensions and CI electrode positional measurements. An international panel of CI researchers and representatives of different manufacturers agreed that angular insertion depth, compared to measurement in millimetres, made allowance for variety in individual cochlear dimensions and intra-cochlear trajectories of the CI electrode. They recommended using a cylindrical coordinate system, which defined measurements of rotational insertion angle of a selected point along the trajectory of the CI electrode, such as different CI electrode contacts.

Concerning the influence of insertion depth, a variety of sometimes contradictory correlations are found in literature. In last decade, studies have reported findings of a positive [8, 9], negative [6] or no demonstrated relationship [10-13] between insertion depth and speech perception with CI. There is, however, need for evidence-based conclusions on the influence of insertion depth.

Objective

In this systematic review, we have systematically summarized available evidence on the influence of angular insertion depth on speech perception in CI patients. By discussing design, findings, strengths, and weaknesses of available studies, we intend to assess the status of current evidence for the influence of angular insertion depth on speech perception, which might contribute to determination of optimal CI electrode position.

Methods

Protocol registration

The review protocol can be accessed at the website of PROSPERO, the International Prospective Register of Systematic Reviews (www.crd.york.ac.uk/PROSPERO). The protocol was registered under the number CRD42018099186 on July 02, 2018.

Eligibility criteria

Participants

Studies in adults with post-lingual onset of deafness, normal cochlear anatomy on pre-operative imaging and implanted with any type of CI system were considered eligible for inclusion in this systematic review.

Predictive factor (PF)

Included studies had to investigate angular insertion depth measured on post-operative CT-scan, using the measurement method as advised by the Consensus Panel in Verbist et al. in 2010 [7], or one of the measurement methods on X-ray described as comparable. Studies measuring insertion depth in millimetres were excluded. Figure 1 shows an example of angular insertion depth measurement according the advised method of the Consensus Panel [7].
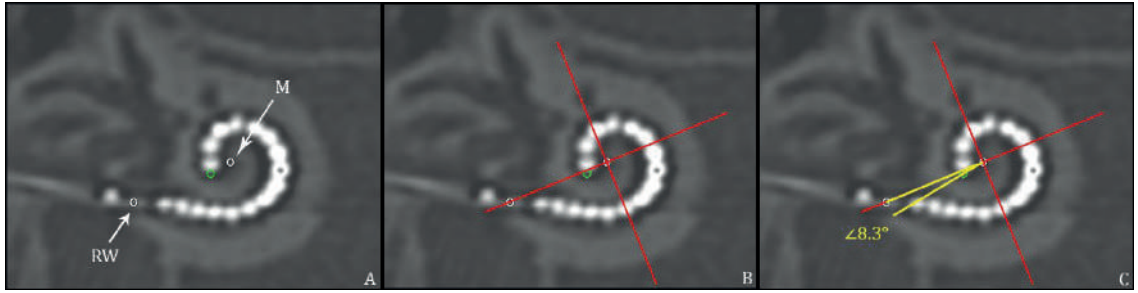
Figure 1. Method for angular insertion depth measurement on CT-scan of an implanted electrode array with 16 electrode contacts. Within a 3 dimensional cylindrical coordinate system all spatial information of the cochlea and an implant is measurable. By consensus this cochlear framework is defined by a plane of rotation through the basal turn of the cochlea and a z-axis through the modiolus. This can be applied on CT of the temporal bone by making a multiplanar reconstruction along the basal turn of the cochlea (Fig.1A, Fig.1B, Fig.1C), and placing the z-axis through the centre of the cochlea; the modiolus (M). Figure 1A: An angular measurement of the insertion depth can then be made by indicating the centre of the round window (RW) and the tip of the electrode array (green circle). Figure 1B: A 0° reference line between the modiolus (M) and the middle of the round window (RW), and a perpendicular line from the modiolus on the 0° reference line line is drawn (red cross). Figure 1C: An angle is drawn (in yellow) from the modiolus over the 0° reference line, and through the most apical point the tip of the electrode array (green circle). In this example the angular insertion depth of the most apical electrode contact is 368.3°; the sum of four quadrants equal to 360° plus the measured yellow angle equal to 8.3°.

Outcome measurement

There were no restrictions on type of speech perception test, setting of testing (quiet or in-noise) or loudness of stimulus. In the first year after implantation, speech perception is rising [10, 14]. Yet, after approximately 1 year, most CI recipients (about 90%) have reached a stable speech perception [10, 13]. Therefore, studies analyzing participants with speech

perception measurements within first 12 months post-implantation were excluded.

Other eligibility criteria

Papers written in any language were eligible for inclusion. There were no restrictions in year of publication.

Data sources and search strategy

Assisted by a trained librarian, we systematically searched PubMed, Ovid EMBASE, Web of Science and Cochrane Library up to June 01, 2018 for studies investigating influence of angular insertion depth on speech perception in adults with CI. Terms, and their synonyms, related to patient population, predictive factor and outcome measurements were combined in the search strategy. Both keywords (MESH and Emtree) and free-text terms in title and abstract were used. Supplement I contains the full electronic search strategy in PubMed. Additionally, articles' reference lists were scanned for any applicable studies.

Study selection

Results of the search strategy were merged and duplicates were removed using EndNote reference management software (version X7, Thomas Reuters, New York City, NY, USA). Two review authors (FH and SdR) individually screened titles and abstracts to identify relevant reports based on eligibility criteria outlined above. Full text versions of these potentially relevant studies were retrieved and independently assessed for eligibility by two review authors (FH and SdR). Any disagreements were resolved by discussion with the third reviewer (WH).

Data extraction

Data were extracted using a pre-defined form that included: study design, participant details (total number of implantations, etiology of hearing loss, age at implantation, gender, history of hearing loss and pre-operative hearing ability), CI system, type of electrodes, type and details of surgical approach used, imaging details (type of imaging, timing of imaging, method used for measurement of angular insertion depth and measurement of other electrode positional factors), speech perception measurement details (mean speech perception score, type of speech perception test, loudness of stimuli used and timing of speech perception measurement), data on measured angular insertion depth(s) and speech perception outcome(s), correlation between angular insertion depth and outcome, and authors' conclusions. Corresponding authors of included papers were contacted if relevant data was missing with the request to provide this information.

Risk of bias assessment

Risk of bias was independently assessed by two review authors (FH and SdR). Included studies were assessed using the Quality-in-Prognostic-Studies (QUIPS) tool[15]. This tool contains six items judging risk of bias due to patient selection, attrition, measurement of prognostic factors, outcome measurement, confounding on statistical analysis and confounding on reporting. Each of the six items in included studies were judged as low, moderate or high risk. Confounding factors that were considered important because they possibly influence angular insertion depth, or relation of angular insertion depth on speech perception, were: age at implantation, history of hearing loss, pre-operative speech perception score, pre-

operative residual hearing, electrode type(s), electrode scalar location and electrode – to – modiolus proximity. Results of risk of bias assessment were graphically summarized using ReviewManager 5 (RevMan5) software (version 5.3.5, Cochrane Collaboration, London, England).

Data synthesis

Details of included studies were structured, and an overview of effect sizes was created for the influence of angular insertion depth on speech perception. Ultimately, the studies included in our systematic review were too heterogeneous to perform the planned meta-analyses, as seen in Table 1. For this reason, effect estimates reported in individual studies are presented.

Results

Study selection

A flow diagram of study selection is shown in Figure 2, derived from The Preferred Reporting Items for Systematic Reviews and Meta-Analyses (PRISMA) Group [16]. After screening, based on title and abstract, full-texts of 63 studies were reviewed and 55 articles were excluded [1, 3, 6, 9, 11, 12, 14, 17-64]. Reasons for exclusion are listed in Figure 2. Eight papers [8, 10, 13, 65-69] seemed eligible for inclusion.

After contact with corresponding authors, it was found the eligible study of van der Marel et al. [13] with 162 participants included a part of the 45 participants of the study in 2005 of van der Beek et al. [68], and included all 130 participants of the study of van der Beek et al. in 2016 [69]. In this systematic review only unique, eligible participants (n=15) of the study by van der Beek in 2005 [68] were included. The study of van der Beek et al. in 2016 [69] was excluded. In total, seven papers [8, 10, 13, 65-68] were included in this systematic review.
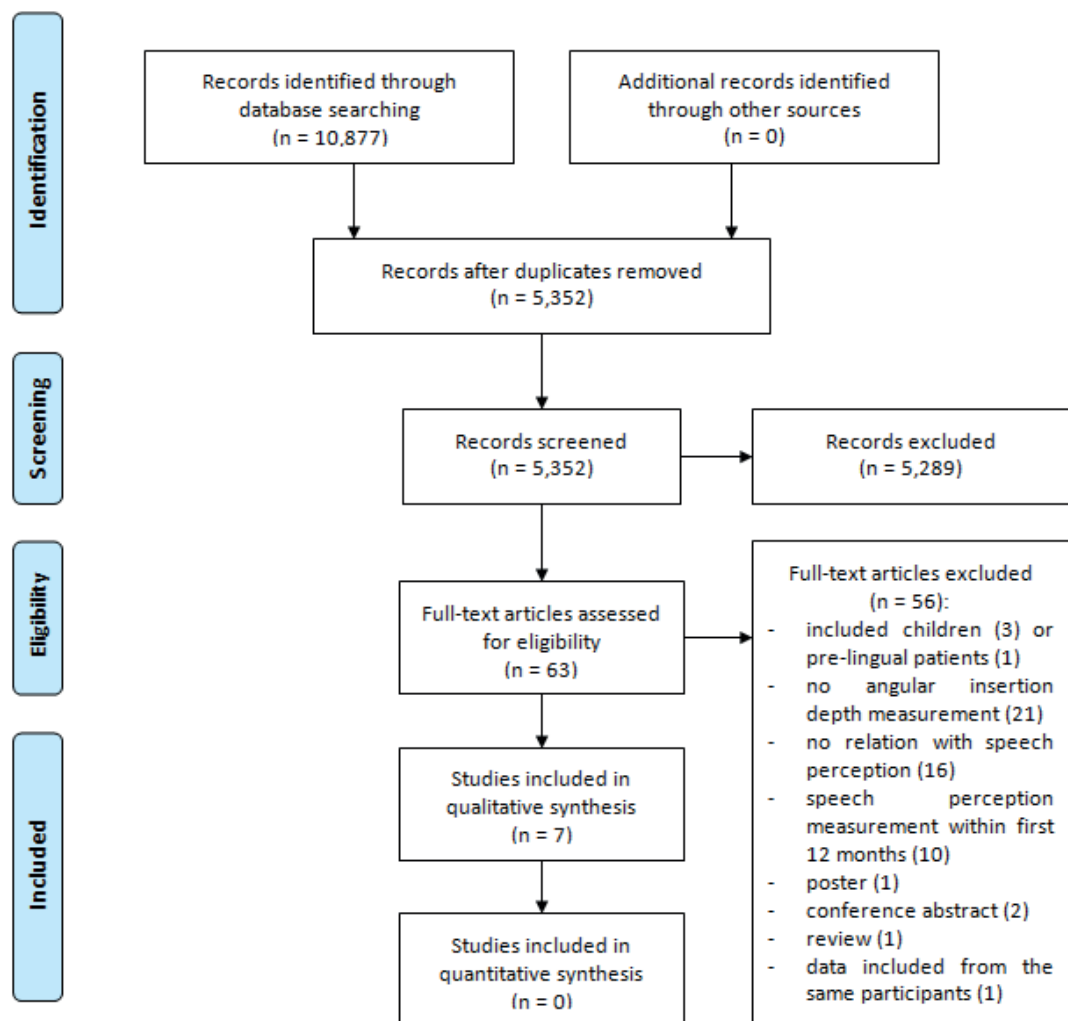
Figure 2. Flow diagram of the study selection.

First author, year	Number of implants, *Study Design*, Surgical approach	Electrodes implanted	Angular insertion depth details		Outcome measurements			Confounders	Included in analysis
			Mean (SD)	Range	Type of test	Mean (SD)	Range	Collected	
De Seta 2016	26 *Prospective* NR[1]	M1	643 (93)	510 – 880	Fournier word test In quiet @ 70dB In noise @ SNR +5, SNR +10, SNR+15	64 (6)	NR[1]	Age at implantation, History of hearing loss, Hearing aid use, Cochlear diameter, Cochlear height, Electrode to modiolus distance @ 180 and 360 degrees	-
Hilly 2016	120 *Retrospective* C	AB1	382 (98)	180 – 720	HINT sentence test In quiet @ 60dB	76 (26)	NR[1]	Age at implantation, Pre-operative outcome score, Pre-operative residual hearing, Number of intracochlear contacts	-
Holden 2013	114 *Prospective* C	AB1, AB2, AB3, C2, C3	NR[1]	NR[1]	CNC word test In quiet @ 60dB	62 (21)	3 - 89	Age at implantation, Educational level, Cognitive measures, History of hearing loss, Hearing aid use, Lip-reading ability, Pre-operative outcome score, Pre-operative residual hearing, Electrode type, Scalar location, Basal angular insertion depth, Electrode to modiolus proximity	-
Marrinan 2004	28 *Retrospective* NR[1]	C2	NR[1]	NR[1]	CNC word test In quiet @ 70dB CUNY sentence test In quiet @ 70dB In noise @ SNR+10	NR[1]	NR[1]	Age at implantation, History of hearing loss, Pre-operative outcome score	-

2

Study	N / Design	Electrode type	Insertion depth mean (SD)	Range	Test	Score mean (SD)	Range	Covariates considered	Covariates not considered
O'Connell 2016	137 107 *Retrospective* RW 39% ERW 34% C 37%	M1, M2, M3, M4, C1, C3, AB1, AB4	420 (99)	208 – 715	CNC word test In quiet @ 60dB AzBio sentence test In quiet @ 60dB	47 (23) 57 (28)		Age at implantation, Category of electrode type, Surgical approach, Cochlear volume, Scalar location	Age at implantation, Category of electrode type, Surgical approach, Cochlear volume, Scalar location
Van der Beek 2005	15 *Prospective* C	AB2	439 (73)	105-559	CVC word test In quiet @ 65 and 75dB	NR[1]	NR[1]	Age at implantation, Duration of deafness, Preoperative outcome score, Pre-operative residual hearing, Electrode to modiolus proximity	-
Van der Marel 2015	162 *Retrospective* ERW	AB1, AB2	477 (70)	303 – 678	CVC word test In quiet average @ 65 + 75dB	Word score 54 (22) Phoneme score 74 (19)	0 – 93 0 - 97	Age at implantation, History of hearing loss, Preoperative outcome score, Electrode to modiolus proximity, Linear insertion depth in millimeters	Duration of deafness, Pre-operative phoneme score, Pre-operative word score

Table 1. Characteristics of included studies. Abbreviations:[1] NR: Not reported in paper and missing information not able to retrieve after contact with author.

Study Characteristics

Table 1 shows characteristics of the seven included studies.

None of the included studies had a randomized design. Four studies [8, 13, 66, 67] reviewed a retrospective acquired database and three [10, 65, 68] combined retrospective and prospectively collected data. Number of cochlear implantations in included studies varied between 15 and 220 implantation. Eleven different types of electrodes were implanted and 10 different speech perception tests were used. Measurement of, and correction for confounding factors varied widely between studies.

Risk of bias

QUIPS – risk of bias assessment Risk of bias assessment, using the QUIPS - tool, is summarized in figures 3 and 4. Three included studies [8, 10, 13] had noticeable lower risk on bias compared to the other four studies [65-68].
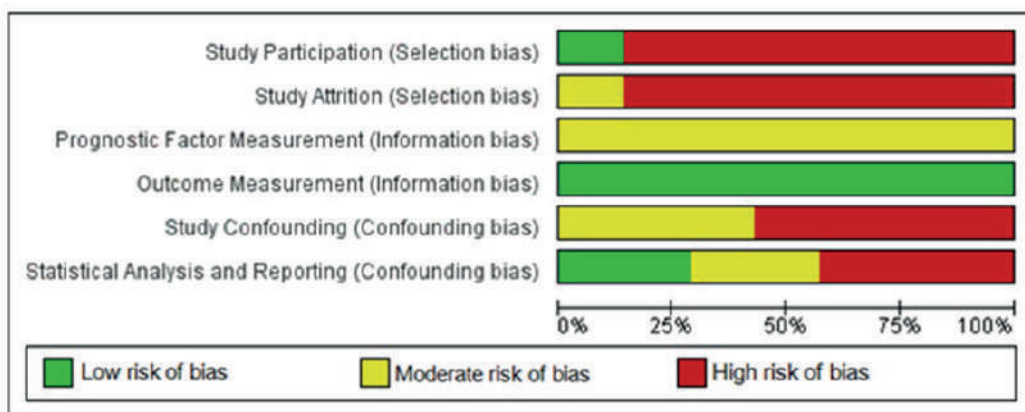
Figure 3. Risk of bias graph: review authors' judgements about each risk of bias item presented as percentages across all included studies.

Figure 4. Risk of bias summary: review authors' judgements about each risk of bias item for each included study.

Selection bias

Overall risk on selection bias was high in most included studies. In six studies [8, 10, 13, 65-67], eligible participants were excluded because of missing information, which mostly concerned imaging data. Additionally, two studies [8, 10] included participants with different CI systems without stating criteria for allocation.

Information bias

Overall risk on information bias was low in included studies. Even though two studies [66, 67] used X-ray, and five studies [8, 10, 13, 65, 68] used CT-scan; all seven included studies measured angular insertion depth using one of the comparable methods advised by Verbist et al. [7]. However, in all studies a time interval between imaging and speech perception measurement was present or at risk. When a time interval between imaging and outcome measurement is present, a non-negligible possibility

exists of intra cochlear changes to the electrode array position during this interval, e.g. extruding of electrode array outside the cochlea [70]. In all studies, speech perception was measured at 12 months post-operatively. In four papers timing of imaging was provided: intra-operatively [67], first weeks post-operatively [13, 68] or 5 years post-operatively [65]. In three papers [8, 10, 66] timing of imaging was reported as "post-operative", without reporting further details.

Confounding bias

Overall risk on confounding bias was moderate to high in all included studies. Only one study [10] measured all confounding factors that we indicated as important. However, this study correlated angular insertion depth with speech perception without correction for these confounding factors. Four other studies [65-68] investigated the relationship between angular insertion depth and speech perception in univariate analysis, without reporting on possible confounding factors. Two studies [8, 13] did include measured confounding factors in analysis, but measured confounders were incomplete.

The most important confounding factor, might be type(s) of electrode array implanted. In Table 1 types of electrodes implanted per study is shown. Table 2 shows an overview of characteristics and technical differences between different types of CI electrodes. Direct comparison of different electrode types can lead to bias in the following ways; Firstly, different electrode designs might yield different results in speech perception in more ways than just angular insertion depth. For example, electrode types vary with respect to a) electrode–to–modiolus proximity, b) number of active contacts, c) spatial distance between active contacts along

the array d) length of the array in millimetres or e) size of electrode contacts. Secondly, inserting a specific electrode too shallow or overly deep, compared to the design goals and prescription of manufacturers,

Brand	Name	Abbreviation code in this study	Type of electrode[1]	Total length in millimetres	Active length / Number of active electrodes	Spatial distance between electrodes	Basal diameter	Tip diameter
Med-El	Standard	M1	S	31.5	26.4 / 12	2.4	1.2	0.5
	Flex 28	M2	S	28	23.1 / 12	2.1	0.8	0.48-0.36
	Flex 24	M3	S	24	20.9 / 12	1.9	0.8	0.48-0.36
	Medium	M4	S	24	20.9 / 12	1.9	0.8	0.38-0.36
Cochlear	Slim straight	C1	S	25	20 / 22	0.95	0.6	0.3
	Contour	C2	MH	18	15 / 22	0.71	0.8	0.5
	Contour advanced	C3	MH	18	15 /22	0.71	0.8	0.5
Advanced Bionics	HiFocus 1	AB1	S	20	17 / 16	1.13	0.8	0.4-0.6
	HiFocus 1J	AB2	S	20	17 / 16	1.13		0.4-0.6
	Helix	AB3	MH	18.5	13.25 / 16	0.85	1.1	0.6
	Mid-Scala	AB4	MH	18.5	15 / 16	1.0	0.7	0.5

Table 2. Characteristics of different electrodes implanted in included studies. Abbreviations: [1] S: Straight electrode, MH: Modiolus hugging; precurved electrode.

might suggest a correlation between angular insertion depth and speech perception, while actually these studies might have found a difference in speech perception for surgical correctly placed electrode arrays when compared to surgically too shallow or overly-deep electrode placement. The surgical variation in depth of implantation should therefore be described in all studies on this topic. Degree of surgical insertion depth, or

marker until were the electrode(s) in study participants were inserted, was not reported in five studies [8, 65-68], therefore potential bias due to surgical depth of insertion in these studies was unclear. Two out of seven included studies [10, 13] did address the possibility of shallow or deep inserted electrodes in more detail, as these studies measured angular insertion depth of the basal electrode contact and used this as a reference for degree of surgical insertion depth.

Study results

A summary of reported effect sizes is presented in Table 3.

Speech perception in quiet

Speech perception in quiet is reported in all included studies. One out of seven studies [8] found a significant relationship between angular insertion depth and speech perception in quiet, and six studies [10, 13, 65-68] reported no correlation. Out of three studies [8, 10, 13] with noticeable lower risk of bias, Holden et al. and van de Marel et al., found no correlation between angular insertion depth and speech perception in quiet, while O'Connell et al. did find a significant relationship. These studies are discussed in more detail in following paragraphs.

Holden et al. [10], found no correlation between angle of apical electrode insertion depth and speech perception in quiet. This study was the only included study measuring all confounding factors that were indicated as important in this systematic review. However, no multivariate analysis was performed. Interestingly, angular insertion depth of most basal electrode contact, and length of the electrode array measured in millimetres were

First author, year	Number of implants	Type(s) of analysis	Effect size	Authors' conclusion
De Seta 2016	26	Pearson's Correlation	*NR[1]*	No correlation
Hilly 2016	120	Spearman's Correlation	R=0.16, p=0.09	No correlation
Holden 2013	114	Spearman's Correlation	*NR[1]*	No correlation
Marrinan 2004	28	Linear Regression	*NR[1]*	No correlation
O'Connell 2016	137	Pearson's Correlation	*CNC: r=0.23, p=0.006*	Significant positive correlation between angular insertion depth and CNC word scores.
	107		*AzBio: NR[1]*	No correlation
	137	Multivariate Linear Regression	*CNC:* Coefficient 0.0006, 95%CI 0.0002–0.001, p=0.009	CNC word score increases 0.6% with every 10 degrees increase in angular insertion depth.
Van der Beek 2005	45	Pearson's Correlation	R=0.01, p>0.8	No correlation
Van der Marel 2015	162	Multivariate Partial Correlation	R=0.03, p=0.69	No correlation

Table 3. Effect size(s) in included studies.

found to significantly negatively correlate with speech perception outcome. Authors divided their participants in 6 outcome groups based on percentile ranking of participants CNC final score, and calculated mean values of independent variables of interest in these outcome groups. The effect size of linear relationship across the outcome groups mean angular insertion

2

depth of most basal electrode contact was -2.42 (p≤0.05) and of the groups mean array trajectory length was -2.10 (p≤0.05). The negative relationship of these two variables suggest that electrodes of participants with deepest insertion in this study were probably inserted overly deep in comparison with design goals of included electrodes. In theory, this could decrease performance for two reasons[6]. First, if such overly deep insertion occurs, the first part of the basal cochlea might be bypassed by the electrode, which otherwise would have been stimulated. Secondly, when the tip of the electrode array approaches the apex this might cause trauma which may reduce residual hearing. Furthermore, the tip might translocate to scala vestibuli, or the tip might fold inside scala tympani which might cause a decrease in apical stimulation [6]. Authors concluded measurement of angular basal electrode contact, could be used to judge surgically too shallow or overly-deep surgical insertions [10].

Van de Marel et al. [13] found no correlation between angular insertion depth and post-operative CVC word scores, while correcting for age at implantation, duration of deafness, pre-operative phoneme score and pre-operative word score (p=0.89). In their analysis, van de Marel et al. did not correct for electrode scalar location and electrode-to-modiolus proximity. All participants were implanted with the same type of electrode (HiFocus I/IJ) and with the same surgical technique (extended round window approach). This homogeneity in implantation characteristics prevented bias of results caused by differences in CI systems and by differences in electrode designs which is a strength of this study. On the other hand, conclusions of this study only apply to this specific combination of electrode type and surgical technique.

O'Connell et al. [8] reported 0.6% increase of CNC word score for every 10 degrees increase in angular insertion depth (coefficient 0.0006, p=0.03), while corrected for age at implantation, category of electrode type (lateral wall, perimodiolar or mid-scalar electrode), surgical technique, cochlear volume and scalar location. O'Connell et al. did not measure possible confounding audiologic factors or electrode-to-modiolus proximity. Besides, the study of O'Connel et al. included eight different electrode types, and despite grouping these electrodes into three categories, electrode types within these groups remained to differ significantly, as shown in Table 2. Thus, influence of array length and width, number of active electrodes, space between electrode contacts and differences in fitting programs is unclear. Additionally, authors did not account for possible influence of shallow and/or deep inserted electrode arrays. Furthermore, O'Connell et al. [8] found no correlation between angular insertion depth and AzBio-sentence test scores in quiet.

Speech perception in noise

Speech perception in noise is reported in two studies [65, 67]. No correlation between angular insertion depth and CUNY-sentences and Fournier-word test in noise was found in these studies.

2

Discussion

Summary of evidence

This systematic review includes seven studies investigating the influence of angular insertion depth on speech perception, one year or more after CI surgery in adults with post-lingual onset of deafness. Included studies demonstrate substantial heterogeneity in study design, electrodes implanted, speech perception test characteristics and confounding factors measured and accounted for in analysis. Risk of bias was judged high in all studies. Therefore, we did not perform a meta-analysis, but present effect size(s) reported in individual studies. Most studies found no relationship between angular insertion depth and speech perception test score in quiet. In all included studies correction for possible confounding factors was poor. None of the included studies found a relationship between angular insertion depth and speech perception in noise.

Contemplation of evidence in light of non – included literature

The objective of present systematic review was to investigate the influence of angular insertion depth on speech perception performance. Since the increase in performance during rehabilitation is beyond the scope of this study, we only included studies describing analysis on stable speech perception scores. The exclusion criterion was therefore set at follow-up of less than 12months. The decision to use the 12 months follow-up criterion is based on data of Holden et al. [10] who showed that most CI recipients reach stable speech perception performance after one year CI experience. Ten studies that were excluded from this review [6, 9, 11, 14, 44, 53, 56, 59, 61, 64] investigated speech perception *within* the first year. Four out of ten studies (40%), reported a significant positive correlation between angular

insertion depth and speech perception, compared to one out of seven of the included studies (14%) . Buchman et al. [14] randomly assigned thirteen participants to receive either the standard electrode array (31,5mm; mean angular insertion depth 657°; SD 82°), or the medium electrode array (24mm; mean angular insertion depth 423°; SD 23°). A significant higher mean speech perception score, increasing over time in the first year was found in the standard electrode array group compared to the medium electrode array group. Comparing the percentage of studies showing a positive correlation of angular insertion depth with speech perception measured within the first year (4 out of 10; 40%) to the studies included in the present systematic review investigating speech perception at or beyond the first year (1 out of 7; 14%) suggests that deeper insertion might only make a difference in the period shortly after activation.

This hypothesis is supported by a recent study conducted by Buchner et al. [71], who compared three electrodes with different lengths. At 3-months post-activation, significant higher scores were found for FLEX28 electrode group for three measured speech perception tests when compared to FLEX20 group, and for two out of three tests when compared to FLEX24 group. However, these significant findings diminished at 6-months post-activation. It can be hypothesised that long electrodes used in this study give a better match to natural frequency placement after 3 months, but at 6 months brain plasticity copes with the mismatch for shorter electrodes, and early effect of electrode length diminishes. Further exploration of this theory goes beyond the scope of this review but should be addressed in future research.

Strengths and limitations

This is the first systematic evaluation of evidence on the topic of influence of electrode insertion depth, measured in angular insertion depth, on speech perception performance beyond one year after CI surgery in adults with post-lingual onset of deafness. Considering the possibility to influence CI electrode position within the cochlea, potentially through surgical technique and more easily by electrode design, determination of influence of electrode position on performance is of high relevance to healthcare providers and patients. We conducted this systematic review with strict allegiance to our registered research protocol and followed PRISMA guidelines of reporting [16].

Several limitations are present in our systematic review. Most importantly, included individual studies were low to moderate quality, mainly due to risk of selection and confounding bias. Study designs were mostly retrospective, participants were excluded due to missing data, important confounding factors were not taken into account and reporting of data on angular insertion depth and outcome measurement was incomplete. Between study comparison was limited, due to ten different outcome measurement tests being used, eleven different electrode types investigated and large variation in number and definition of measured confounding factors. Investigating influence of angular insertion depth, on speech perception in non randomized, observational research is difficult because (1) differences in angular insertion depth are mostly due to differences in lengths in millimetres of used electrodes, and not due to surgical variation in insertion depth or anatomical variation in the cochlea of participants, and (2) comparing electrodes of different manufactures is automatically accompanied with other differences between electrodes

then angular insertion depth, such as factors mentioned in this systematic review and shown in Table 2. These difficulties stress the need for randomized designs in future studies addressing insertion depth.

Clinical / Future implications

Identifying factors that may influence variability in CI outcome, which could be influenced by patient, surgeon or manufactures, could potentially improve future speech discrimination capability after cochlear implantation. However, all studies investigating optimal insertion depth of CI electrode array are characterized by methodological flaws, and evidence-based conclusions regarding influence of angular insertion cannot be drawn to date. To fully assess influence of angular insertion depth on speech perception, a randomized trial with multiple identical electrodes of different lengths is preferred. Learning and developmental effects due to brain plasticity should be taken into account, and therefore it is recommended to measure speech perception outcomes beyond 12 months after implantation. Alternatively, prospective cohort studies addressing this topic should conduct analysis including important confounding audiologic, biographic and electrode positional factors.

Conclusions

Although angular insertion depth is a much debated topic over the past decade in cochlear implantation research, the current body of evidence does not support firm conclusions on the effect of insertion depth on speech perception at one year or more after CI surgery.

References

1.   Baskent, D. and R.V. Shannon, *Interactions between cochlear implant electrode insertion depth and frequency-place mapping.* J Acoust Soc Am, 2005. **117**(3 Pt 1): p. 1405-16.
2.   Faulkner, A., S. Rosen, and C. Norman, *The right information may matter more than frequency-place alignment: simulations of frequency-aligned and upward shifting cochlear implant processors for a shallow electrode array insertion.* Ear Hear, 2006. **27**(2): p. 139-52.
3.   Gani, M., et al., *Implications of deep electrode insertion on cochlear implant fitting.* J Assoc Res Otolaryngol, 2007. **8**(1): p. 69-83.
4.   Suhling, M.C., et al., *The Impact of Electrode Array Length on Hearing Preservation in Cochlear Implantation.* Otol Neurotol, 2016. **37**(8): p. 1006-15.
5.   Causon, A., C. Verschuur, and T.A. Newman, *A Retrospective Analysis of the Contribution of Reported Factors in Cochlear Implantation on Hearing Preservation Outcomes.* Otol Neurotol, 2015. **36**(7): p. 1137-45.
6.   Finley, C.C., et al., *Role of electrode placement as a contributor to variability in cochlear implant outcomes.* Otol Neurotol, 2008. **29**(7): p. 920-8.
7.   Verbist, B.M., et al., *Consensus panel on a cochlear coordinate system applicable in histologic, physiologic, and radiologic studies of the human cochlea.* Otol Neurotol, 2010. **31**(5): p. 722-30.
8.   O'Connell, B.P., et al., *Electrode Location and Angular Insertion Depth Are Predictors of Audiologic Outcomes in Cochlear Implantation.* Otol Neurotol, 2016. **37**(8): p. 1016-23.
9.   O'Connell, B.P., et al., *Electrode Location and Audiologic Performance After Cochlear Implantation: A Comparative Study Between Nucleus CI422 and CI512 Electrode Arrays.* Otol Neurotol, 2016. **37**(8): p. 1032-5.
10.   Holden, L.K., et al., *Factors affecting open-set word recognition in adults with cochlear implants.* Ear Hear, 2013. **34**(3): p. 342-60.
11.   Kos, M.I., et al., *Measurements of electrode position inside the cochlea for different cochlear implant systems.* Acta Otolaryngol, 2005. **125**(5): p. 474-80.
12.   Lee, A., et al., *Electric acoustic stimulation of the auditory system: experience and results of ten patients using MED-EL's M and Flex(EAS) electrodes.* Clinical Otolaryngology, 2010. **35**(3): p. 190-197.
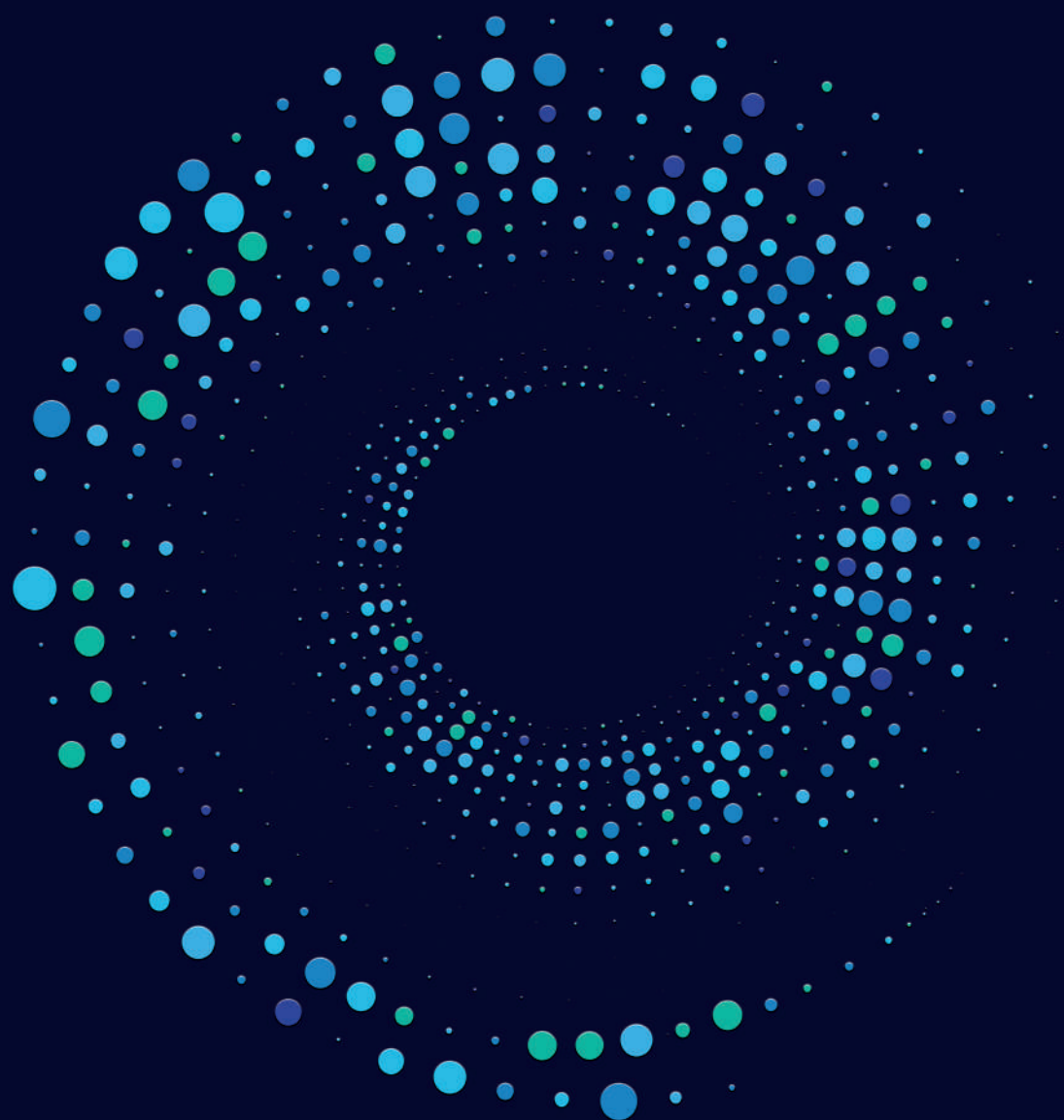
13.   van der Marel, K.S., et al., *The influence of cochlear implant electrode position on performance.* Audiol Neurootol, 2015. **20**(3): p. 202-11.

14.   Buchman, C.A., et al., *Influence of cochlear implant insertion depth on performance: a prospective randomized trial.* Otol Neurotol, 2014. **35**(10): p. 1773-9.

15.   Hayden, J.A., et al., *Assessing bias in studies of prognostic factors.* Ann Intern Med, 2013. **158**(4): p. 280-6.

16.   Moher, D., et al., *Preferred reporting items for systematic reviews and meta-analyses: the PRISMA statement.* BMJ, 2009. **339**: p. b2535.

17.   Adamczyk, M., et al., *[Cochlear implantation: relationship between speech development and insertion depth in children].* Laryngorhinootologie, 2001. **80**(3): p. 123-6.

18.   Huang, T.C., et al., *Modiolar coiling, electrical thresholds, and speech perception after cochlear implantation using the nucleus contour advance electrode with the advance off stylet technique.* Otol Neurotol, 2006. **27**(2): p. 159-66.

19.   Nayak, G., et al., *Deeper insertion of electrode array result in better rehabilitation outcomes - Do we have evidence?* Int J Pediatr Otorhinolaryngol, 2016. **82**: p. 47-53.

20.   DeVries, L., R. Scheperle, and J.A. Bierer, *Assessing the Electrode-Neuron Interface with the Electrically Evoked Compound Action Potential, Electrode Position, and Behavioral Thresholds.* J Assoc Res Otolaryngol, 2016. **17**(3): p. 237-52.

21.   Albu, S. and G. Babighian, *Predictive factors in cochlear implants.* Acta Otorhinolaryngol Belg, 1997. **51**(1): p. 11-6.

22.   Aschendorff, A., et al., *Quality control after insertion of the nucleus contour and contour advance electrode in adults.* Ear Hear, 2007. **28**(2 Suppl): p. 75s-79s.

23.   Ball, J.B., Jr., G.W. Miller, and S.T. Hepfner, *Computed tomography of single-channel cochlear implants.* AJNR Am J Neuroradiol, 1986. **7**(1): p. 41-7.

24.   Basta, D., I. Todt, and A. Ernst, *Audiological outcome of the pull-back technique in cochlear implantees.* Laryngoscope, 2010. **120**(7): p. 1391-6.

25.   Blamey, P.J., et al., *Factors predicting postoperative sentence scores in postlinguistically deaf adult cochlear implant patients.* Ann Otol Rhinol Laryngol, 1992. **101**(4): p. 342-8.

26.   Bredberg, G. and B. Lindstrom, *Insertion length of electrode array and its relation to speech communication performance and*

nonauditory side effects in multichannel-implanted patients. Ann Otol Rhinol Laryngol Suppl, 1995. **166**: p. 256-8.

27. Chu, K.M., et al., *Short electrode insertion in cochlear implants: performance on speech perception.* Cochlear Implants Int, 2004. **5 Suppl 1**: p. 126-8.

28. Coombs, A., et al., *The role of post-operative imaging in cochlear implant surgery: a review of 220 adult cases.* Cochlear Implants Int, 2014. **15**(5): p. 264-71.

29. Fitzgerald, M.B., et al., *The effect of perimodiolar placement on speech perception and frequency discrimination by cochlear implant users.* Acta Otolaryngol, 2007. **127**(4): p. 378-83.

30. Hartrampf, R., et al., *Insertion depth of the Nucleus electrode array and relative performance.* Ann Otol Rhinol Laryngol Suppl, 1995. **166**: p. 277-80.

31. Hiraumi, H., et al., *Cochlear implants in post-lingually deafened patients.* Acta Oto-Laryngologica, 2007. **127**(SUPPL. 557): p. 17-21.

32. Johnston, J.D., et al., *Computed Tomography Estimation of Cochlear Duct Length Can Predict Full Insertion in Cochlear Implantation.* Otol Neurotol, 2016. **37**(3): p. 223-8.

33. Kumakawa, K., H. Takeda, and N. Ujita, *Determining the optimum insertion length of electrodes in the cochlear 22-channel implant: results of a clinical study.* Adv Otorhinolaryngol, 1997. **52**: p. 129-34.

34. Long, C.J., et al., *Examining the electro-neural interface of cochlear implant users using psychophysics, CT scans, and speech understanding.* J Assoc Res Otolaryngol, 2014. **15**(2): p. 293-304.

35. Rader, T., et al., *Management of Cochlear Implant Electrode Migration.* Otol Neurotol, 2016. **37**(9): p. e341-8.

36. van Besouw, R.M., et al., *Simulating the effect of interaural mismatch in the insertion depth of bilateral cochlear implants on speech perception.* J Acoust Soc Am, 2013. **134**(2): p. 1348-57.

37. Wanna, G.B., et al., *Impact of electrode design and surgical approach on scalar location and cochlear implant outcomes.* Laryngoscope, 2014. **124 Suppl 6**: p. S1-7.

38. Wanna, G.B., et al., *Assessment of electrode placement and audiological outcomes in bilateral cochlear implantation.* Otol Neurotol, 2011. **32**(3): p. 428-32.

39. Zhou, X., et al., *Effects of insertion depth on spatial speech perception in noise for simulations of cochlear implants and single-sided deafness.* Int J Audiol, 2016: p. 1-8.

2

40. Zuniga, M.G., et al., *Tip Fold-over in Cochlear Implantation: Case Series.* Otol Neurotol, 2017. **38**(2): p. 199-206.

41. Boyle, P.J., *The rational for a mid-scala electrode array.* Eur Ann Otorhinolaryngol Head Neck Dis, 2016. **133 Suppl 1**: p. S61-2.

42. Boex, C., et al., *Acoustic to electric pitch comparisons in cochlear implant subjects with residual hearing.* J Assoc Res Otolaryngol, 2006. **7**(2): p. 110-24.

43. Boyer, E., et al., *Scalar localization by cone-beam computed tomography of cochlear implant carriers: a comparative study between straight and periomodiolar precurved electrode arrays.* Otol Neurotol, 2015. **36**(3): p. 422-9.

44. Chen, J.M., et al., *Depth and quality of electrode insertion: a radiologic and pitch scaling assessment of two cochlear implant systems.* Am J Otol, 1999. **20**(2): p. 192-7.

45. Deman, P.R., et al., *Pitch estimation of a deeply inserted cochlear implant electrode.* Int J Audiol, 2004. **43**(6): p. 363-8.

46. Doshi, J., et al., *Straight Versus Modiolar Hugging Electrodes: Does One Perform Better Than the Other?* Otology & Neurotology, 2015. **36**(2): p. 223-227.

47. Esquia Medina, G.N., et al., *Is electrode-modiolus distance a prognostic factor for hearing performances after cochlear implant surgery?* Audiology and Neurotology, 2015. **18**(6): p. 406-413.

48. Fama, A., et al., *The Use of Micro-CT to Evaluate Cochlear Implant Electrode Position and Intracochlear Damage.* Laryngoscope, 2010. **120**: p. S205-S205.

49. Fischer, N., et al., *Radiologic and functional evaluation of electrode dislocation from the scala tympani to the scala vestibuli in patients with cochlear implants.* AJNR Am J Neuroradiol, 2015. **36**(2): p. 372-7.

50. Grasmeder, M.L., C.A. Verschuur, and V.B. Batty, *Optimizing frequency-to-electrode allocation for individual cochlear implant users.* J Acoust Soc Am, 2014. **136**(6): p. 3313.

51. Hassepass, F., et al., *Radiologic Results and Hearing Preservation With a Straight Narrow Electrode via Round Window Versus Cochleostomy Approach at Initial Activation.* Otol Neurotol, 2015. **36**(6): p. 993-1000.

52. Jolly, C.N., et al., *Principles and outcome in perimodiolar positioning.* Ann Otol Rhinol Laryngol Suppl, 2000. **185**: p. 20-3.

53. Lazard, D.S., et al., *Pre-, per- and postoperative factors affecting performance of postlinguistically deaf adults using cochlear implants: a new conceptual model over time.* PLoS One, 2012. **7**(11): p. e48739.

54.   Marsh, M.A., et al., *Radiologic evaluation of multichannel intracochlear implant insertion depth.* Am J Otol, 1993. **14**(4): p. 386-91.

55.   Noble, J.H., et al., *Clinical evaluation of an image-guided cochlear implant programming strategy.* Audiol Neurootol, 2014. **19**(6): p. 400-11.

56.   O'Connell, B.P., et al., *Insertion depth impacts speech perception and hearing preservation for lateral wall electrodes.* Laryngoscope, 2017.

57.   Puyalto De Pablo, P., et al., *Relationship between the insertion depth and the auditory results in patients with cochlear implants.* Neuroradiology, 2017. **59 (2)**: p. 186-187.

58.   Roy, A.T., et al., *Deeper Cochlear Implant Electrode Insertion Angle Improves Detection of Musical Sound Quality Deterioration Related to Bass Frequency Removal.* Otol Neurotol, 2016. **37**(2): p. 146-51.

59.   Skinner, M.W., et al., *In vivo estimates of the position of advanced bionics electrode arrays in the human cochlea.* Ann Otol Rhinol Laryngol Suppl, 2007. **197**: p. 2-24.

60.   Skinner, M.W., et al., *CT-derived estimation of cochlear morphology and electrode array position in relation to word recognition in Nucleus-22 recipients.* J Assoc Res Otolaryngol, 2002. **3**(3): p. 332-50.

61.   van der Jagt, M.A., et al., *Comparison of the HiFocus Mid-Scala and HiFocus 1J Electrode Array: Angular Insertion Depths and Speech Perception Outcomes.* Audiol Neurootol, 2016. **21**(5): p. 316-325.

62.   Wang, J., et al., *Cochlear implant outcomes with perimodiolar-positioned electrodes.* Otolaryngology - Head and Neck Surgery (United States), 2016. **155**: p. P105.

63.   Wanna, G.B., et al., *Impact of Intrascalar Electrode Location, Electrode Type, and Angular Insertion Depth on Residual Hearing in Cochlear Implant Patients: Preliminary Results.* Otol Neurotol, 2015. **36**(8): p. 1343-8.

64.   Yukawa, K., et al., *Effects of insertion depth of cochlear implant electrodes upon speech perception.* Audiol Neurootol, 2004. **9**(3): p. 163-72.

65.   De Seta, D., et al., *The Role of Electrode Placement in Bilateral Simultaneously Cochlear-Implanted Adult Patients.* Otolaryngol Head Neck Surg, 2016. **155**(3): p. 485-93.

2

66.   Hilly, O., et al., *Depth of Cochlear Implant Array Within the Cochlea and Performance Outcome.* Ann Otol Rhinol Laryngol, 2016. **125**(11): p. 886-892.

67.   Marrinan, M.S., et al., *Degree of modiolar coiling, electrical thresholds, and speech perception after cochlear implantation.* Otol Neurotol, 2004. **25**(3): p. 290-4.

68.   van der Beek, F.B., et al., *Clinical evaluation of the Clarion CII HiFocus 1 with and without positioner.* Ear Hear, 2005. **26**(6): p. 577-92.

69.   van der Beek, F.B., et al., *Intracochlear Position of Cochlear Implants Determined Using CT Scanning versus Fitting Levels: Higher Threshold Levels at Basal Turn.* Audiol Neurootol, 2016. **21**(1): p. 54-67.

70.   van der Marel, K.S., et al., *Electrode migration in cochlear implant patients: not an exception.* Audiol Neurootol, 2012. **17**(5): p. 275-81.

71.   Buchner, A., et al., *Investigation of the effect of cochlear implant electrode length on speech comprehension in quiet and noise compared with the results with users of electro-acoustic-stimulation, a retrospective analysis.* PLoS One, 2017. **12**(5): p. e0174900.

3

Factors Influencing Speech Perception in Adults With a Cochlear Implant.

Floris Heutink, Berit M. Verbist, Willem-Jan van der Woude,
Tamara J. Meulman, Jeroen J. Briaire, Johan H.M. Frijns, Priya Vart,
Emmanuel A.M. Mylanus, Wendy J. Huinck

Abstract

Objectives: The primary objective of this study is to identify the biographic, audiologic, and electrode-position factors that influence speech perception performance in adult cochlear implant (CI) recipients implanted with a device from a single manufacturer. The secondary objective is to investigate the independent association of the type of electrode (precurved or straight) with speech perception.

Design: In a cross-sectional study design, speech perception measures and ultra-high-resolution computed tomography (UHR-CT) scans were performed in 129 experienced CI recipients with a postlingual onset of hearing loss. Data were collected between December 2016 and January 2018 in Radboud university medical center, Nijmegen, the Netherlands. The participants received either a precurved electrode (N=85) or a straight electrode (N=44), all from the same manufacturer. The biographic variables evaluated were age at implantation, level of education, and years of hearing loss. The audiometric factors explored were pre- and post-operative pure tone average residual hearing and preoperative speech perception score. The electrode-position factors analyzed, as measured from images obtained with the UHR-CT scan, were the scalar location, angular insertion depth of the basal and apical electrode contacts, and the wrapping factor (i.e., electrode-to-modiolus distance), as well as the type of electrode used. These 11 variables were tested for their effect on three speech perception outcomes: consonant–vowel–consonant words in quiet tests at 50 dB SPL (CVC50) and 65 dB SPL (CVC65), and the digits-in-noise test (DIN).

Results: A lower age at implantation was correlated with a higher CVC50 phoneme score in the straight electrode group. Other biographic variables did not correlate with speech perception. Furthermore, participants implanted with a precurved electrode and who had poor preoperative hearing thresholds performed better in all speech perception outcomes than the participants implanted with a straight electrode and relatively better preoperative hearing thresholds. After correcting for biographic factors, audiometric variables, and scalar location, we showed that the precurved electrode led to an 11.8 percentage points (95%CI: 1.4–20.4%; p=0.03) higher perception score for the CVC50 phonemes compared with the straight electrode. Furthermore, contrary to our initial expectations, the preservation of residual hearing with the straight electrode was poor, as the median preoperative and the postoperative residual hearing thresholds for the straight electrode were 88 dB and 122 dB, respectively.

Conclusions: Cochlear implantation with a precurved electrode results in a significantly higher speech perception outcome, independent of biographic factors, audiometric factors, and scalar location.

Introduction

Since the first cochlear implant (CI) in 1973, the overall speech perception performance with a CI has increased as a result of technical, surgical, and audiologic improvements, such as the optimization of the speech processor program [1]. However, performance still varies across CI recipients. As a result, the factors explaining speech perception with a CI have been discussed in an extensive number of studies over the past three decades.

The factors of interest affecting the variation in contemporary CI speech perception can be divided into three categories: biographical factors, audiometric factors, and electrode (positional) factors. Rapid developments in the CI field means that the influence of these factors on speech perception could be constantly changing, as shown by Blamey et al. [2, 3]. Blamey and colleagues studied the influence of several biographic and audiologic factors on speech perception in two multicenter studies using the same study method (N=800 in 1996 and N=2251 in 2013). Compared with the results of the 1996 study, the authors showed less of an influence for biographic and audiologic factors (i.e., age at implantation, age at onset of deafness, duration of deafness, etiology of hearing loss, and CI experience) on speech perception in the 2013 study, explaining 21% and 10% of the variation in speech perception, respectively. This decrease was attributed to less stringent CI patient selection criteria and the improved clinical management of hearing loss and cochlear implantation in 2013 [3].

Since their initial introduction, CIs have been developed from devices that only provide sound to deaf patients into devices that also improve speech perception in patients with moderate to severe hearing loss. In the last two decades, early implantation, when there still is some functional residual hearing, has been shown to positively affect the

postoperative speech perception performance with CI [4-8]. As a result, the preservation of residual hearing became an important goal, both to reduce intracochlear damage but also because residual hearing can, in some CI recipients, be used in a combined electric–acoustic stimulation. Following this, post-operative imaging has become more important for checking the relationship between the electrode position post-implantation and the residual hearing. Several post-operative imaging studies have shown that translocation from the desired scala tympani (ST) to the scala vestibuli (SV) causes a higher loss of residual hearing and reduced speech perception [9-13]. Recently, the influence of electrode positional factors on speech perception has gained more interest, with studies exploring the effect of scalar location, insertion depth [10, 14-16], and 'electrode-to-modiolus' distance [10, 17-19]. In 2012, Lazard et al. [20] used [3] data and added several additional factors: gender, years of education, preoperative hearing aid use, preoperative pure tone average (PTA) of the implanted ear, PTA of the best ear, preoperative speech score in quiet conditions, surgical approach, CI device brand, angular insertion depth, and percentage of active electrodes. Besides the five factors that [3] found to be significantly correlated with speech perception, [20] also observed an impact for the PTA of the best ear, the CI device brand, the percentage of active electrodes, and preoperative hearing aid use.

Blamey's and Lazard's multicenter studies significantly contributed to our understanding of the factors influencing cochlear implantation. The large number of subjects in multicenter studies mean a high statistical power can be reached; however, multicenter research into CI has the disadvantage of introducing data heterogeneity caused by various clinical approaches and study methodologies (e.g., population, electrode selection,

surgical approach, and audiometric measurements). Considering this limitation, [10] conducted a single-center study with a relatively large number of participants implanted between 2003 and 2008 (N=114). In addition to most of the biographic and audiometric factors described before, Holden and colleagues also found cognition and electrode-position factors (scalar location, insertion depth, and electrode-to-modiolus proximity) to be correlated with CI performance, which was in line with the outcomes of other studies [21, 22]. In Holden et al.'s study, however, the age at implantation and the cognitive function were found to be correlated, and after the authors reanalyzed the data controlling for the age at implantation, no significant correlation was found between cognition and speech perception. Several factors (electrode scalar position, angular insertion depth of the most basal electrode, CI sound field threshold, insertion depth in millimeters, duration of severe-to-profound deafness, and wrapping factor) remained significantly correlated with speech perception, however.

In current CI research, there might also be a risk of confounding variables when multiple CI systems and/or multiple electrode types are included in one study. Electrode type could introduce selection bias because the choice of electrode type is based on clinic-specific preoperative decision criteria (e.g., residual hearing, cochlear anatomy, and the surgeon's preference; [14]. The potential correlations between the 'electrode choice' criteria and the speech perception outcome may obscure the true correlation between electrode type and speech perception. Moreover, when analyzing multiple electrode designs in one study, the correlation between the electrode position and speech perception may be affected by electrode type-specific factors, the influence of which cannot be

3

determined using different CI brands as they may be substantially different, e.g., the number of contacts [23].

The present study investigates the factors influencing the CI outcome using a cross-sectional study design. The population represents a homogeneous group of adult CI recipients with a postlingual onset of hearing loss, implanted between 2010 and 2016 at Radboud university medical center (Radboudumc), Nijmegen, the Netherlands. The included patients received either a precurved or straight electrode made by a single CI manufacturer.

Objectives

The primary objective of this study was to identify the biographic, audiologic, and electrode-position factors that influence the speech perception performance in adult CI recipients implanted with a device from a single manufacturer. The secondary objective was to investigate the independent association of the type of electrode with speech perception.

Material and Methods

Study design

This cross-sectional study was conducted between December 2016 and January 2018 at Radboudumc (Nijmegen, the Netherlands) and approved by the Institutional Review Board (Medical Ethics Committee Arnhem-Nijmegen; NL510071.091.14). All participants signed their informed consent. Eleven biographic, audiometric, and electrode-position variables were evaluated in a cohort of CI recipients (N=129), in terms of their effect on speech perception in quiet and noisy conditions (Table 1). The biographic and pre-implantation data were retrospectively collected from the electronic patient files, whereas the post-implantation ultra-high-resolution computed tomography scan (UHR-CT) and audiometric tests were prospectively collected. The moment at which the study variables and outcome measurements were taken is referred to as the Study Variables and Outcome Evaluation (SVOE). The time between the surgery and the SVOE ranged from 14 to 92 months due to the selected time window of inclusion: CI recipients who were implanted between 2010 and 2016 were invited to participate in this study.

Participants

All participants were diagnosed with a bilateral postlingual onset of hearing loss, defined as the onset of severe or profound hearing loss (SPHL), after the age of 5 years. Participants had at least one year of experience with their CI before SVOE (mean 3.8 years; SD 1.7; range 1.2–7.7 years). Patients with a prelingual onset of hearing loss, a congenital or acquired mental disorder, congenital or acquired anomalies of the vestibulocochlear system identified in preoperative imaging (CT or magnetic resonance imaging), or

3

fewer than 12 months of experience with CI were not included in this study. In total, 211 patients met the inclusion criteria and received information about the study, of whom 129 agreed to participate and signed informed consent. The exact reasons not to participate or respond to the invitation were not evaluated for each patient, but most recipients refrained either due to (1) the effort and time involved or (2) the radiation dose of the UHR-CT. None of the 82 participants who did not participate had failed devices nor complicated procedures in which they differed from the study population. Table 1 summarizes the biographic, audiometric, and electrode (position) data and study outcomes of the 129 participants.

Sixty-three males and 66 females with an average age at implantation of 62.6 (SD 12.7; range 27–85) years were included in the study. The highest achieved level of education, ranked according to the Dutch educational system, was recorded for all participants. An educational level of a Bachelor of Science (BSc) or higher was defined as a "high level of education", and had been attained by 23 of the 129 participants. The average duration between the onset of hearing loss and implantation was 26.7 (SD 15.3; range 0–72) years. Due to the lack of audiologic data in the referred patients, the

Independent variables[1]		All (n=129)	Precurved (n=85)	Straight (n=44)	P-value[2]
Biographical factors					
1	Age at implantation (years)	62.6 (13)	62.6 (12)	62.6 (14)	0.995
2	Level of Education (cat.)	18% ≥ BSc	16% ≥ BSc	20% ≥ BSc	0.58
3	Years of Hearing loss (years)	25 (0 – 72)	25 (0 – 72)	25 (6 – 58)	0.26
Audiological factors					
4	Preoperative CVC – phonemescore (%)	9 (0 – 68)	0 (0 – 60)	29 (0 – 68)	<0.001
5	Preoperative PTA3 (dB)	100 (62 – 130)	108 (78 – 130)	88 (62 – 122)	<0.001
6	Postoperative PTA3 (dB)	130 (85 – 130)	130 (102 – 130)	122 (85 – 130)	<0.001
Electrode positional factors					
7	Electrode type (cat.)	66% Precurved			
		34% Straight			
8	Scalar trajectory[a] (cat.)	48% all ST	44% all ST	56% all ST	<0.001
		22% all SV	32% all SV	2% all SV	
		30% Trans.	24% Trans.	42% Trans.	
9	Angle of insertion basal contact[b] (°)	19.4 (16)	25.9 (13)	7.2 (13)	<0.001
10	Angle of insertion apical contact[b] (°)	372.8 (46)	386.2 (47)	347.6 (30)	<0.001
11	Wrapping Factor[b,e]	0.73 (0.59 – 0.92)	0.66 (0.05)	0.85 (0.03)	<0.001
Dependent outcomes		All	Precurved	Straight	P-value
1	CVC50[c] (%)	63 (0 – 92)	65 (23 - 92)	61 (0 – 90)	0.03
2	CVC65 (%)	81 (33 - 100)	83 (45–100)	81 (33-100)	0.12
3	DIN[d] (dB SNR)	-1.3 (-7.2 – 14.3)	-2.5 (-7.2 – 12.7)	0.1 (-6.5 – 14.3)	0.02

Table 1. Descriptive data for all, precurved electrode and straight electrode participant groups. Abbreviations: BSc = Bachelor of Science; Cat. = Categorical CVC = Consonant – Vowel – Consonant; PTA3 = Pure Tone Average (in dB) over frequencies 0.5, 1 and 2 kHz, ST = Scala Tympani, SV = scala vestibuli, Trans. = Translocation, dB = decibels, CVC50 = CVC phoneme score in quiet at 50dB, CVC65 = CVC phoneme score in quiet at 65dB, DIN = Digits – in – Noise test, SNR = Signal – Noise Ratio.

[1] Mean values (with standard deviation in brackets) are presented for normally distributed variables (variable 1, 9 and 10 for all data, and variable 11 for the data on precurved and straight electrode), Median values (with range in brackets) are presented for not normally distributed variables (variables 3, 4, 5 and 6 for all data, and variable 11 for the data on all participants; and for all data on outcomes 1,2 and 3), and proportions of the sample are presented for categorical variables (variables 2, 7 and 8).

[2] Differences in continuous independent variables and dependent outcomes were compared between the precurved and straight electrode groups using t-test (if normally distributed) or Mann –Whitney test (if not normally distributed), and differences in categorical variables were compared using chi-square test.

[a] the quality of 6 UHR-CT scan was too poor (due to movement artifacts) to score variable 8.

[b] the quality of 5 UHR-CT scans was too poor (due to movement artifacts) to score variables 9 - 11.

[c] Outcome measurement of CVC50 was missing in 5 participants.

[d] Outcome measurement of DIN test was missing in 4 participants.

[e]Wrapping Factor was compared only in participants with Scala Tympani (ST) position; 59 participants had a ST position in All group, of which 35 had a precurved electrode and 24 a straight electrode.

duration of SPHL was mostly unknown. As the retrospective recall of start of SPHL is prone to bias, the duration of SPHL was not evaluated. The etiologies of hearing loss were: hereditary–unspecified (25); sudden deafness (8); autosomal dominant non-syndromic hearing loss – i.e., DFNA-9 (13) and DFNA-22 (1); autosomal recessive non syndromic hearing loss – i.e., DFNB-3 (1); trauma (3); Meniere's disease (2); Usher syndrome (4); ototoxic medication (2); maternal rubella (2); mumps infection (1); otosclerosis (5); and unknown (60). The preoperative PTA at 500, 1000, and 2000 Hz (PTA3) and the postoperative PTA3, measured at SVOE, were analyzed. If a participant experienced a vibrotactile sensation at any frequency before the audiometric threshold was found, the threshold of the stimulated frequency was recorded as a missing value. If a participant had no response at the maximum stimulated frequency, the threshold was set to 130 dB. The preoperative speech perception phoneme score of the CI ear, used as the independent variable, was measured using the consonant–vowel–consonant words in quiet test (CVC) at 65 dB SPL in the best aided condition using a hearing aid. Patients that had ceased using a hearing aid in the ear to be implanted were tested with a clinic hearing aid. The contralateral ear was plugged.

Surgery and CI details
All 129 participants were unilaterally implanted by one of the four CI surgeons at the Radboudumc CI center (Nijmegen, the Netherlands). Each surgeon implanted between 24 and 38 participants. In terms of the preoperative PTA3 threshold, 98 participants were implanted in the poorer ear (mean difference between the best ear and the implanted poorer ear was 16.8 dB), five participants showed an exactly symmetric preoperative

hearing loss, and 26 participants were implanted in the best ear (mean difference between the implanted best ear and the poorer ear was 13.9 dB). Implantation in the best ear was considered when there was a risk of vestibular function loss when implanting the poorer ear with significant residual vestibular function, or when the poorer ear was expected to have less hearing opportunities with CI. Sixty-six participants were implanted in the right ear and 63 were implanted in the left ear. All participants were implanted with a CI system from Cochlear Ltd. (Sydney, Australia), of whom 85 participants were implanted with a precurved electrode [the Cochlear Contour advanced (CI512/CI24RE)] and 44 were implanted with a straight electrode [the Cochlear slim straight electrode (CI422/522)]. The choice of electrode was based on the local selection criteria used in the Radboudumc CI center between 2010 and 2016. In general, patients with (functional) residual hearing received a straight electrode and patients without residual hearing received a precurved electrode, based on the assumption that the less traumatic insertion of the straight electrode better preserved the residual hearing. No strict definition or cut-off point was used for (functional) residual hearing, and the choice of electrode type was made by the CI team clinician in consensus with the patient in view of the reported functionality of the ear by the patient, the presence of vestibular function, and the preoperative audiometry. This resulted in two groups of participants based on electrode type, with different median values in the pre-op thresholds and speech perception but with overlapping ranges (Table 1). The precurved electrode was inserted via a cochleostomy approach (n=85), while the straight electrode was inserted using the round window approach (n=35). If the round window membrane could not be clearly identified, the straight electrode had to be inserted via a

cochleostomy approach (n=9). The location for the cochleostomy was anterior and inferior to the round window. In all participants, the standard mastoidectomy and facial recess approach was used to expose the round window. All patients underwent a complete insertion of the electrode array during surgery.

Fitting protocol

After implantation, all participants attended the standard clinical rehabilitation program of the Radboudumc CI center. The CI processor was fitted by experienced CI audiologists, all of whom used the local standard fitting protocol. This protocol is based on the conventional threshold and comfort levels established for each electrode, following the manufacturer's guidance.

The loudness of complex speech-like sounds was assessed by presenting the vowels [ʊː], [ɑː], and [iː], and the consonants [tʃ] and [s], through a loudspeaker. The participants responded by pointing at a seven-item loudness scale from "nothing" to "too loud". Together, these sounds covered the speech spectrum. Each sound was presented nine times without pause and therefore allowed a loudness summation across electrodes and summation over a timespan similar to that of a short sentence. Each sound was spectrally filtered to minimize the spectral overlap between sounds, which ensured that aberrant responses were traceable to specific electrodes and could be adjusted as the clinician deemed fit. Presentation at 75 dB SPL was used to assess the occurrence of discomfort; sounds presented at 65 dB SPL were expected to be of moderate loudness. All participants had the same generation of CI

processor (Nucleus 6; Cochlear Ltd., Sydney, Australia). The default processing strategy was ACE, with a stimulation rate of 900 pps.

Imaging details and electrode-position variables of interest

A UHR-CT (Aquilion Precision; Canon Medical Systems, Otawara, Japan) scan was taken at the time of SVOE to be able to measure the electrode-position variables. The imaging was conducted in one sequential (volume) scan with the following settings: 160 × 0.25 collimation, 120 kVp, 80 mA, and a 1.5-s rotation time. The images were reconstructed with a filtered back projection in bone kernel (FC81) from images with a 0.25-mm slice thickness with 0.125-mm intervals, a 90-mm field of view, and using a 1024 × 1024 matrix. Oblique multi-plane reconstruction (MPR) images were obtained through the cochlea, parallel to the basal turn of the cochlea. For image processing, the images were magnified to 500% and centered on the vestibulocochlear system. The window width and level were adjusted until both cochlear walls and the individual electrode contacts were visualized. The UHR-CT MPRs were used to measure the four electrode-position variables of interest for all participants. The scalar location of all 22 contacts along the electrode array were reviewed in midmodiolar sections. Every contact was scored as either (1) located in the ST, (2) located in the SV or (3) located in an undefined position inside the cochlea. The independent variable scalar trajectory was categorically defined as (1) all contacts in ST, (2) all contacts in SV, or (3) contacts translocated between ST and SV. Examples of electrode contacts with different scalar positions are presented in Figure 1.
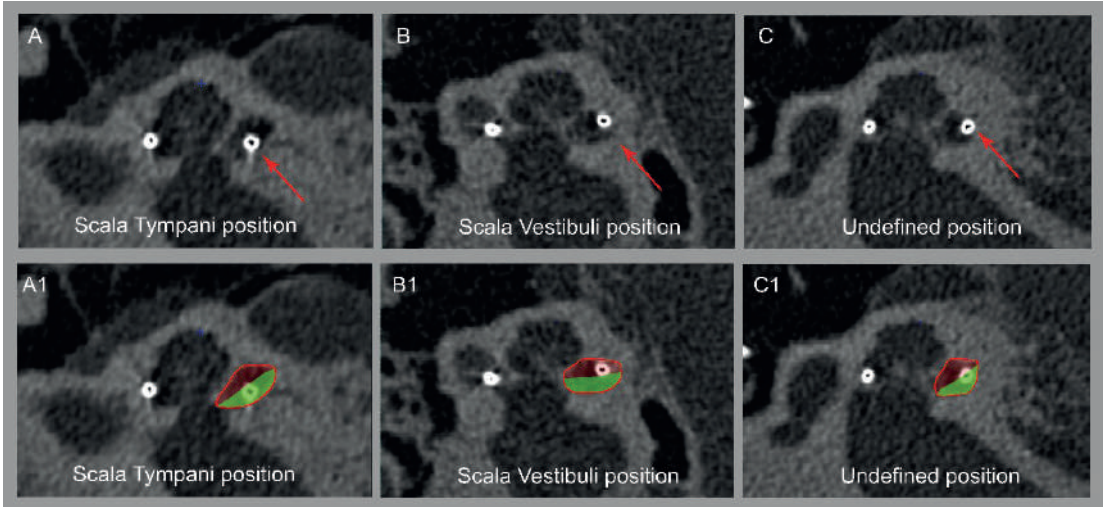
Figure 1. Method for measuring scalar location using mid-modiolar sections of an ultra-high-resolution computed tomography (UHR-CT) scan. Examples of electrode contacts in different scalar positions: In the panels A1, B1, and C1, the scala tympani (ST) is roughly denoted by the green area, and the scala vestibuli (SV) is roughly indicated as the red area. The scala media is not visible. Dependent of the location of the electrode contact, the position was defined as contact in ST position (A and A1), SV position (B and B1), or undefined (C and C1). An undefined position, defined as a contact located between the two scalas, was only found if the electrode translocated from one scala to the other. The independent variable scalar trajectory was categorically defined as (1) all contacts in ST, (2) all contacts in SV, or (3) translocation between ST and SV.

For all 22 contacts along the electrode array, the angular insertion depth was measured. An angular measurement of the insertion depth was made by indicating the center of the round window and the modiolus on a multiplanar reconstruction along the basal turn of the cochlea. Next, a 0° reference line between the modiolus and the middle of the round window, as well as a line between the contact from which the angular insertion

depth has to be measured and the modiolus, are drawn. The angular insertion depth is the angle between these two lines. The method of measurement used to measure the angle of insertion is shown in detail in Figure 2.
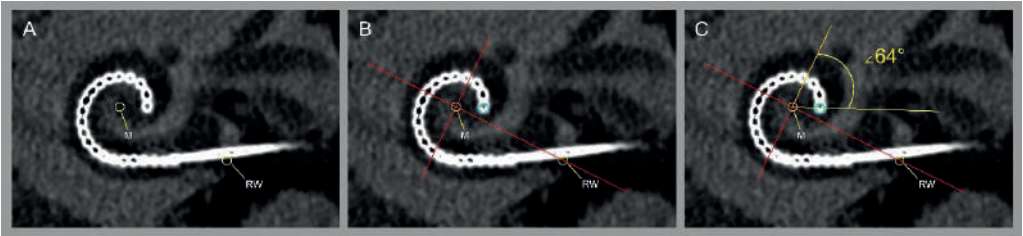

Figure 2. Method for the measurement of the angular insertion depth from a multiplanar reconstruction along the basal turn of the cochlea (A, B, and C) in an ultra-high-resolution computed tomography (UHR-CT) scan. A: An angular measurement of the insertion depth can be made by indicating the center of the round window (RW) and the modiolus (M). B: A 0° reference line was drawn between the modiolus (M) and the middle of the round window (RW), and a perpendicular line was drawn from the modiolus on the 0° reference line is drawn (red cross). The contact for which the angular insertion depth is to be measured is indicated (turquoise circle); in this case this is the most apical contact. C: An angle was drawn (in yellow) from the modiolus over the 270° reference line, and onto the most apical point of the electrode array (turquoise circle). In this example, the angular insertion depth of the most apical electrode contact is 334° (the sum of the three quadrants, equal to 270°, plus the measured yellow angle of 64°). The independent variables of interest were defined as the angle of insertion for the most basal (AOI1) and apical (AOI22) contacts.

The independent variables of interest were defined as the angle of insertion of the most basal (AOI1) and apical (AOI22) contacts (Figure 2).

The last independent electrode-position variable of interest was the wrapping factor, shown in Figure 3. The wrapping factor was defined as the proximity of the electrode array relative to the modiolus, and was

calculated and compared only in participants with a ST-located CI (N=59; [10]. The wrapping factor (WF) is calculated as: $WF = \frac{L\text{Electrode}}{L\text{Lateral Wall}}$ The length of the lateral wall (LLateral Wall) and the length of the electrode (LElectrode) were measured (in millimeters) by first defining the center of the round window and the modiolus. Then, two lines were drawn; one to indicate the onset, a "starting point line" perpendicular to the first contacts on the electrode, and the "end point line", drawn between the modiolus and the contact located at 360° or, if below 360°, the most apical contact. This resulted in a score between 0 and 1, with 0 indicating the closest possible proximity to the modiolus and 1 reflecting the closest possible proximity to the lateral wall of the cochlea.
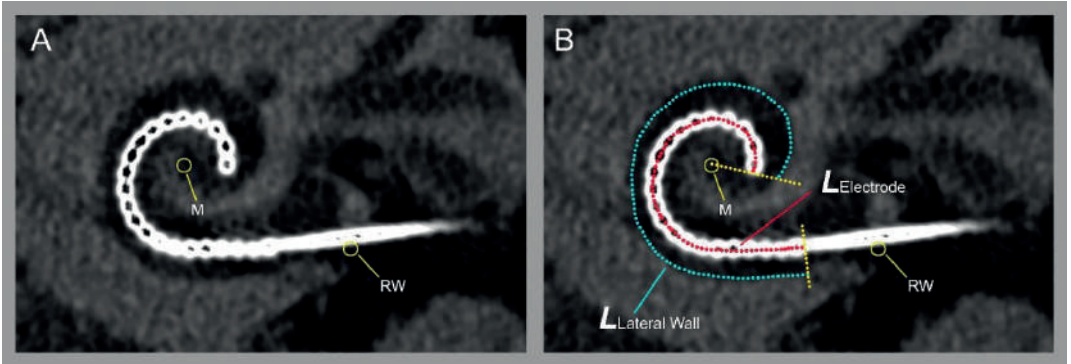
Figure 3: Method for measuring the wrapping factor (WF) on a multiplanar reconstruction along the basal turn of the cochlea (A and B) in an ultra-high-resolution computed tomography (UHR-CT) scan. WF was defined as the proximity of the electrode array relative to the modiolus, and was calculated and compared only in participants with a ST-located CI [10]. WF is calculated as: $WF = \frac{L\text{Electrode}}{L\text{Lateral Wall}}$. The length of the lateral wall (LLateral Wall) and the length of the electrode (LElectrode) were measured (in millimeters) by first defining the center of the round window (RW) and the modiolus (M). Then, two lines were drawn; one to indicate the onset, a "starting point line" perpendicular to the first contacts on the electrode, and the "end point line", drawn between the modiolus (M) and the contact located at 360° or, if below 360°, the most apical contact. This resulted in a score between 0 and 1, with 0 indicating the closest possible proximity to the modiolus and 1 reflecting the closest possible proximity to the lateral wall of the cochlea.

Speech perception outcome measurements

Three speech perception outcome measurements, measured at SVOE, were used as dependent outcome variables: the consonant–vowel–consonant words in quiet test at 50 dB SPL (CVC50) and at 65 dB SPL (CVC65) and the digits-in-noise (DIN) test. The CVC test is the standard speech perception test used by the Dutch Society of Audiology, consisting of phonetically balanced CVC word lists. The CVC test was presented at 50 dB SPL and 65 dB SPL using a loudspeaker 1 m in front of the participant, who was positioned in a quiet soundproof booth, and the average phoneme score of three CVC lists was calculated. The DIN test [24] consists of 24 pairs of three consecutively presented digits (a digit triplet) with background noise. If the digit triplet is repeated correctly, the signal-to-noise ratio (SNR) of the next digit triplet is lowered until the participant makes an error. If a digit triplet is not heard or incorrectly repeated, the SNR of the next digit triplet is increased until the participant hears and repeats it correctly. The score of the DIN test (in dB SNR) represents the 50% speech recognition threshold of the DIN test (dependent outcome DIN). In this study, the DIN was presented in a small soundproof case, developed for CI-audiometric testing, called the OtoCube (Otocube Limited, Geertruidenberg, the Netherlands). Speech perception testing with the Otocube gives similar results to soundbooth testing [25]. Using the Otocube, the CI processor of the participant is connected to the CI coil with an extended wire. The processor is placed inside this soundproof case while the coil remains connected to the CI implant in the participant's head. In the soundproof case, a speaker orientated in front of the processor presents both the background noise and the digit triplets (signal) of the DIN test. A DIN score above a +15 dB SNR is considered unreliable because the adaptive procedure does not work

properly at these levels and, therefore, results above +15 dB do not reflect the ability to recognize speech in noise [26]. In the present study, three participants had a score >15 dB SNR and were therefore not included in the DIN-test analysis. In all conditions, participants were tested using the speech processor program, volume, and sensitivity settings they used in everyday life. If the participant was using a hearing aid in the contralateral ear, this device was removed. In all participants the contralateral ear was plugged before audiometric testing.

Statistical approach

Data were presented for all participants (as is common in the literature), and for groups by electrode type: (1) "precurved group", i.e., the participants with a precurved electrode, and (2) "straight group", i.e., the participants with a straight electrode. Study characteristics were summarized using the mean (SD) for normally distributed variables or the median (range) for non-normally distributed variables. Categorical variables were summarized in percentages.

Differences in continuous independent variables and dependent outcomes were compared between the precurved and straight electrode groups using a t-test (if normally distributed) or a Mann–Whitney test (if non-normally distributed). Differences in categorical variables were compared using a chi-square test. To assess the relationships between continuous independent variables and dependent outcomes, Spearman's correlation coefficient was calculated. A Mann–Whitney U test or Kruskal–Wallis test was used to assess differences in the level of dependent outcomes across the levels of categorical independent variables.

A multivariable linear regression analysis was used to assess the relationship between the independent variable of interest, i.e., electrode type, and the dependent speech perception outcome. A squared outcome transformation was used to normalize the skewed data for the CVC50 and CVC65 outcomes, and a log transformation was used for the DIN test. The model assumptions were assessed by examining the distribution of residuals. For all statistical tests, $p \leq 0.05$ was used as the level of significance.

3

Results

In Table 1, the descriptive data for all participants and both electrode-type groups (precurved and straight) are presented. The biographical factors did not differ between the two electrode-type groups; however, all audiological factors were significantly poorer in the precurved group compared with the straight group (p<0.001). Additionally, all electrode-position factors showed significant differences between the precurved and straight electrode groups (p<0.001). In particular, the ranges of the proximity to the modiolus, i.e., the wrapping factor, observed in both groups barely overlapped. On average, the precurved electrodes were positioned 11.1% deeper inside the cochlea and were 22.4% closer to the modiolus than the straight electrodes. The partial extrusion of one or more of the most basal contacts on the electrode array was seen in 13 participants. In the precurved group, one participant had four electrode contacts outside the cochlea. In the straight group, eight participants had one contact outside the cochlea, three participants had three contacts outside the cochlea, and one participant had four contacts outside the cochlea. These partial extrusions did not cause a statistically significant difference in the speech perception of the affected participants relative to those without an extrusion. With respect to the scalar position, 56% of the straight electrodes and 44% of the precurved electrodes were positioned in the ST. A complete SV position was found more often for the precurved electrode (32%) compared with the straight electrode (2%; one participant, whose straight electrode was, like all precurved electrodes, inserted through a cochleostomy approach). Translocation between the ST and SV along the trajectory of the electrode array occurred in 24% of the participants with a precurved electrode and in 42% of the participants with a straight electrode.

Speech perception was higher in the precurved electrode group than in the straight electrode group. The median CVC50 phoneme score for all participants was 63% (0–92%); however, the scores were significantly different (p=0.03) for the precurved and straight groups [65% (23–92%) and 61% (0–90%), respectively]. The median CVC65 phoneme score was 83% (45–100%) in the precurved group and 81% (33–100%) in the straight electrode group (p=0.12). The median DIN score was –2.5 dB SNR (–7.2 – 12.7 dB SNR) in the precurved electrode group and 0.1 dB SNR (–6.5 – 14.3 dB SNR) in the straight electrode group (p=0.02). All three outcome measures, CVC50, CVC65, and DIN, significantly correlated with each other (p≤0.003); scatter plots and Pearson's correlations between the three outcome measures are presented in Supplemental Digital Content A. Overall, the results of the CVC50, CVC65 (Supplemental Digital Content B; Table B1), and DIN tests (Supplemental Digital Content B; Table B2) showed the same trends in the influence of independent variables on speech perception; however, the results were most distinct in the CVC50 outcome.

In Table 2, univariate Spearman correlations between the CVC50 outcome and the 10 independent factors are reported (see Table 1 for the differences between electrode type). Besides the factor "electrode type", the age at implantation, preoperative PTA3, and the angle of insertion of the basal and apical electrode contacts were significantly correlated with the CVC50 phoneme score for the group containing all participants. In the precurved group, however, none of the independent factors showed a significant correlation with CVC50. In the straight group, only the age at implantation was significantly correlated with CVC50 (Spearman ρ = –0.4; p=0.01). The correlation coefficient of the preoperative CVC phoneme score for the straight group was higher than

3

that of the group comprising all participants (Table 2). While a higher incidence of translocations was observed in the straight electrode group than in the precurved electrode group (respectively 42% and 24%), a correlation between the scalar location and the CVC50 outcome was not seen (Table 2).

		Spearman ρ (p-value)			
	Continuous variables	All		Precurved	Straight
1	Age at implantation[a]	**-0.21 (0.02)**		-0.12 (0.28)	**-0.40 (0.01)**
3	Years of Hearing loss[a]	0.06 (0.53)		0.06 (0.61)	0.04 (0.81)
4	Preoperative CVC – phonemescore[a]	0.01 (0.94)		0.07 (0.55)	0.21 (0.18)
5	Preoperative PTA3[a]	**0.20 (0.04)**		0.14 (0.21)	-0.05 (0.74)
6	Postoperative PTA3[a]	0.07 (0.46)		0.003 (0.98)	-0.04 (0.79)
9	Angle of insertion basal contact[b]	**0.22 (0.02)**		0.04 (0.74)	-0.003 (0.98)
10	Angle of insertion apical contact[b]	**0.23 (0.01)**		0.05 (0.67)	0.16 (0.33)
11	Wrapping factor[d]	-0.21 (0.11)		0.20 (0.24)	0.003 (0.99)
	Categorical variables	P- value of Mann – Whitney / Krusskall – Wallis test[e]			
2	Level of Education (cat.)[a]	0.53		0.98	0.26
8	Scalar trajectory (cat.)[c]	0.90		0.61	0.35

Table 2. Univariate correlations for independent variables of interest with CVC50 in all, precurved electrode and straight electrode participant groups. Abbreviations: BSc = Bachelor of Science; CVC = Consonent – Vowel – Consonant; PTA3 = Pure Tone Average (in dB) over frequencies 0.5, 1 and 2 kHz.
[a] 124 participants had complete measurements of both CVC50 and variables 1 – 6 of which 82 participants had a precurved electrode and 42 participants had a straight electrode.
[b] 121 participants had complete measurements of both CVC50 and variables 9, 10 and 11 of which 81 had a precurved electrode and 41 participants had a straight electrode.
[c] 120 participants had complete measurements of both CVC50 and variable 8 of which 79 had a precurved electrode and 41 participants had a straight electrode.
[d] 57 participants had complete measurements of both CVC55 and variable 11, and had a Scala Tympani position, of which 35 had a precurved electrode and 22 had a straight electrode.
[e] Mann – Whitney test was performed for variable 2, Krusskall – Wallis test was performed for variable 8.

A multivariable linear regression model was conducted to investigate the extent to which the favorable CVC50 speech perception outcome in the precurved group was independent of the influence of biographic variables, audiometric variables, and scalar electrode location.

	Independent variable	Coefficient	95% Conf. Interval		p-value
1	Age at implantation	-0.30	-0.67	0.07	0.11
2	Level of education (cat.)				
	< BSc	Ref.			
	≥ BSc	0.15	-10.04	10.28	0.98
3	Years of Hearing loss	-0.01	-0.30	0.28	0.93
4	Preoperative CVC – phonemescore[a]	0.14	-0.16	0.44	0.35
5	Preoperative PTA3	0.17	-0.20	0.54	0.37
6	Postoperative PTA3	-0.19	-0.65	0.26	0.40
7	Electrode type				
	Precurved	Ref.			
	Straight	-11.79	-20.42	-1.39	0.03
8	Scalar trajectory (cat.)				
	All scala tympani	Ref.			
	All scala vestibuli	-1.00	-11.26	9.66	0.87
	Translocation	-0.53	-9.70	8.84	0.92

Table 3. Multivariate linear regression on dependent outcome CVC50 in all participants with complete measurements (n=120). Abbreviations: BSc = Bachelor of Science; CVC = Consonent – Vowel – Consonant; PTA3 = Pure Tone Average (in dB)

3

The model presented in Table 3 shows that the CVC50 phoneme score is 11.8 percentage points (95%CI: 1.4–20.4%; p=0.03) higher with a precurved electrode than with a straight electrode, independent of the influence of age at implantation, level of education, years of hearing loss, preoperative CVC phoneme score, preoperative PTA3, postoperative PTA3, and scalar trajectory. This trend of an independent higher speech perception outcome for the precurved electrode was similar for the CVC65 (Supplemental Digital Content B; Table B1) and DIN tests (Supplemental Digital Content B; Table B2). The proportion of variance explained by the multivariable model on CVC50 (Table 3) was 11%, and the degrees of freedom were 9, 110, and 119, respectively, for the model, the residual, and the total. Nine participants with missing data were excluded from the model; four were excluded due to the inability to score the scalar location from poor-quality CT scans resulting from movement artifacts, three were excluded due to missing CVC50 outcome measurements, and two were excluded for both reasons. The multivariable linear regression model in

Table 3 did not show apparent violation of the assumption regarding the distribution of residuals (Supplemental Digital Content C: Figure C1).

Sensitivity analysis of the multivariable model

In the present study, speech perception was measured after at least 12 months to ensure that participants were in a phase of stable speech perception. The average time from CI implantation to the SVOE ranged from 14 to 92 (mean 45.5; SD 20.7) months. The correlation between the time from CI to the SVOE and the outcomes was evaluated (Supplemental Digital Content A; Figure A1). The time between the CI and the SVOE showed a weak correlation with CVC50 (r=0.19; p=0.04); however, there was no correlation with CVC65 (r=0.06; p=0.5) or DIN (r=–0.09; p=0.3). The correlation between the time from CI to the SVOE and the CVC50 was insignificant if participants with a CI more recently than 18 months previously were excluded. As a sensitivity analysis, a multivariable linear regression model was conducted on the CVC50, excluding the participants for whom the time from CI to SVOE was less than 18 months (Supplemental Digital Content C; Table C1). Like the original model, this model showed the same significant influence of electrode type on CVC50 independent of the other variables of interest (Table 3). This confirmed that the time from CI to SVOE was not a significant factor in the present study.

Discussion

The primary objective of this study was to identify the biographic, audiologic, and electrode-position factors that influence the speech perception performance in adult CI recipients implanted with devices from a single manufacturer. The secondary objective was to investigate the independent association of the type of electrode with speech perception.

We found that participants implanted with a precurved electrode and who had poor preoperative hearing thresholds performed better with their CI on all speech perception outcomes than those participants implanted with a straight electrode and with relatively better preoperative hearing thresholds (Table 1). The average absolute CVC50 score was 4 percentage points higher in the group with the precurved electrodes than for those implanted with the straight electrodes (p=0.03). For speech perception in a noisy background, evaluated using the DIN test, the absolute difference was –2.6 dB SNR in favor of the precurved electrode (p=0.02). This is an important result, as hearing in noisy situations is challenging for CI users; for example, a 1-dB improvement in SNR was shown to correspond to a 10 percentage point improvement in speech understanding in quiet conditions [27, 28].

After correction for the influence of biographic, audiometric, and scalar position factors, the independent positive effect of the precurved electrode on the CVC50 outcome was found to be 11.8% (95%CI: 1.4–20.4%; p=0.03), as determined using a multivariate model. This effect size is almost three times higher than the 4% absolute difference in CVC50 outcome between the two electrode groups (Table 1), indicating that the pre-implantation factors (in particular, the audiometric factors) probably obscured the real added value of using a precurved electrode over a

3

straight electrode. Similar to the CVC50 outcome, the effect size for the electrode type in the multivariable model was greater than the absolute differences between the two electrode type groups in terms of the DIN outcome and the CVC65 outcome (Supplemental Digital Content B; Tables B2 and B1, respectively).

In our clinic, the choice of electrode type depends on several factors, including audiometric parameters. As a result, the electrode type is a mediating factor in the known relationship between lower preoperative audiometric factors and an increased speech perception [4-6, 8]. As shown in Table 2, the univariate correlations in all patients indicate that audiometric variables have a significant positive relationship with speech perception, suggesting that poorer preoperative hearing results in better postoperative CI speech perception. This correlation is misleading however, since this effect was caused by the fact that participants with limited or no residual hearing were implanted with the better-performing precurved electrode. Moreover, in the Spearman correlations, after stratification by electrode type, no correlations were found for the audiometric factors (Table 2), despite the variation in preoperative hearing within the electrode groups. The explanation for not finding a correlation between audiometric factors and speech perception in the stratified analysis could be that, in the precurved electrode group, the pre-implantation residual hearing might have been too poor to positively affect the postoperative speech perception (Table 1 shows a median preoperative PTA3 of 108). In the straight electrode group, there was a positive trend (the correlation coefficient of the preoperative CVC phoneme score with the CVC50 outcome was higher than for the group containing all participants; Table 2);

however, the number of participants might have been too low to detect a statistical significance (n=44).

The positive effect of the precurved electrode is likely to be related to the different intracochlear electrode position compared with the straight electrode. The precurved electrode is positioned significantly deeper inside the cochlea and significantly closer to the modiolus (Table 1). While it is valuable to determine the independent influence of these two factors (insertion depth and wrapping factor) on speech perception, these factors are inseparable from the electrode type and each other. The electrode type (which has either a straight or modiolus-hugging design) determines the wrapping factor and, to a lesser degree, the depth of insertion (an electrode of the same length with a close modiolus position is deeper than a with a lateral wall position). The correlation between the wrapping factor, position of the most apical electrode, and electrode type is demonstrated in a scatter plot in Figure 4. Whether the wrapping factor or the insertion depth is the main factor for improved speech perception using the precurved electrode cannot be statistically inferred from this study.

Theoretically, however, better speech perception due to a greater angular insertion depth may be the result of a larger coverage of the cochlear spiral ganglion cells by the electrode or by an improved frequency match between electric stimulation and natural frequency tonotopy [15, 29, 30]. In this study, the absolute difference between the average angular insertion depth of the most apical electrode contact (AIO22) between the two electrode types was only 40° (Table 1). In theory, if only the angular insertion depth influenced speech perception, this 40° would have to
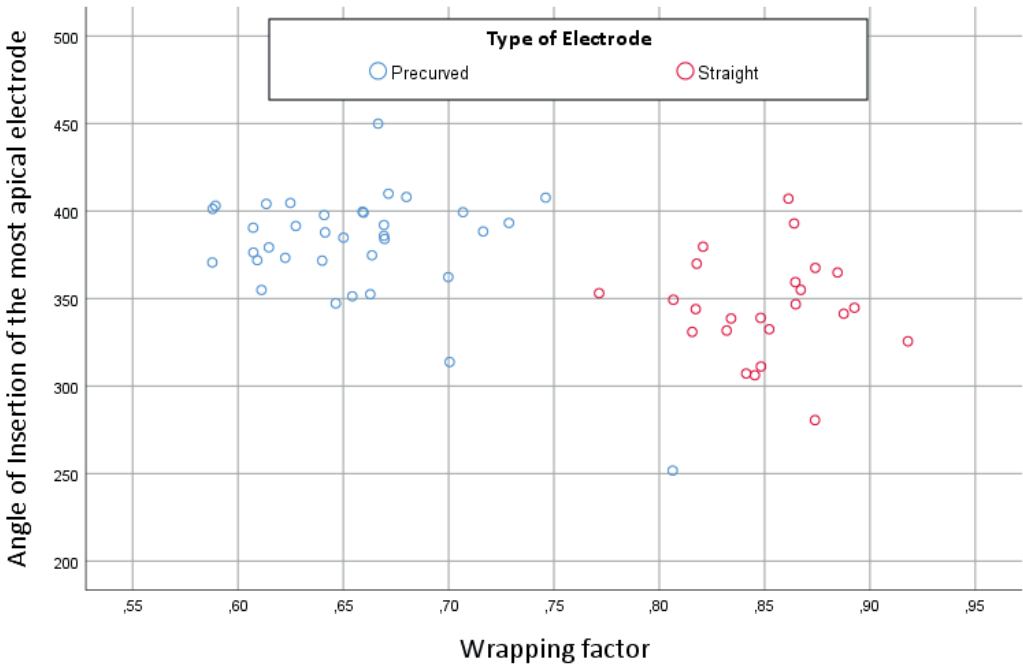
3

Figure 4. A scatter plot between the wrapping factor and the angle of insertion of the most apical electrode contact (AOI22), in which individual cases are marked by type of electrode, indicating the influence of electrode type on the electrode position.

explain the 11.8% higher speech perception scores. The ranges of the AIO22 within the electrode type is 264° and 144°, respectively, for the precurved and straight electrodes. Considering that in the stratified univariable analysis within these electrode types, no correlations were found between the AOI22 and speech perception (Table 2), suggests that deeper insertion does not explain the higher speech perception scores in the recipients of the precurved electrodes. This is consistent with the results of a number of other studies evaluating the influence of angular insertion depth on speech perception outcome [10, 14, 16].

The theory that a small wrapping factor positively influences speech perception is based on the improved electrophysiological properties that a small electrode-to-modiolus distance provides. A perimodiolar position has been shown to lead to lower stimulation thresholds, the reduced spread of excitation, and, therefore, to the stimulation of a more specific region of spiral ganglion cells [19, 31-35]. It is likely that these electrophysiological properties are the explanatory factors underpinning the significantly better performance of the precurved electrodes in this study. Moreover, other studies [10, 17-19] also demonstrated a positive influence on speech perception when the electrode array was in close proximity to the modiolus.

A number of other studies [11, 36-41] compared speech perception in precurved and straight electrodes; however, the results of these studies are somewhat divisive. [41] found that children who were bilaterally implanted with a precurved and a straight electrode had significantly better speech perception in the ear with the precurved electrode. Four studies in adults reported significantly higher speech perception for the precurved electrodes [19, 36, 39, 42], whereas four other adult studies found no difference between electron types [11, 37, 38, 43]. One study reported better speech perception scores for straight electrodes [40]. The reason for the variation between these studies is unknown; however, observational studies investigating cochlear implantation are prone to different forms of bias, potentially causing these differences in findings. The physiological process of converting sound to electricity and stimulating the auditory nerve into comprehensive speech perception is complex, and many patient-specific factors can influence long-term speech perception. Moreover, every CI implant center has specific clinical procedures, leading to

3

differences in the indication of participants, in choices for CI systems and electrode types, and in surgical techniques. As shown in this study, these clinical choices and differences can cause selection (present study) or information and confounding bias, which is not accounted for in a univariable analysis. Therefore, the clinical differences in combination with the observational design of most CI studies most likely explain the variation between findings in the current CI literature.

One example of a strong confounding factor, which has been addressed in the present study, is the influence of the type of electrode and its correlation with factors related to it, such as electrode insertion and placement. Since CI surgeons strive for structure and therefore the preservation of residual hearing, the electrode choice is usually based on clinical decision parameters (e.g., audiometric parameters), and thus may influence the results of all recent non-randomized CI research. Moreover, the covariance between electrode type and electrode-position factors in the present paper showed that the electrode type mainly determines the position of the electrode inside the cochlea; thus, the electrode position is only partly influenced by other factors such as the variation in surgical approach and cochlear anatomy [44, 45]. This indicates that the analysis of electrode-position factors in a group of participants with multiple types of electrodes is merely analyzing the differences between the types of electrodes and not the variation in electrode position. Considering this potential influence, one may wonder about the possible bias in studies analyzing multiple CI systems incorporating several CI clinics. Based on these findings, it is important that future non-randomized studies investigating factors affecting CI outcomes should take into account that the electrode type has an effect on the three position factors (angular

insertion depth, scalar location, and wrapping factor) and that the clinician's choice of a specific electrode type is likely to be dependent on the patient's (audiologic) profile. In hindsight, the rationale for implanting participants who retained a certain degree of residual hearing with a straight electrode seemed to be incorrect. In the current study, we observed that 1) the overall results when using the precurved electrode were better than the results with the straight electrode, and 2) adults who received a straight electrode eventually lost, to a great extent, their residual hearing post implantation. The overall preoperative and postoperative residual hearing for the straight electrode were 88 dB and 122 dB, respectively.

Compared with other studies [9-13], we identified a high number of SV locations and translocations. Interestingly, however, the scalar trajectory did not significantly influence the speech perception performance (Tables 2 and 3). It is unclear why we did not observe a negative effect for a SV position or translocation, and future research should explore this.

Beside the electrode position and audiometric factors, the correlation between speech perception and the three included biographic factors (age at implantation, level of education, and years of hearing loss) was evaluated (Table 2). Regarding age at implantation, a univariate analysis suggested that higher speech perception scores would be detected in the younger participants than in the older participants. This was observed for the straight electrode but not the precurved electrode, which might be due to a potentially confounding correlation in which younger adults more commonly had higher pre-implantation speech perception scores in straight electrode implants. Some studies found a positive effect

3

for the age at implantation on speech perception [2, 3, 10, 46], while others found no effect [47, 48].

The reason why no correlation was found between the level of education and speech perception might be that the level of education, as defined in this study, did not reflect the level of cognitive functioning, which was previously shown to influence speech perception in CI [10, 21, 22]. Several studies also reported a negative effect for the duration of deafness [2, 3, 10, 20]; however, we calculated the duration of hearing loss instead of the duration of deafness, and did not find a correlation. Studies investigating the duration of deafness often define it as the time since the start of SPHL, which is an average hearing level higher than 70 dB. In our clinic, however, we found that it often is quite difficult to pinpoint the exact onset of deafness in adults with a late onset of hearing loss. Most adults cannot recall this because their hearing loss happened slowly over time, and there is often a lack of audiometric history in referred patients. In addition, the retrospective recall of start of SPHL is prone to bias; therefore, duration of deafness was not evaluated here. The duration of hearing loss is easier to recall as it is often a more memorable event from the patient's perspective, and is therefore less prone to recall bias. Another potential reason for not finding an effect for the duration of hearing loss is the effect of the time frame in which studies are conducted. Blamey et al. [2, 3] showed that the influences of biographic and audiometric factors decrease over time. Since the indication criteria for adult CI candidates have become less stringent, today most adult CI candidates still have some residual hearing that is rehabilitated with hearing aids.

Strengths and limitations

The present paper is the first single-center study to identify factors that affect speech perception in a large, homogeneous group of patients implanted with a CI device from a single manufacturer, in which the data was stratified according to the type of electrode. The main limitation of this study is that it is observational and thus not randomized. The present study was designed to limit bias arising from the electrode type used, and any potential bias is considered in the statistical analysis and addressed in the discussion; however, not all factors that theoretically might influence speech perception have been measured (e.g., cognition and brain plasticity). Second, the variation of some of the independent factors investigated was limited in the present study (Table 1). Limited variation restricts the extent to which the conclusions can be generalized to patients fitted with different CI brands. The electrodes of some other CI models can extend up to 880° [49], while the maximum angular insertion depth in our study was 498°. An effect of angular insertion depth above our maximum insertion depth cannot be ruled out. Finally, stratifying the analysis by the electrode type results in a reduced number of participants per group. This could have resulted in some of the statistically insignificant univariate correlations (Table 2), particularly in the audiometric analysis in the straight electrode group (n=44).

Conclusion

In this study, cochlear implantation with a precurved electrode resulted in a significantly higher speech perception outcome, independent of biographic factors, audiometric factors, or scalar location. The clinical selection process for choosing the type of electrode can significantly influence correlations

3

between speech perception and the biographic, audiometric, and electrode positional factors. Nevertheless, because the study was limited to two electrode types from one CI manufacturer, we gained insights into the importance of electrode choice.

References

1.   Holden, L.K., et al., *Optimizing the perception of soft speech and speech in noise with the Advanced Bionics cochlear implant system.* Int J Audiol, 2011. **50**(4): p. 255-69.

2.   Blamey, P., et al., *Factors affecting auditory performance of postlinguistically deaf adults using cochlear implants.* Audiol Neurootol, 1996. **1**(5): p. 293-306.

3.   Blamey, P., et al., *Factors affecting auditory performance of postlinguistically deaf adults using cochlear implants: an update with 2251 patients.* Audiol Neurootol, 2013. **18**(1): p. 36-47.

4.   Huinck, W.J., E.A.M. Mylanus, and A.F.M. Snik, *Expanding unilateral cochlear implantation criteria for adults with bilateral acquired severe sensorineural hearing loss.* Eur Arch Otorhinolaryngol, 2019. **276**(5): p. 1313-1320.

5.   Snel-Bongers, J., et al., *Evidence-Based Inclusion Criteria for Cochlear Implantation in Patients With Postlingual Deafness.* Ear Hear, 2018. **39**(5): p. 1008-1014.

6.   Francis, H.W., et al., *Central effects of residual hearing: implications for choice of ear for cochlear implantation.* Laryngoscope, 2004. **114**(10): p. 1747-52.

7.   Friedland, D.R., H.S. Venick, and J.K. Niparko, *Choice of ear for cochlear implantation: the effect of history and residual hearing on predicted postoperative performance.* Otol Neurotol, 2003. **24**(4): p. 582-9.

8.   Gomaa, N.A., et al., *Residual speech perception and cochlear implant performance in postlingually deafened adults.* Ear Hear, 2003. **24**(6): p. 539-44.

9.   Chakravorti, S., et al., *Further Evidence of the Relationship Between Cochlear Implant Electrode Positioning and Hearing Outcomes.* Otol Neurotol, 2019. **40**(5): p. 617-624.

10.   Holden, L.K., et al., *Factors affecting open-set word recognition in adults with cochlear implants.* Ear Hear, 2013. **34**(3): p. 342-60.

11.   O'Connell, B.P., et al., *Electrode Location and Angular Insertion Depth Are Predictors of Audiologic Outcomes in Cochlear Implantation.* Otol Neurotol, 2016. **37**(8): p. 1016-23.

12.   O'Connell, B.P., J.B. Hunter, and G.B. Wanna, *The importance of electrode location in cochlear implantation.* Laryngoscope Investig Otolaryngol, 2016. **1**(6): p. 169-174.

13.   Wanna, G.B., et al., *Impact of electrode design and surgical approach on scalar location and cochlear implant outcomes.* Laryngoscope, 2014. **124 Suppl 6**: p. S1-7.

3

14.   Heutink, F., et al., *Angular Electrode Insertion Depth and Speech Perception in Adults With a Cochlear Implant: A Systematic Review.* Otol Neurotol, 2019.

15.   Skinner, M.W., et al., *CT-derived estimation of cochlear morphology and electrode array position in relation to word recognition in Nucleus-22 recipients.* J Assoc Res Otolaryngol, 2002. **3**(3): p. 332-50.

16.   van der Marel, K.S., et al., *The influence of cochlear implant electrode position on performance.* Audiol Neurootol, 2015. **20**(3): p. 202-11.

17.   Frijns, J.H., J.J. Briaire, and J.J. Grote, *The importance of human cochlear anatomy for the results of modiolus-hugging multichannel cochlear implants.* Otol Neurotol, 2001. **22**(3): p. 340-9.

18.   Holden, L.K., et al., *Factors Affecting Outcomes in Cochlear Implant Recipients Implanted With a Perimodiolar Electrode Array Located in Scala Tympani.* Otol Neurotol, 2016. **37**(10): p. 1662-1668.

19.   van der Beek, F.B., et al., *Clinical evaluation of the Clarion CII HiFocus 1 with and without positioner.* Ear Hear, 2005. **26**(6): p. 577-92.

20.   Lazard, D.S., et al., *Pre-, per- and postoperative factors affecting performance of postlinguistically deaf adults using cochlear implants: a new conceptual model over time.* PLoS One, 2012. **7**(11): p. e48739.

21.   Heydebrand, G., et al., *Cognitive predictors of improvements in adults' spoken word recognition six months after cochlear implant activation.* Audiol Neurootol, 2007. **12**(4): p. 254-64.

22.   Pisoni, D.B., et al., *Verbal Learning and Memory After Cochlear Implantation in Postlingually Deaf Adults: Some New Findings with the CVLT-II.* Ear Hear, 2018. **39**(4): p. 720-745.

23.   Dhanasingh, A. and C. Jolly, *An overview of cochlear implant electrode array designs.* Hear Res, 2017. **356**: p. 93-103.

24.   Smits, C., S. Theo Goverts, and J.M. Festen, *The digits-in-noise test: assessing auditory speech recognition abilities in noise.* J Acoust Soc Am, 2013. **133**(3): p. 1693-706.

25.   De Matos Magalhaes, A.T., et al., *Evaluation and validation of programming the speech processor with otocube (Electroacoustical test box for cochlear implant users) [Abstract].* Int Arch Otorhinolaryngology, 2014. **18; a2464 DOI: 10.1055/s-0034-1389066**.

26.   Kaandorp, M.W., et al., *Assessing speech recognition abilities with digits in noise in cochlear implant and hearing aid users.* Int J Audiol, 2015. **54**(1): p. 48-57.

27.   Litovsky, R., et al., *Simultaneous bilateral cochlear implantation in adults: a multicenter clinical study.* Ear Hear, 2006. **27**(6): p. 714-31.

28.   Soli, S.D. and L.L. Wong, *Assessment of speech intelligibility in noise with the Hearing in Noise Test.* Int J Audiol, 2008. **47**(6): p. 356-61.

29.   Baskent, D. and R.V. Shannon, *Speech recognition under conditions of frequency-place compression and expansion.* J Acoust Soc Am, 2003. **113**(4 Pt 1): p. 2064-76.

30.   Baskent, D. and R.V. Shannon, *Interactions between cochlear implant electrode insertion depth and frequency-place mapping.* J Acoust Soc Am, 2005. **117**(3 Pt 1): p. 1405-16.

31.   Frijns, J.H., et al., *Initial evaluation of the Clarion CII cochlear implant: speech perception and neural response imaging.* Ear Hear, 2002. **23**(3): p. 184-97.

32.   Hughes, M.L. and P.J. Abbas, *Electrophysiologic channel interaction, electrode pitch ranking, and behavioral threshold in straight versus perimodiolar cochlear implant electrode arrays.* J Acoust Soc Am, 2006. **119**(3): p. 1538-47.

33.   Hughes, M.L. and L.J. Stille, *Effect of stimulus and recording parameters on spatial spread of excitation and masking patterns obtained with the electrically evoked compound action potential in cochlear implants.* Ear Hear, 2010. **31**(5): p. 679-92.

34.   Mens, L.H., P.J. Boyle, and J.J. Mulder, *The Clarion Electrode positioner: approximation to the medial wall and current focussing?* Audiol Neurootol, 2003. **8**(3): p. 166-75.

35.   Todt, I., et al., *Electrophysiological effects of electrode pull-back in cochlear implant surgery.* Acta Otolaryngol, 2008. **128**(12): p. 1314-21.

36.   Bacciu, A., et al., *Comparison of speech perception performance between the Nucleus 24 and Nucleus 24 Contour cochlear implant systems.* Acta Otolaryngol, 2004. **124**(10): p. 1155-8.

37.   Doshi, J., et al., *Straight versus modiolar hugging electrodes: does one perform better than the other?* Otol Neurotol, 2015. **36**(2): p. 223-7.

38.   Fitzgerald, M.B., et al., *The effect of perimodiolar placement on speech perception and frequency discrimination by cochlear implant users.* Acta Otolaryngol, 2007. **127**(4): p. 378-83.

3

39.   Gordin, A., et al., *Evolution of cochlear implant arrays result in changes in behavioral and physiological responses in children.* Otol Neurotol, 2009. **30**(7): p. 908-15.

40.   O'Connell, B.P., et al., *Electrode Location and Audiologic Performance After Cochlear Implantation: A Comparative Study Between Nucleus CI422 and CI512 Electrode Arrays.* Otol Neurotol, 2016. **37**(8): p. 1032-5.

41.   Park, L.R., et al., *Audiological Outcomes and Map Characteristics in Children With Perimodiolar and Slim Straight Array Cochlear Implants in Opposite Ears.* Otol Neurotol, 2017. **38**(9): p. e320-e326.

42.   Holder, J.T., et al., *Matched Cohort Comparison Indicates Superiority of Precurved Electrode Arrays.* Otol Neurotol, 2019. **40**(9): p. 1160-1166.

43.   Fabie, J.E., et al., *Evaluation of Outcome Variability Associated With Lateral Wall, Mid-scalar, and Perimodiolar Electrode Arrays When Controlling for Preoperative Patient Characteristics.* Otol Neurotol, 2018. **39**(9): p. 1122-1128.

44.   van der Marel, K.S., et al., *Diversity in cochlear morphology and its influence on cochlear implant electrode position.* Ear Hear, 2014. **35**(1): p. e9-20.

45.   van der Marel, K.S., et al., *Development of Insertion Models Predicting Cochlear Implant Electrode Position.* Ear Hear, 2016. **37**(4): p. 473-82.

46.   Friedland, D.R., et al., *Case-control analysis of cochlear implant performance in elderly patients.* Arch Otolaryngol Head Neck Surg, 2010. **136**(5): p. 432-8.

47.   Budenz, C.L., et al., *The effects of cochlear implantation on speech perception in older adults.* J Am Geriatr Soc, 2011. **59**(3): p. 446-53.

48.   Leung, J., et al., *Predictive models for cochlear implantation in elderly candidates.* Arch Otolaryngol Head Neck Surg, 2005. **131**(12): p. 1049-54.

49.   De Seta, D., et al., *The Role of Electrode Placement in Bilateral Simultaneously Cochlear-Implanted Adult Patients.* Otolaryngol Head Neck Surg, 2016. **155**(3): p. 485-93

Factors Influencing Speech Perception in Adults With a Cochlear Implant.

Supplemental appendix:

1. Supplemental Digital Content A; Figure A1: Scatter plots and Pearson correlation coefficients of CVC55, CVC70, DIN and Time from CI to Study Variables and Outcome Evaluation (SVOE).

2. Supplemental Digital Content B; Supplemental Digital Content Table 1: Multivariate linear regression on outcome CVC65.

3. Supplemental Digital Content B; Supplemental Digital Content Table 2: Multivariate linear regression on outcome DIN.

4. Supplemental Digital Content C; Figure C1: Distribution of residuals of multivariable linear regression model (Original Paper; Table 3)

5. Supplemental Digital Content C; Table C1: Multivariate linear regression on dependent outcome CVC50 in participants with time from CI to SVOE ≥ 18 months (n=111).

3

1. Supplemental Digital Content A; Figure A1: Scatter plots and Pearson correlation coefficients of CVC55, CVC70, DIN and Time from CI to Study Variables and Outcome Evaluation (SVOE)
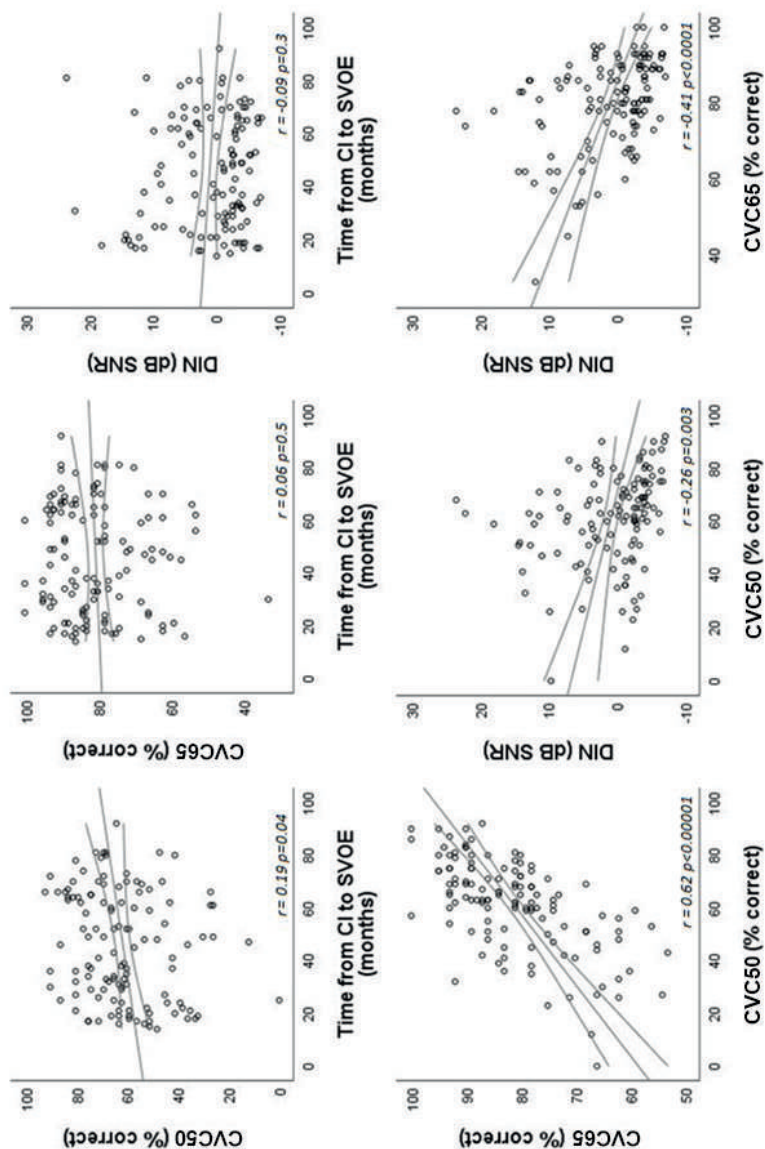
Supplemental Digital Content B.

Supplemental Digital Content Table 1:
Multivariate linear regression of possible electrode selection variables and type of electrode on outcome CVC65 in all participants with complete measurements (n=123). Participants with missing data were excluded from the model (n=6); all six were excluded due to inability to score scalar location due to poor quality CT-scan due to movement artifacts. The proportion of variance explained by the model in the Supplemental Digital Content Table 1 was 9%, the degrees of freedom were 9, 113 and 122, respectively for the model, the residual and the total.

	Independent variable	Coefficient	95% Conf. Interval		p-value
1	Age at implantation	-0,15	-0,48	0,19	0,39
2	Level of education (cat.)				
	< BSc	Ref.			
	≥ BSc	0,87	-8,79	10,21	0,87
3	Years of Hearing loss	0,02	-0,24	0,29	0,88
4	Preoperative CVC – phonemescore[a]	0,19	-0,09	0,46	0,18
5	Preoperative PTA3	0,24	-0,10	0,58	0,16
6	Postoperative PTA3	-0,11	-0,10	0,58	0,60
7	Electrode type				
	Precurved	Ref.			
	Straight	-8,30	-16,80	1,97	0,11
8	Scalar trajectory (cat.)				
	All scala tympani	Ref.			
	All scala vestibuli	-3,75	-12,72	6,38	0,47
	Translocation	0,98	-7,75	9,39	0,84

Supplemental Digital Content Table 2:

Multivariate linear regression of possible electrode selection variables and type of electrode on outcome DIN in all participants with complete measurements (n=117). Participants with missing data were excluded from the model (n=12); five were excluded due to inability to score scalar location due to poor quality CT-scan due to movement artifacts, three were excluded due to missing CVC50 outcome measurement, one was excluded for both these reasons, and three were excluded due to a DIN score above 15 SNR. The proportion of variance explained by the model in table 3 was 11%, the degrees of freedom were 9, 107 and 116, respectively for the model, the residual and the total.

	Independent variable	Coefficient	95% Conf. Interval		p-value
1	Age at implantation	0,04	-0,13	0,22	0,64
2	Level of education (cat.)				
	< BSc	Ref.			
	≥ BSc	-2,43	-6,64	2,97	0,34
3	Years of Hearing loss	0,04	-0,10	0,17	0,59
4	Preoperative CVC – phonemescore[a]	-0,01	-0,15	0,13	0,89
5	Preoperative PTA3	-0,05	-0,23	0,13	0,58
6	Postoperative PTA3	-0,01	-0,22	0,21	0,96
7	Electrode type				
	Precurved	Ref.			
	Straight	5,39	-0,88	13,56	0,10
8	Scalar trajectory (cat.)				
	All scala tympani	Ref.			
	All scala vestibuli	3,47	-2,29	10,94	0,26
	Translocation	4,80	-0,52	11,45	0,08

Supplemental Digital Content C.

Figure C1.
Figure indicating distribution of residuals of multivariable linear regression model (Original Paper; Table 3). On the X-axis the fitted values of the multivariable model (or predicted values) are plotted, and on the Y-axis the residual values; indicating the difference between the predicted values and the found values in our study, are plotted.
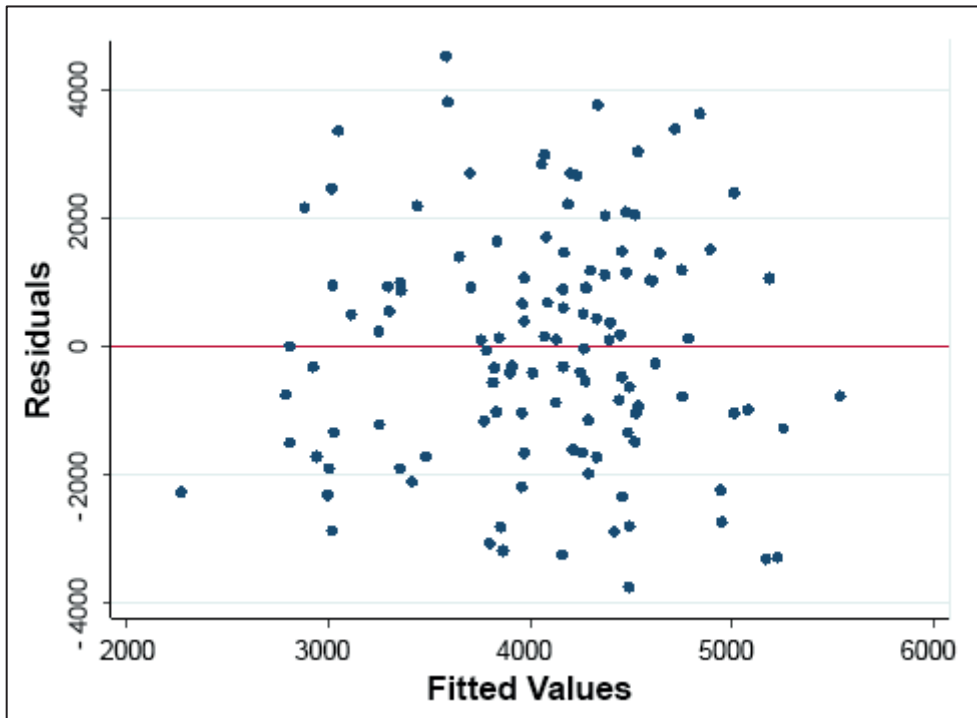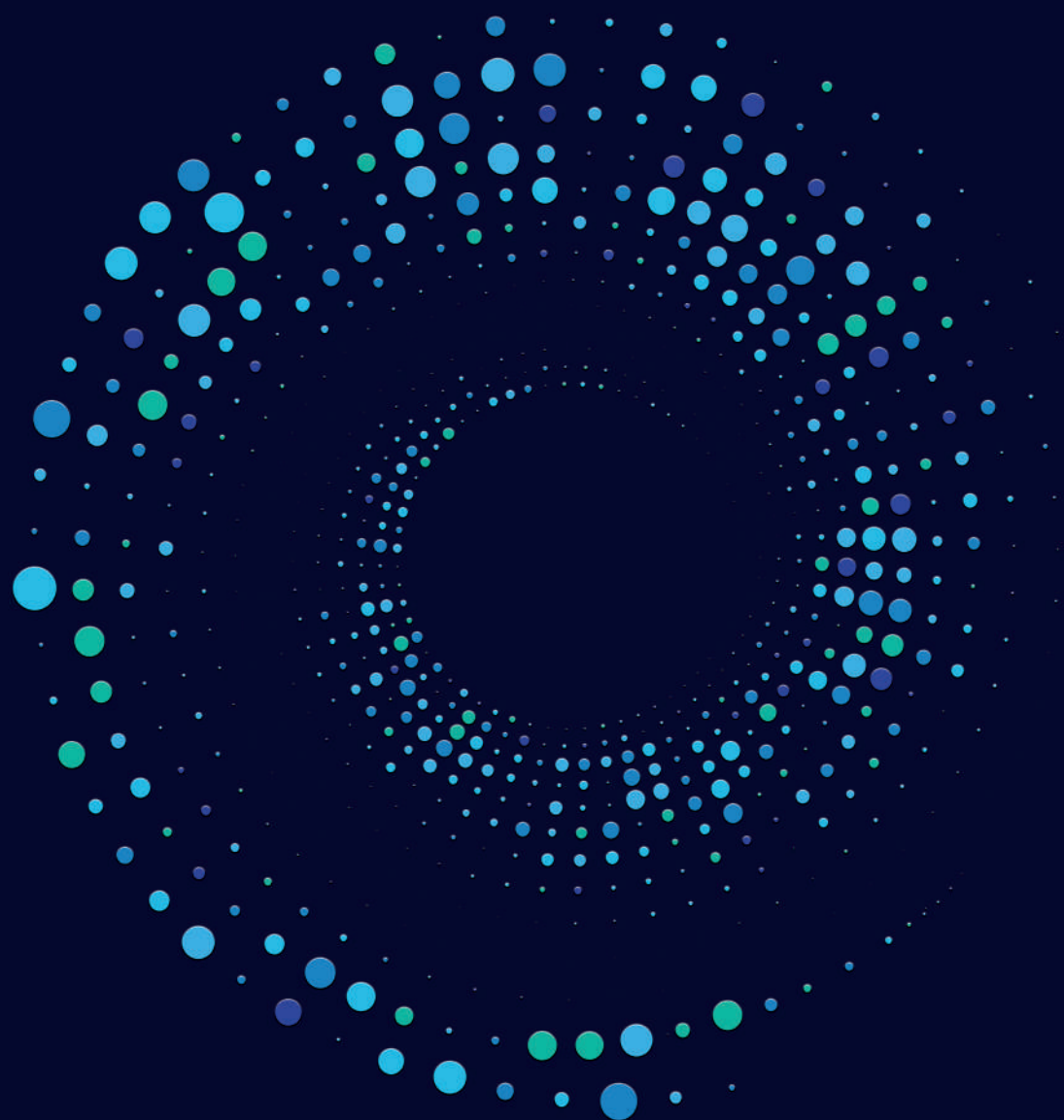
Table C1.
Multivariate linear regression on dependent outcome CVC50 in participants
with time from CI to SVOE ≥ 18 months (n=111).

	Independent variable	Coefficient	95% Conf. Interval		p-value
1	Age at implantation	-0,33	-0,72	0,06	0,09
2	Level of education (cat.)				
	< BSc	Ref.			
	≥ BSc	-2,67	-13,24	8,91	0,67
3	Years of Hearing loss	-0,05	-0,38	0,28	0,77
4	Preoperative CVC – phonemescore[a]	0,15	-0,16	0,46	0,35
5	Preoperative PTA3	0,19	-0,22	0,59	0,37
6	Postoperative PTA3	-0,23	-0,70	0,25	0,35
7	Electrode type				
	Precurved	Ref.			
	Straight	-12,83	-21,90	-1,84	0,03
8	Scalar trajectory (cat.)				
	All scala tympani	Ref.			
	All scala vestibuli	-2,70	-13,13	8,75	0,66
	Translocation	-2,94	-1,50	7,28	0,58

3

4

The evaluation of a slim perimodiolar electrode: surgical technique in relation to intracochlear position and cochlear implant outcomes.

Floris Heutink, Berit M. Verbist, Lucas H.M. Mens,
Wendy J. Huinck, Emmanuel A.M. Mylanus

Abstract

Purpose: In cochlear implantation, the two factors that are determined by the surgeon with a potential significant impact on the position of the electrode within the cochlea and the potential outcome, are the surgical technique and electrode type. The objective of this prospective study was to evaluate the position of the slim, perimodiolar electrode (SPE), and to study the influence of the SPE position on CI outcome.

Methods: Twenty-three consecutively implanted, adult SPE candidates were included in this prospective cohort study conducted between December 2016 and April 2019. Mean age at surgery was 59.5 years. Mean preoperative residual hearing was 92.2dB. Intra-operative fluoroscopy and high-resolution CT-scans were performed to evaluate electrode position after insertion using a cochleostomy approach. Follow-up was 12-months after implantation; residual hearing (6-8 weeks) and speech perception (6-8 weeks and 12 months) were evaluated in relation to the intracochlear SPE position.

Results: In most patients in whom the SPE was positioned in the **s**cala tympani residual hearing was preserved (mean absolute increase in PTA of 4.4dB and 77.2% relative hearing preservation (RHP%)). Translocation into the scala vestibuli occurred in 36% of the insertions, resulting in a mean absolute increase in PTA of 17.9dB, and a RHP% of 19.2%. Participants with a translocation had poorer speech perception scores at 12 months follow-up.

Conclusion: Given the incidence of cochleostomy associated translocations with the SPE and the negative effect on outcome, it is advised to insert the SPE using the (extended) round window approach.

INTRODUCTION

Rationale

The Cochlear Implant (CI) electrode array is the fundamental component of
the CI system, as it provides the interface to the auditory system of the
patient. Current CI electrodes are designed as either "precurved" or
"straight". Precurved electrodes are designed to curl around the medial
wall and to assume a midscalar or perimodiolar position close to the
modiolus, while straight electrodes assume a more lateral position,
following the lateral wall of the cochlea [1]. Several studies have shown that
perimodiolar electrodes, compared to lateral wall electrodes, lead to lower
stimulation thresholds and reduced spread of excitation; stimulating a more
specific, tonotopic region of spiral ganglion cells [2-7]. On the other hand,
conventional perimodiolar electrodes translocate to the scala vestibuli (SV)
at a higher rate compared to lateral wall electrodes [1, 8, 9]. These
translocations are shown to be traumatic and are associated with loss of
residual hearing and poorer speech perception [8, 10, 11].

To reduce intracochlear trauma during insertion, the slim
perimodiolar electrode (SPE) was introduced in 2016. This electrode is 60%
thinner and more flexible than the previous generation perimodiolar
electrode produced by the same manufacturer [12]. The SPE has been
developed for hypo-traumatic insertion and preservation of residual
hearing. The surgical approach to the cochlea for the SPE is described as
feasible using three surgical approaches to the cochlea: round window
(RW), extended round window (eRW) or cochleostomy (CS) [13]. However,
in previous generation electrodes the approach to the cochlea has been
shown to influence electrode position and audiologic outcomes. It was

4

observed that independent of the type of electrode used, full scala tympani (ST) position [8] and preservation of residual hearing [8, 10] is more likely using a RW or eRW approach, compared to the CS approach. These findings might contribute to the fact that to-date, eRW and RW approaches were used in 91.8% (236 / 257) of the participants in the five studies that investigated the SPE [11, 12, 14-16].

The scalar position of the SPE, visualized in high-resolution imaging, was evaluated in 96 out of these 257 participants [11, 12, 15, 16]. Out of these participants, 81 were implanted using the RW or eRW approach [11, 12, 15, 16]; in six participants a translocation had occurred [15]. In the remaining, relatively low number of 15 patients in whom the CS approach was used, no translocation was observed [12}. There is a need for more studies investigating the SPE, specifically that study correlations between the surgical approach and the electrodes' position in the cochlea.

This paper reports on a prospective study with the SPE implanted using the cochleostomy approach in 23 participants. In a previous temporal bone study [17], as well as in clinical papers [12, 15], it was observed that there is a potential risk of tip fold-over when implanting the SPE. The primary objective of this prospective study was to evaluate the position of the SPE after a cochleostomy approach, to detect translocations and tip fold-overs. A rotational flat, cone-beam Computed Tomography (CT)-scan was used for the intra-operative fluoroscopy and CT-scan images. The secondary objective of this study was to investigate preservation of residual hearing in relation to the position of the SPE.

METHODS

Study design and population

In this prospective study, 23 consecutive patients were implanted with the slim, perimodiolar electrode (SPE; Nucleus CI532; Cochlear Ltd, Sydney, Australia) between December 2016 and February 2018. All included patients were indicated for cochlear implantation, based on the Dutch CI indication criteria. As a part of the CI indication procedure, existing hearing aid fitting was optimized, including fitting new hearings aids if deemed necessary. A CI was indicated if results in terms of aided speech performance with hearing aids is insufficient. Patients with functional residual hearing were informed about the study and invited to participate. Both patients with early and late onset of hearing loss were included in this study. Early onset of hearing loss was defined as an onset of hearing loss within the first five years of life. Patients with an early onset of deafness – i.e. prelingual onset of deafness, were excluded from this study.

Demographic data, history of hearing and pre-operative audiologic measurements were collected pre-operatively. All surgeries were performed in a hybrid operating theater equipped with a high-resolution, rotational cone beam CT scan (MITeC, Radboudumc, Nijmegen, the Netherlands). Intra-operative fluoroscopy and high-resolution rotational CT-scans were performed after insertion. Post-operative residual hearing thresholds were measured at two-months follow-up and speech perception, with electric stimulation only, was measured at two- and 12-months follow-up. Approval was obtained from the Institutional Medical Research Ethics Committee (NL57456.091.16) and participants signed informed consent before participating.

4

Electrode and procedure details

The SPE is precurved with an active length of 14mm and a diameter of 0.35mm x 0.4mm at the tip, and 0.45mm x 0.5 mm at the base. It is designed to provide full ST position with all common surgical approaches, including round window, extended round window, or cochleostomy [13]. The SPE is loaded in an external, flexible silicon sheath, shaped as a tube, with a length of 5mm, and then inserted together with the sheath inside the cochlea using two forceps, until the sheath stopper reaches the cochleostomy or round window opening. After insertion of the sheath, the electrode array is further inserted through the sheath at slow speed until full insertion (standardized insertion time ≥120 seconds). After full insertion, the sheath is retracted and removed. Surgery was performed by one surgeon (EM), using the standard mastoidectomy and facial recess approach. As our clinic had been selected by the manufacturer as one of the "early users group", it was mandatory to undergo training with the SPE. In this training, the approach was an anterior - inferior positioned cochleostomy of which the diameter is checked with a silicone seizer tool which is included in the sterile blister package. All participants received a single dose of 1.8mg/kg intravenous methylprednisolone during surgery. After full insertion of the electrode, the cochleostomy site was sealed with fragments of periosteum and fibrin glue.

Electrode position evaluation

The Artis Zeego system (Siemens Healthcare, Forchheim, Germany), a multi-axis system for interventional imaging with a flat-panel detector, was used for intra-operative 3D imaging. Immediately after insertion, the surgeon used fluoroscopy imaging to rule out the presence of a tip fold-over. Post-

operatively, the position of the SPE was evaluated on the CT images by an experienced Head- and Neck Radiologist (BV). For each of the 22 electrode contacts the location was determined as either an ST or SV position.

Audiologic assessment

Pre- and post-operative (two-months) unaided pure-tone thresholds at 125 Hz, 250 Hz, 500 Hz, 1000 Hz and 2000 Hz were measured both of the CI ear and the contralateral (CL) ear using a headphone in a soundproof room according to standard audiometric procedures. If the air-conduction threshold of the CI ear was 45dB or higher - i.e. worse (Table 1), audiometric masking of the CL ear was performed using the standard plateau method according to J.D. Hood [18]. If a participant did not respond to an auditory stimulus, the threshold for that specific frequency was set at the maximum stimulation level (MSL). The MSL for the collected frequencies were 90dB, 105dB, 110dB, 120dB and 120dB, respectively. This was in accordance with the consensus paper by Skarzynski et al. [19] on reporting on Hearing Preservation (HP). The Absolute Pure Tone Average of Low frequencies (PTALow) was defined as the average threshold over frequencies: 250 Hz, 500 Hz and 1000 Hz. If a participant did not respond to two or more frequencies used for the calculation of PTALow, the PTALow was defined as Non Measurable Hearing (NMH). Fourteen patients were implanted in the poorer hearing ear, one had equal hearing thresholds in both ears and eight were implanted in the best hearing ear. Three patients who were implanted in the better hearing ear had limited difference in thresholds between the ears pre-implantation and symmetric vestibular function. These patients chose their ear to be implanted. One patient received his implant in the (slightly) better hearing ear because of good

vestibular function in the worst ear and lack of vestibular function in the implanted ear. In the four patients that were implanted in the better hearing ear, the better hearing ear was the only ear with potential to reach speech perception performance with CI. Pre-implantation this ear had functional residual hearing, whereas in the CL there had been a lack of auditory input for a long period and therefore poor performance was expected. These patients were advised to be implanted in the one hearing ear (Table 1). The mean absolute difference between the PTALow of both ears was 9.7 dB (Standard Deviation (SD) 8). The difference between the pre-operative PTALow (prePTALow) and the post-operative PTALow (postPTALow) for the CI ear was defined as the absolute loss of the residual hearing (PTALowDiff). We used the Hearing Preservation classification system of Skarzynski et al. [19] to calculate the Relative Hearing Preservation (RHP%): $RHP\% = \left[1 - \frac{(PTALowDiff)}{(PTALowMax - prePTALow)} * 100\right]$. PTALowMax -defined as the average MSL over the frequencies 250Hz, 500Hz and 1000Hz- was 111.7dB. Based on their RHP%, each participant was categorized into one of the three defined categories of Hearing Preservation (HP): (1) "Minimal HP" defined as RHP% between 0 and 25%, (2) "Partial HP" defined as RHP% greater than 25% to 75%, (3) "Complete HP" defined as RHP% greater than 75%.

In our clinic, speech perception in quiet is routinely measured at two- and 12-months after implantation. The standard Dutch speech perception test of the Dutch Society of Audiology, which consists of phonetically balanced monosyllabic Consonant – Vowel – Consonant (CVC) word lists, was used [20]. The average of three CVC lists (99 phonemes in total) was calculated. The test was carried out at 65dB SPL, in a quiet

audiometric booth, using a loudspeaker that was placed in front of the participant.

Statistical analysis

Individual absolute and relative residual hearing thresholds and electrode position of participants are presented in Table 1. The results are grouped according to scalar position. Average absolute residual hearing thresholds and average RHP% were reported per group and between-group comparisons were performed using Student *t* Tests (IBM SPSS Statistics 25.0) with the significance level set at 0.05 (Table 2). Speech perception scores of participants are reported in Table 1. As this was not an objective of the present study, and due to the heterogeneity of the data, these scores were not statistically analyzed.

4

Participant [a,b]	Age / Gender	Duration of HL (years)	Etiology	CI Side	Translocation to SV [b]	Pure Tone Average of Low Frequencies (in dB) [e]			Relative hearing preservation [f]		Post – operative speech perception (CVC – phoneme scores)		
						prePTALow CL ear	prePTALow CI ear	PTALowDiff CI ear	RHP%	Cat. HP	Pre-operative	2 months [c]	12 months [d]
1	56 / M	21	Hereditary	L	Y	23	52	31.7	47	P	0	0	65
2	65 / M	20	Hereditary	L	Y	77	83	21.7	24	M	3	56	-
3	45 / F	45	Unknown	L	Y	88	90	20.0	8	M	9	45	44
4	64 / M	10	M. Meniere	L	Y	92	92	20.0	0	M	20	56	56
5	67 / M	14	Unknown	L	Y	87	95	15.0	10	M	0	63	65
6	58 / F	20	Meningitis	L	Y	77	98	11.7	13	M	0	55	-
7	50 / M	49	Meningitis	L	Y	82	103	7.5	25	M	9	39	48
8	58 / F	57	Meningitis	L	Y	107	NMH	NA	NA	NA	6	45	47
9	60 / F	52	Unknown	R	Y	62	NMH	NA	NA	NA	0	75	82
10	66 / M	11	Unknown	L	N	62	67	11.7	74	P	42	69	95
11	44 / F	42	Unknown	L	N	93	88	-	NA	NA	0	-	15
12	64 / M	64	Unknown	R	N	92	88	8.3	64	P	46	45	45
13	55 / M	37	Unknown	R	N	70	92	6.7	67	P	0	51	-
14	73 / M	73	Unknown	L	N	105	95	11.7	30	P	6	71	62
15	43 / F	43	Unknown	R	N	93	97	1.7	89	C	40	61	70

16	57 / M	57	Usher Synd.	L	N	NMH	98	-2.5	125	C	0	-	-
17	44 / M	44	Unknown	R	N	100	98	0.0	100	C	0	12	65
18	85 / F	55	Unknown	L	N	NMH	102	0.0	100	C	6	-	-
19	56 / M	51	Hereditary	R	N	NMH	103	5.0	40	P	0	66	56
20	69 / F	25	Unknown	R	N	90	103	8.33	0	M	15	89	98
21	49 / F	49	Unknown	R	N	103	108	-2.5	160	C	0	-	-
22	78 / F	30	Hereditary	L	N	80	NMH	NA	NA	NA	0	81	86
23	63 / M	11	Unknown	L	N	73	NMH	NA	NA	NA	0	72	74

Table 1. Characteristics of participants.

[a] Participants numbers 1, 2, 4, 5, 6, 9, 10, 13, 18, 20, 22 and 23 were defined as having late onset of hearing loss and participants numbers 3, 7, 8, 11, 12, 14, 15, 16, 17, 19 and 21 were defined as having early onset of hearing loss.

[b] Participant number 3 is the one participant with tip fold-over and translocation of the four most apical electrode contacts.

[c] CVC-measurement was not conducted at three months for participants 16, 18 and 21; as there was no understanding or use of spoken words in everyday life.

[d] CVC-measurement was not conducted at 12 months f

or participants 16, 18 and 21; as there was no understanding or use of spoken words in everyday life, and for participants 2, 6 and 13; because these participants were lost to follow-up during the first year.

[e] Non Measurable Hearing (NMH) is defined as a participant without response at maximum stimulation level on two or more frequencies.

[f] Relative hearing preservation (RHP) is defined by Skarzynski et al. using the following formula: RHP $=100 * (1 - PTALowDiff / (PTALowMax - prePTALow))$

4

RESULTS

Demographics

Twenty-three consecutive participants were included in this study, 13 males and 10 females. Twelve participants had a late onset of hearing loss. The average age at implantation was 59.5 (SD 11.0; range 43-85) years old and the mean preoperative residual hearing was 92.2dB.

Tip fold-over

Intra-operatively, no tip fold-over was identified on fluoroscopy imaging. However, post-operative evaluation of the CT-images showed a tip fold-over of the four most apical electrode contacts in one of the 23 participants (4.3%). In retrospect, this tip fold-over was present on intra-operative fluoroscopy imaging, which was not recognized intra-operatively.
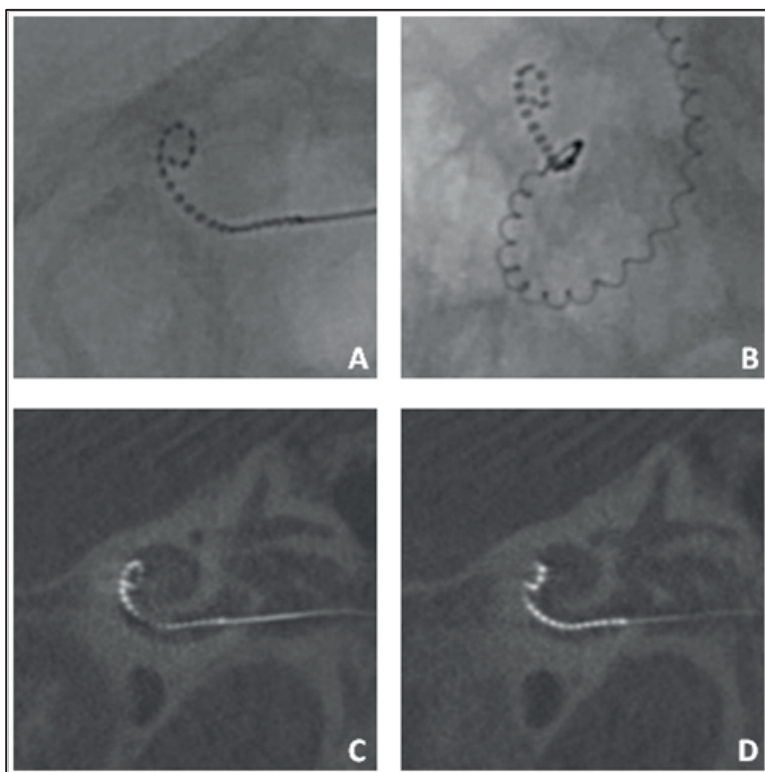
Figure 1. Images of the patient with a tip fold-over (Figures A and B: Fluoroscopy, Figures C and D: CT – scan).

Additionally, the SPE of this participant translocated from the ST into the SV
at the location of this tip fold-over (Figure 1). The participant, with early
onset of hearing loss, decided not to be re-implanted; as speech perception
was subjectively satisfactory and in-line with pre-implantation expectations.
Loss of residual hearing (PTALowDiff) in this patient was 25 dB and CVC -
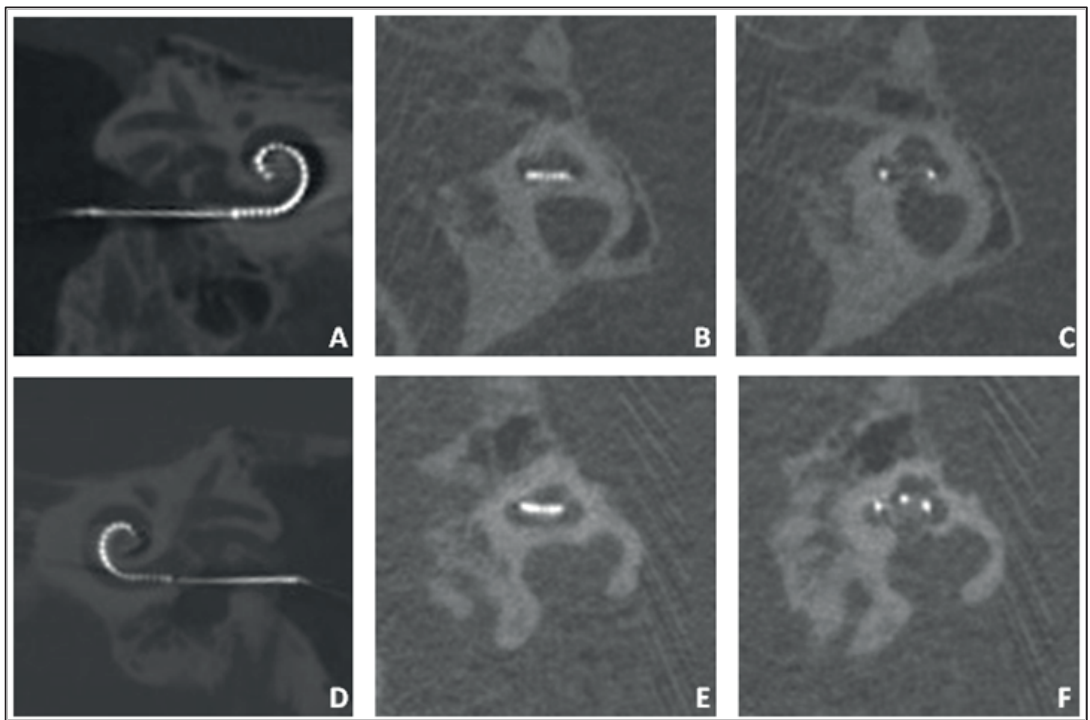phoneme scores at two- and 12-months post-operatively were 45% and
44%, respectively.

Figure 2. Position of different scalar locations (Figures A,B and C Scala Tympani position.
Figures D, E and F Scala vestibuli position).

Scalar position

In evaluation of the SPE scalar position of the 22 participants without tip fold-over, we found that 14 of the 22 participants (63.6%) had all electrode contacts positioned inside the ST. In eight participants (36.4%), the SPE translocated to the SV. All eight translocations occurred in near proximity of the cochleostomy. In seven participants, all 22 electrode contacts were placed in the SV. In one participant, the first two contacts were located in the ST, before the SPE translocated to the SV. In Figure 2, CT-scan images of an SPE in an ST position and in an SV position are shown.

Audiometric outcomes

Table 1 shows the residual hearing thresholds for both ears and speech perception scores with CI for individual participants. The average loss of residual hearing was 9.8dB (SD 9) across all participants with measurable pre-operative residual hearing and without a tip fold-over (n=18). Table 2 shows an average absolute loss of residual hearing (PTALowDiff) of 17.9dB (SD 9) in participants with translocation to the SV, while this was 4.4 dB (SD 5) in the participants without translocation (p=0.001). Moreover, relative hearing preservation in participants with and without translocation showed a similar statistically significant difference (p=0.01); RHP% was 19.7% (SD 16) in patients with translocation and 77.2% (SD 45) when there was no translocation. With respect to the categorical relative HP, there was no participant of the translocation group (n=7) with complete HP; one showed partial HP and six minimal HP. In the group of participants without translocation (n=11), five showed complete HP, five had partial HP and in one patient there was minimal HP.

	No translocation (SD)	Translocation (SD)	P-value of Student's t-test[e]
Number of participants[a,b,c]	11	6	
Pre-op residual hearing (prePTALow in dB)[d]	95.4 (11)	87.1 (19)	*0.26*
Difference score[e] (PTAlowDiff)	4.4 (5)	17.9 (9)	0.001
Relative hearing preservation according to Skarzynski et al.[f] (%)	77.2 (45)	19.7 (16)	0.01

Table 2. Mean loss of residual hearing in dB in participants with and without translocation to the scala vestibuli.

[a] one participant showed a tip fold-over and a translocation of the four most apical electrodes and was not included in the analysis.

[b] one participant was lost to follow-up before post-operative residual hearing measurement and was not included in the analysis.

[c] four participants; two in each group, had no measurable hearing (NMH) pre-operatively and were not included in the analysis.

[d] PTALow is defined as average pure-tone threshold over frequencies 250, 500 and 1000Hz.

[e] PTAlowDiff is defined as average difference between post- and pre-operative PTALow thresholds.

[f] Relative hearing preservation (RHP) is defined by Skarzynski et al. [19] using the following formula: RHP $=100 * (1 - PTALowDiff / (PTALowMax - prePTALow))$

The speech perception scores of participants with an early onset of hearing loss at two- and 12-months post-implantation was lower (mean phoneme score respectively 48% and 50%) compared to the scores of participants with a late onset of hearing loss (mean phoneme score 61% and 78%, respectively). As shown in Table 1, overall, the individual speech perception scores at two- and 12-months post-implantation of participants with complete ST position tend to be higher compared to scores of participants with translocation to the SV. No statistical analysis was

performed on the differences in speech perception, as this was not an objective of the study, the population was too heterogeneous and the number of participants was too low to enable appropriate conclusions to be drawn.

DISCUSSION

The primary objective of this study was to evaluate the position of the SPE inside the cochlea after implantation using the cochleostomy approach. Intra-operative fluoroscopy and cone beam CT-scan were used for, evaluation of tip fold-over and scalar position, respectively. The secondary objective was to investigate the relationship between the position of the SPE and residual hearing preservation.

Tip fold-over

One tip fold-over was found in this study (4.3%). In two other studies that investigated the SPE, 4.5% and 7.7% tip fold-over was reported [12, 15]. For comparison, in three studies, including conventional precurved CI electrode types, tip fold-over was found in 0.8%, 2% and 5.6% of the cases [21-23]. The slim and flexible design of the electrode is the obvious explanation for the higher frequency of tip fold-over in the SPE compared to conventional precurved electrodes. McJunkin et al. [15] and Ashendorff et al. [12] reported that, 88.9% (8/9) and 50% (1/2), respectively, of the tip fold-overs in the SPE were recognized in intra-operative imaging, and successfully re-inserted immediately. While this emphasizes the usefulness of intra-operative tip fold-over evaluation, it also demonstrates that recognizing a tip fold-over on fluoroscopy or plain X-Ray imaging may be challenging, especially if it concerns a limited number of apical electrode contacts. In the present study, the tip fold-over was missed during surgery. On the intra-operative fluoroscopy images, the tip fold-over had been misjudged as having a peri-modiolar position(Figures 1A and 1B). The tip fold-over became apparent once post-operative evaluation of the CT images clearly showed the relation to the cochlear wall (Figures 1C and 1D). Surgeons

implanting precurved electrodes, in particular the SPE, should perform intra-operative imaging, but should be aware of the challenges in evaluation the of fluoroscopy images.

Scalar position

In 63.6% of the participants without a tip fold-over (n=22), all electrode contacts were placed inside the ST, whereas 36.4% showed a translocation from the ST to the SV. In comparison, Aschendorff et al. [12], Ramos et al. [16] and Shaul et al. [11] found that 100% of in total 73 participants had full ST placement of the SPE; a CS approach was used in 15 participants, and the eRW or RW approach in 58 participants. While evaluating scalar location in 23/117 participants, McJunkin et al. [15] found 73.9% to have full ST insertion all implanted using the eRW approach. Interestingly, in this latter study, the participants with translocation to the SV had between nine and 11 most basally located electrode contacts located in the ST; suggesting that the translocations occurred more apically compared to the translocations in our study. The fact that all translocations in our study were located directly at the cochleostomy site indicates a correlation with the used surgical technique. This hypothesis is strengthened by two studies [8, 24] with a large number of participants (n=116 and n=220); in which it was reported that a cochleostomy approach, compared to an (extended) RW approach, is associated with higher risk of translocation, independent of the implanted conventional electrode type. Our study is the first to report cochleostomy associated translocations for the slim, periomodiolar electrode, which was designed to be non-traumatic with any surgical approach [13].

Based on anatomical studies, it is advised that a cochleostomy should be located anterior – inferiorly or inferiorly to the round window to avoid direct translocation into the SV or direct damage to the basilar membrane [25-27]. The most straightforward explanation for the early translocations in the present study is that the cochleostomy was positioned too superiorly; resulting in the direct insertion in the SV, or in a scalar translocation, immediately after the electrode is inserted into ST. On the other hand, it seems unlikely that the position of the cochleostomy provides the full explanation. In this prospective study, following extensive training by the manufacturer in insertion of the SPE with positioning of an anterior – inferior cochleostomy, and meticulous use of the silicone gauge for size of the cochleostomy of 0.8mm provided in the sterile implant package, the experienced surgeon was highly focused on a correct implementation of the cochleostomy position. A theoretical explanation, possibly relevant to the present study, is that a combination of factors, including the anterior – inferior cochleostomy, the size of the cochleostomy, the design of the insertion tool and flexible sheath, the angle of insertion, the force applied during insertion, and, in particular, the anatomical variation of the cochlea, play a role. Illustrative is an anatomical study of 73 cochleae in which the, for example, the height of the basal turn ranged from 1.6mm to 2.6mm (Mean 2.1, SD 0.2mm) [28]. Clinical relevance of anatomical variation in CI surgery was studied by Atturo et al. in 23 temporal bones [29]; the distances between the oval window, round window and spiral lamina were measured, and specifically compared in relation to cochleostomy sites located anterior – inferiorly, and inferiorly to the round window. The authors concluded that in a cochlea with small dimensions, only a very inferior cochleostomy could guarantee access to

the ST without trauma to the spiral lamina. The obvious solution -to position the cochleostomy inferior to the round window- could be very challenging. Due to the fact that the SPE insertion is a two-hand procedure, the tool itself represents volume and the area inferior to the round window is difficult to access.

While the exact explanation for the (cochleostomy associated) translocations in present paper remains unclear, based on the findings of this study and the reports in the literature, in favor of the round window approach rather than the cochleostomy [8, 24], it was decided to convert our surgical approach for the SPE to the RW approach to ensure highest probability on the ST position. Extending the round window approach, which involves removal of the crista semilunaris and some of the anterior bony edge of the window with a diamond drill size 0.8 or even 0.6mm, is necessary for the SPE to facilitate the insertion of the sheath of the insertion tool. Moreover, as in the present study the CI surgeon is experienced and was specifically trained in inserting the SPE using the cochleostomy approach, it might be expected that other surgeons inserting the SPE using the cochleostomy approach also have a high risk on translocation. This emphasizes the importance of quality control with imaging.

Audiologic outcomes

In this study, it was shown that the SPE can provide preservation of residual hearing (defined as RHL% > 75%), however only if inserted non-traumatically. Participants with full ST position of the SPE array had an average loss of low frequency residual hearing (PTA3lowDiff) of 4.4 dB and relative hearing preservation (RHP%) of 77.2%. Yet, in participants with a

translocation to the SV, we found a statistically significant higher average loss of low frequency residual hearing of 17.9 dB and low relative hearing preservation of only 19.7%. The only other study that described translocations in the SPE [15] did not report on residual hearing thresholds specifically for the participants with translocation. The found average loss of PTA3lowdiff in participants without translocation (4.4dB) was lower compared to the median loss of residual hearing (8.3.dB) found in an large multicenter study [30] that investigated the Hybrid-L electrode; a short straight electrode that was specifically designed for preservation of residual hearing.

In this study, it was observed that participants with translocation to the SV had lower speech perception scores compared to participants with a ST position. These differences indicate that scalar position might not only be of importance for residual hearing, but also for speech perception results. While the finding that ST position is important for the best speech perception is in line with similar findings in literature [8, 10, 11, 31]; speech perception is influenced by several factors, which were not accounted for in this paper. Moreover, our study population was relatively small and heterogeneous due to variation in biographic and audiologic factors; e.g. etiology, duration of hearing loss, pre-operative speech perception and age at implantation. Authors of this paper would like to emphasize the findings on speech perception should, therefore, be interpreted with caution.

Conclusion

In this prospective study, it was confirmed that the slim perimodiolar electrode carries a risk of tip fold-over - underscoring the need for intra-operative control. The slim perimodiolar electrode, once positioned in the
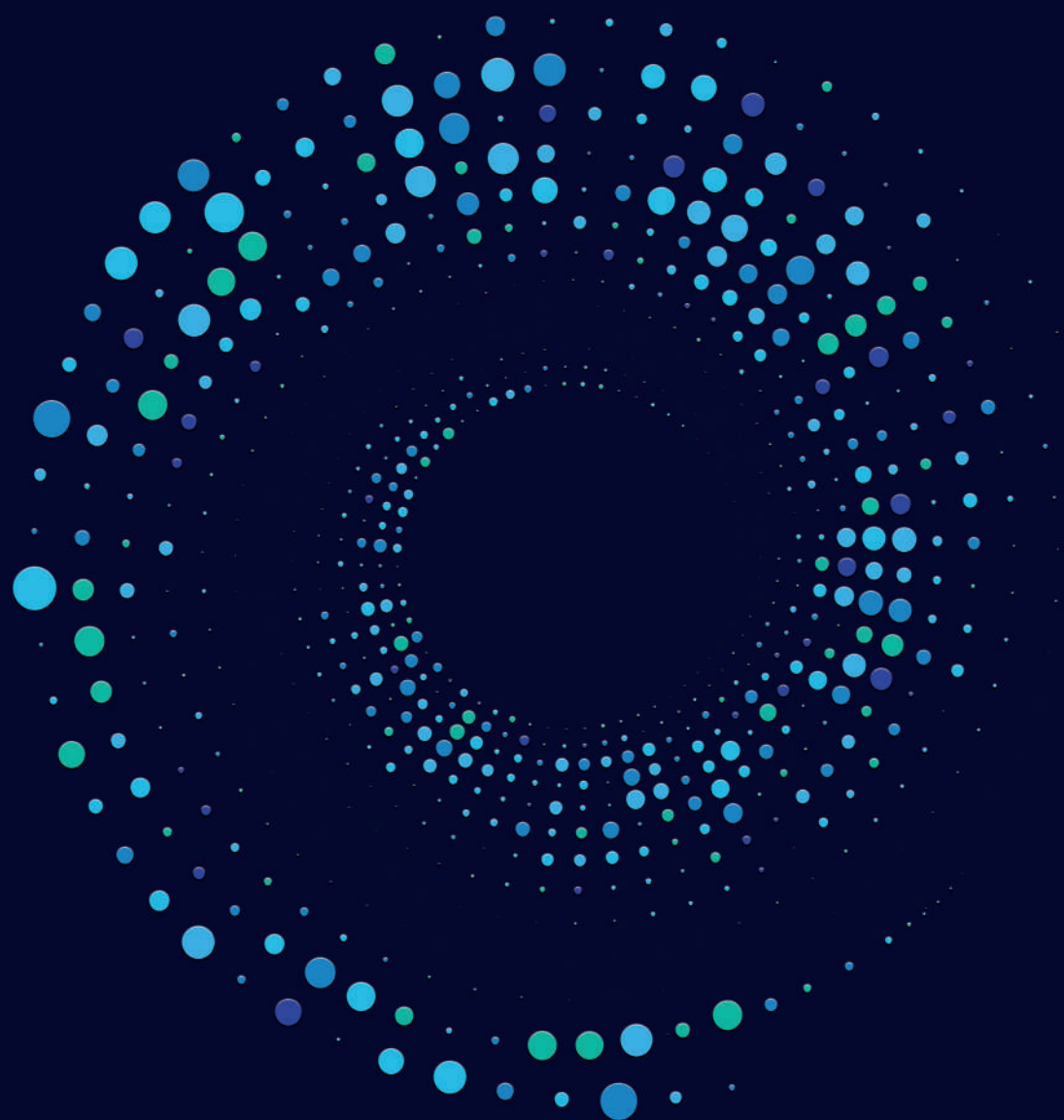
scala tympani can provide preservation of residual hearing. However, cochleostomy associated translocation to the scala vestibuli occurred in more than one-third of the participants and was shown to be detrimental for residual hearing thresholds. Based on the results of the present study and evaluation of literature, if the anatomical situation allows it, we advise to insert the slim perimodiolar electrodes using the eRW approach.

References

1.   Dhanasingh, A. and C. Jolly, *An overview of cochlear implant electrode array designs.* Hear Res, 2017. **356**: p. 93-103.

2.   Hughes, M.L. and P.J. Abbas, *Electrophysiologic channel interaction, electrode pitch ranking, and behavioral threshold in straight versus perimodiolar cochlear implant electrode arrays.* J Acoust Soc Am, 2006. **119**(3): p. 1538-47.

3.   Hughes, M.L. and L.J. Stille, *Effect of stimulus and recording parameters on spatial spread of excitation and masking patterns obtained with the electrically evoked compound action potential in cochlear implants.* Ear Hear, 2010. **31**(5): p. 679-92.

4.   Todt, I., et al., *Electrophysiological effects of electrode pull-back in cochlear implant surgery.* Acta Otolaryngol, 2008. **128**(12): p. 1314-21.

5.   Frijns, J.H., et al., *Initial evaluation of the Clarion CII cochlear implant: speech perception and neural response imaging.* Ear Hear, 2002. **23**(3): p. 184-97.

6.   van der Beek, F.B., et al., *Clinical evaluation of the Clarion CII HiFocus 1 with and without positioner.* Ear Hear, 2005. **26**(6): p. 577-92.

7.   Mens, L.H., P.J. Boyle, and J.J. Mulder, *The Clarion Electrode positioner: approximation to the medial wall and current focussing?* Audiol Neurootol, 2003. **8**(3): p. 166-75.

8.   Wanna, G.B., et al., *Impact of electrode design and surgical approach on scalar location and cochlear implant outcomes.* Laryngoscope, 2014. **124 Suppl 6**: p. S1-7.

9.   O'Connell, B.P., et al., *Electrode Location and Angular Insertion Depth Are Predictors of Audiologic Outcomes in Cochlear Implantation.* Otol Neurotol, 2016. **37**(8): p. 1016-23.

10.   Wanna, G.B., et al., *Impact of Intrascalar Electrode Location, Electrode Type, and Angular Insertion Depth on Residual Hearing in Cochlear Implant Patients: Preliminary Results.* Otol Neurotol, 2015. **36**(8): p. 1343-8.

11.   Shaul, C., et al., *Scalar localisation of peri-modiolar electrodes and speech perception outcomes.* J Laryngol Otol, 2018. **132**(11): p. 1000-1006.

12.   Aschendorff, A., et al., *Clinical investigation of the Nucleus Slim Modiolar Electrode.* Audiol Neurootol, 2017. **22**(3): p. 169-179.

13.   Cochlear Ltd., *Cochlear Nucleus CI532: https://www.cochlear.com/uk/ci532* (April 2019).

4

14.   Cuda, D. and A. Murri, *Cochlear implantation with the nucleus slim modiolar electrode (CI532): a preliminary experience.* Eur Arch Otorhinolaryngol, 2017. **274**(12): p. 4141-4148.

15.   McJunkin, J.L., et al., *Early Outcomes With a Slim, Modiolar Cochlear Implant Electrode Array.* Otol Neurotol, 2018. **39**(1): p. e28-e33.

16.   Ramos-Macias, A., et al., *Hearing Preservation with the Slim Modiolar Electrode Nucleus CI532(R) Cochlear Implant: A Preliminary Experience.* Audiol Neurootol, 2017. **22**(6): p. 317-325.

17.   Briggs, R.J., et al., *Development and evaluation of the modiolar research array--multi-centre collaborative study in human temporal bones.* Cochlear Implants Int, 2011. **12**(3): p. 129-39.

18.   Hood, J.D., *The principles and practice of bone conduction audiometry: A review of the present position.* Laryngoscope, 1960. **70**: p. 1211-28.

19.   Skarzynski, H., et al., *Towards a consensus on a hearing preservation classification system.* Acta Otolaryngol Suppl, 2013(564): p. 3-13.

20.   Bosman, A.J. and G.F. Smoorenburg, *Intelligibility of Dutch CVC syllables and sentences for listeners with normal hearing and with three types of hearing impairment.* Audiology, 1995. **34**(5): p. 260-84.

21.   Dirr, F., et al., *Value of routine plain x-ray position checks after cochlear implantation.* Otol Neurotol, 2013. **34**(9): p. 1666-9.

22.   Grolman, W., et al., *Spread of excitation measurements for the detection of electrode array foldovers: a prospective study comparing 3-dimensional rotational x-ray and intraoperative spread of excitation measurements.* Otol Neurotol, 2009. **30**(1): p. 27-33.

23.   Zuniga, M.G., et al., *Tip Fold-over in Cochlear Implantation: Case Series.* Otol Neurotol, 2017. **38**(2): p. 199-206.

24.   O'Connell, B.P., J.B. Hunter, and G.B. Wanna, *The importance of electrode location in cochlear implantation.* Laryngoscope Investig Otolaryngol, 2016. **1**(6): p. 169-174.

25.   Briggs, R.J., et al., *Cochleostomy site: implications for electrode placement and hearing preservation.* Acta Otolaryngol, 2005. **125**(8): p. 870-6.

26.   Gantz, B.J., et al., *Preservation of hearing in cochlear implant surgery: advantages of combined electrical and acoustical speech processing.* Laryngoscope, 2005. **115**(5): p. 796-802.

27.   Zhou, L., et al., *Does cochleostomy location influence electrode trajectory and intracochlear trauma?* Laryngoscope, 2015. **125**(4): p. 966-71.

28. Erixon, E., et al., *Variational anatomy of the human cochlea: implications for cochlear implantation.* Otol Neurotol, 2009. **30**(1): p. 14-22.

29. Atturo, F., M. Barbara, and H. Rask-Andersen, *On the anatomy of the 'hook' region of the human cochlea and how it relates to cochlear implantation.* Audiol Neurootol, 2014. **19**(6): p. 378-85.

30. Lenarz, T., et al., *European multi-centre study of the Nucleus Hybrid L24 cochlear implant.* Int J Audiol, 2013. **52**(12): p. 838-48.

31. Holden, L.K., et al., *Factors affecting open-set word recognition in adults with cochlear implants.* Ear Hear, 2013. **34**(3): p. 342-60.

4

5

Detecting in vivo intracochlear new bone formation following cochlear implantation using ultra-high resolution CT

Floris Heutink, Tim M. Klabbers, Wendy J. Huinck, Federica Lucev,
Willem Jan van der Woude, Emmanuel A.M. Mylanus, Berit M. Verbist

Abstract

Background: Histopathological studies reported that cochlear implantation (CI), a well-established means to treat severe-to-profound sensorineural hearing loss, may induce inflammation, fibrosis and new bone formation (NBF) with possible impact on loss of residual hearing and hearing outcome.

Purpose: To assess NBF in vivo after CI with ultra-high spatial resolution CT (UHRCT) and its implication on long-term residual hearing outcome.

Materials and Methods: In a secondary analysis of a prospective single-center cross-sectional study, conducted between December 2016 and January 2018, patients with at least 1 year of CI-experience underwent temporal bone UHRCT and residual hearing assessment. Two observers evaluated presence and location of NBF independently and tetrachoric correlations were used for inter-observer reliability. Additionally, scalar location of each electrode was assessed. After consensus agreement, two groups were formed: 1) with NBF (NBF+, n=83 participants) and 2) without NBF (NBF-, n=40). The association between NBF and clinical parameters, including electrode design, surgical approaches and long-term residual hearing loss, was tested using chi-square test and student's t-test.

Results: 123 participants (63+/-13; 63 female) were enrolled. NBF was found in 83/123 (68%) participants, at 466/2706 (17%) electrode contacts, and mostly around the 10 most basal contacts (428/466 (92%)) with an

interobserver agreement of 86% (2297/2683 contacts). Associations between electrode types and surgical approaches were significant (58/79 with NBF in precurved group vs. 24/43 with NBF in straight group, p=0.04 and 64/88 with NBF in cochleostomy group vs. 18/34 in the round window group, p = 0.03, respectively). NBF was least often seen in full scala tympani insertions, but there was no significant association between scalar position and NBF (p=0.15). Long-term residual hearing loss was significantly larger in the NBF+ group compared to NBF- group (22.9dB (SD14) versus 8.6dB (SD18), respectively, p=.04).

Conclusion: In vivo detection of new bone formation after CI is possible using UHRCT. The majority of CI recipients develop NBF, predominately located at the base of the cochlea. NBF adversely affects long-term residual hearing preservation.

Introduction

A cochlear implant (CI) is a neuroprosthetic device that forms an effective solution for patients with severe-to-profound hearing loss (HL). Today, even patients with functional residual hearing may receive a CI. By using soft-surgery techniques, e.g., low drill speeds and slow insertion, the extent of insertional trauma can be reduced.[1, 2] However, long-term changes within the cochlea caused by introducing a foreign body are neither treated nor prevented in current practice.[3]

Although CI electrode arrays are commonly made from biocompatible polymers, they can elicit an inflammatory response in two ways. First, insertional trauma can induce an *acute*, intracochlear tissue response, resulting in formation of iatrogenic scar tissue around the array.[4-6] Second, a *delayed* inflammatory reaction due to the natural host tissue response can lead to encapsulation of the array in a fibrous sheath.[7, 8] In its most pronounced form the fibrosis can progress to neo-ossification. This new bone formation (NBF) has been observed in animal and histopathological studies [5, 6, 9-13]. However, *in vivo* detection of NBF has not yet been described.

The presence of NBF around the CI electrode is relevant for several reasons. First, NBF alters the intracochlear electrophysiology. At the electrode contact-level, the electrical 'impedance' is increased, resulting in higher power consumption and more out-of-compliance issues.[14-16] Furthermore, the spread of electrical current within the cochlea is affected, leading to complex device fitting, channel interaction and poorer worse overall hearing outcome.[16] Second, new tissue formation has been theorized to cause long-term residual acoustic HL due to stiffening of the round window membrane and damping of the scala tympani.[3] Lastly, the

presence of NBF may complicate future therapies or re-implantations. Therefore, it seems desirable to control and reduce NBF, but this requires a method to detect and monitor NBF *in vivo*.

Recently, ultra-high spatial resolution CT (UHRCT) with 0.25mm detector elements and up to 2048 matrix, was introduced, showing better delineation of the fine anatomical temporal bone structures than conventional multidetector-CT (MDCT), which has detector elements of 0.5mm or larger and a matrix of 512.[17, 18] The UHRCT system has various focal spot sizes, the smallest being of nominal size 0.4 x 0.5mm^2,[19] while the smallest focus size in standard MDCT is 0.8 x 0.9 mm^2. UHRCT was used to evaluate intracochlear electrode location, revealing the presence of bone densities alongside the CI electrode contacts.[20]

The primary objective of this study was to describe the amount and location of NBF in a cohort of CI patients and to test the reliability of detecting NBF using UHRCT. The secondary objective was to investigate the association between NBF and two clinical parameters: (1) surgical factors – i.e., insertion location, electrode type and intracochlear scalar position, and (2) long-term residual HL.

Materials and Methods

This prospective single-center cross-sectional study, conducted between December 2016 and January 2018, was approved by the local and regional medical ethics committees (NL510071.091.14). All participants signed informed consent. The dataset of this study was previously used to find factors associated with CI speech perception outcome. These results are reported in a separate manuscript.[20] The current study is a secondary analysis of this prospective trial.

Study design

All participants were evaluated for: 1) the presence and location of post-operative NBF (relative to the implanted electrode), 2) the association between NBF and surgical parameters – i.e., surgical approach, type of electrode and intracochlear scalar position, and 3) the relation between NBF and long-term residual HL. The time point of conducting the UHRCT-scan of the temporal bone and measuring the residual hearing was named the Study Variable and Outcome Evaluation (SVOE). The time between CI implantation and the SVOE (tCI) varied, with an average tCI of 3.8 years (SD 1.7; Range 1.2–7.7 years).

Participants

The 129 participants included in this study met the following inclusion criteria: 1) post-lingual onset of HL, defined as an onset of severe-to-profound HL after the age of 5 years and 2) cochlear implantation between January 2010 and July 2016. Patients with a prelingual onset of HL, cognitive dysfunction, anomalies of the cochleovestibular system on pre-

operative imaging (CT or MRI) or less than 12 months experience with CI, were excluded.

CT technique – Evaluation of New Bone Formation

All participants underwent UHRCT (Canon Aquilion Precision, Canon Medical Systems, Otawara, Japan) at the SVOE measurement. This scan was used to evaluate the presence of NBF. Scans were acquired in sequential scan mode with a collimation of 160 x 0.25 mm resulting in a scan range of 4 cm. The scan parameters were: 140 kV, 100 mA, a rotation time of 1.5 ms, $CTDI_{vol}$ of 29.9 mGy and DLP 119.40 resulting in an effective dose of 0.25mSv (K-factor 0.001). Images were reconstructed with filtered back projection in bone kernel (FC81), 0.25 mm slice thickness every 0.125 mm overlapping, field of view of 90 mm with a 1024x1024 matrix resulting in a pixel spacing of 0.09 mm and a voxel size of 0.09 x 0.09 x 0.25 mm. The scan parameters were chosen such that image noise - inherently increasing with higher spatial resolution - was ameliorated and artifacts were reduced. By using axial acquisition, windmill artifacts due to presence of the cochlear implant were averted.
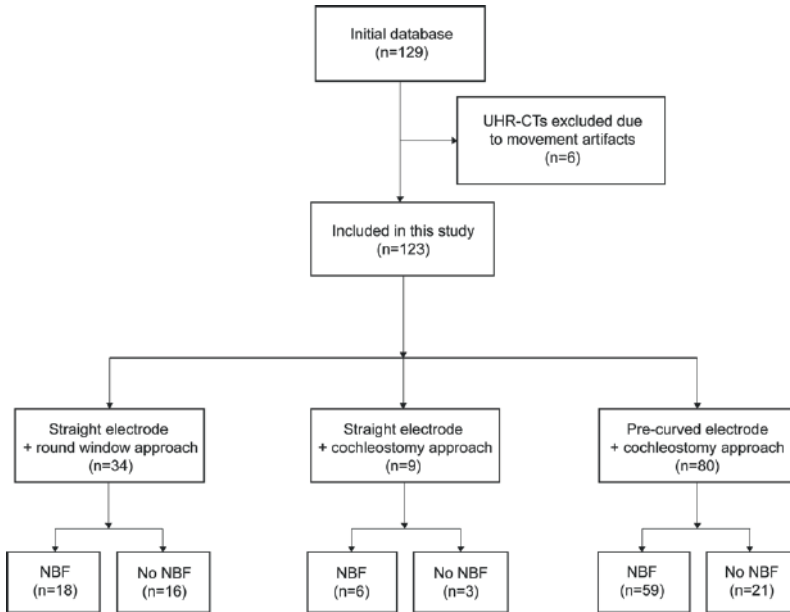
Figure 1: Flowchart of included CI-recipients with ultra-high resolution (UHR) CT-scans for intracochlear new bone formation (NBF) evaluation.
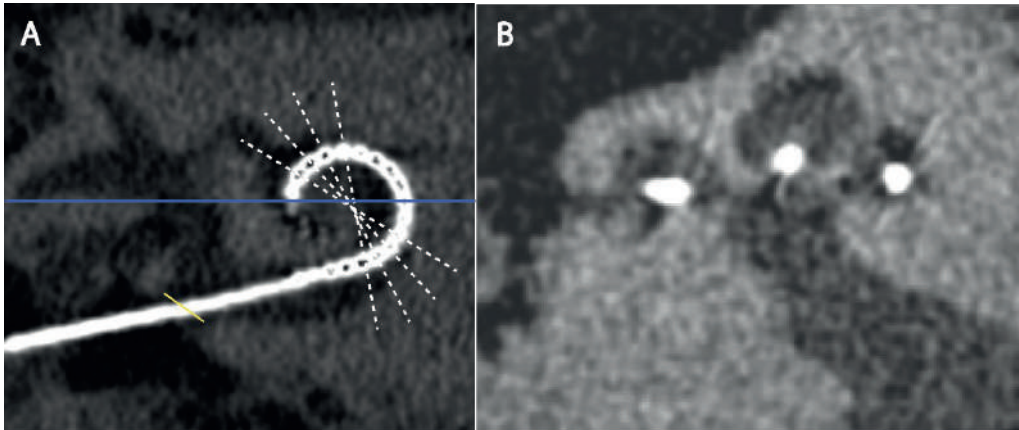
5

Figure 2: Methods for CT assessment: An oblique multi-planar reconstruction (MPR) through the basal turn of the cochlea was made (A) and mid-modiolar slices were obtained (B) with radial MPRs through the center of the cochlea (white lines in A). On such mid-modiolar images the presence or absence of NBF and the scalar position was assessed at each electrode contact. Angular insertion depth was measured from the top of the horizontal semicircular canal (blue line), using a correction factor to the center of the round window (yellow line) of 34 degree.[21, 22]
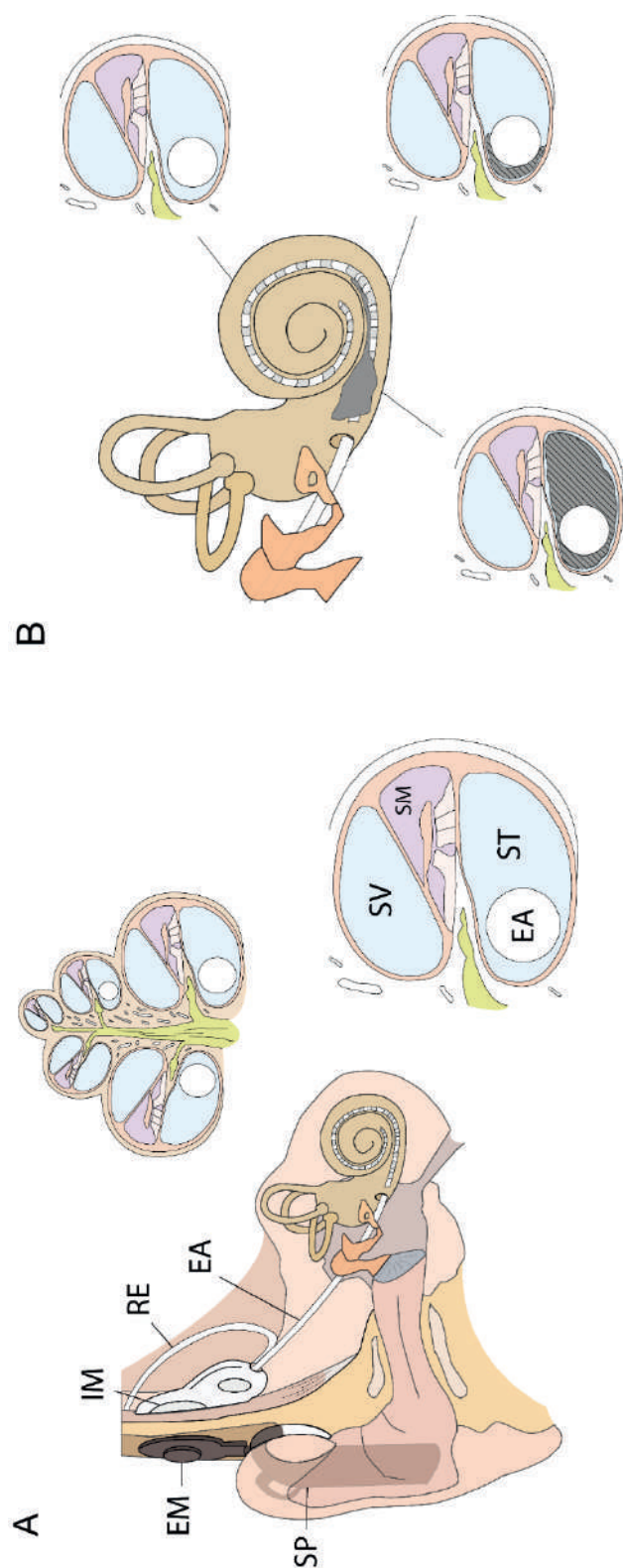
Figure 3: Schematic depiction of a right ear with cochlear implant, mid-modiolar cross-section and close-up of the different compartments within the cochlea (A), and an example of proximal new bone formation (in gray) in the scala tympani (ST) encasing the electrode array, gradually diminishing towards the apex of the cochlea (B).
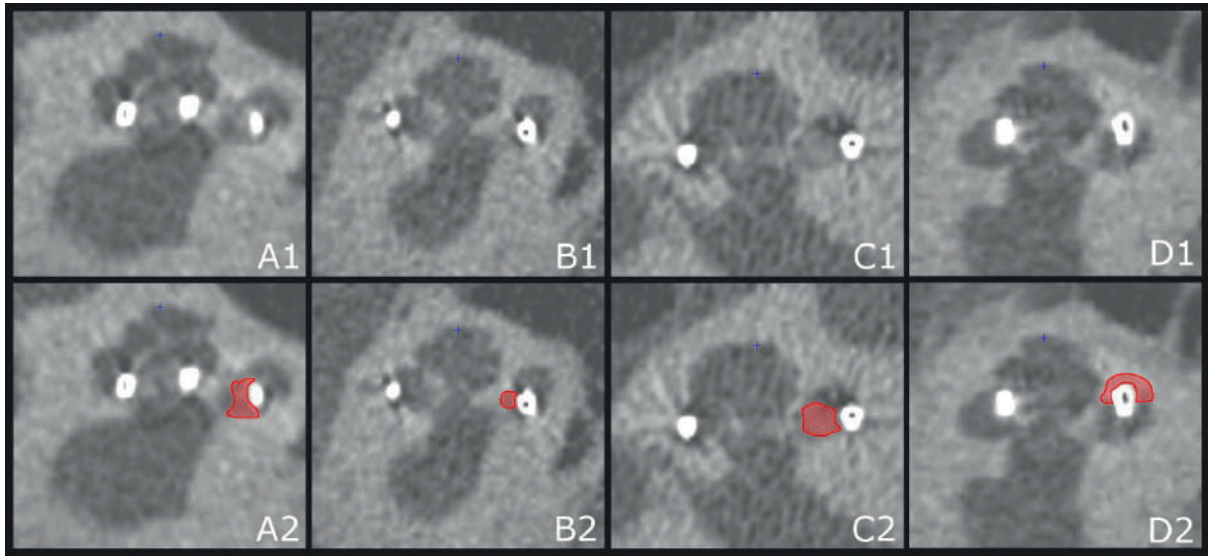
SP = speech processor, EM = external magnet, IM = internal magnet, RE = reference electrode, EA = electrode array, SV = scala vestibuli, SM = scala media, ST = scala tympani

Figure 4: Four mid-modiolar sections of UHRCT scans (A1-D1) with corresponding annotations indicating new bone formation in red (A2-D2). Note the varying appearance of NBF ranging from slightly increased density, resembling the density of the modiolus in (A), to frank ossification with a density similar to the otic capsule surrounding a translocated contact in the scala vestibuli in D. In B, the ossification in-between the peri-modiolar positioned electrode contact and the medial cochlear wall is difficult to discern and caused interrater disagreement.

First, oblique multi-planar reconstructions were obtained through the cochlea, parallel to the basal turn of the cochlea and next, mid-modiolar sections were obtained with radial reconstructions through the center of the cochlea (figure 2). Window width and level were freely adjustable. Two observers (BV and FL), with respectively 19 years of experience in head and neck radiology and 4 in-training years of experience, of which 1.5 years was focused on subspecialty training in head and neck radiology, independently scored presence of NBF around every CI electrode contact for each participant. In six participants the quality of the scan was too poor for NBF evaluation due to movement artifacts (figure 1). In total 22 electrode

5

contacts of 123 participants were evaluated (2706 contacts). Each contact identified as located inside the cochlea was scored as either 1) NBF absent or 2) NBF present (see figures 3 and 4). The scores of both radiologists were compared and the interobserver reliability was calculated using tetrachoric correlations and percentage agreement. The differences in scoring NBF were evaluated and solved during a consensus meeting between the two radiologists. The consensus score was used for further analysis. Additionally, scalar location and angular insertion depth of each electrode contact were assessed (figure 2). The method for both measurements was previously reported.[20-22]

Hearing preservation

The Pure Tone Average over 3 frequencies (PTA3), defined as the average residual hearing threshold over 500, 1000 and 2000Hz, was measured in both ears during follow-up at first fitting – i.e., 4-6 weeks after surgery, and compared with long-term follow-up – i.e., during the SVOE. Two residual hearing outcomes were evaluated: (1) The absolute residual HL (PTA3Diff), defined as the difference between the PTA3 at long-term follow-up (SVOE) and the PTA3 at first fitting (PTA3FirstFit), and (2) the relative residual hearing preservation percentage (RHP%). We used the Hearing Preservation classification system of Skarzynski et al.[23] to calculate the RHP%:

$$RHP\% = \left[1 - \frac{(PTA3Diff)}{(PTA3Max - PTA3FirstFit)} * 100\right].$$

PTA3Max - which was the same for all patients and is defined as the average maximum stimulation level over the frequencies 500Hz, 1000Hz, and 2000Hz The PTA3Max - was 116.7dB.

Statistical methods

Statistical analyses were performed in SPSS (IBM SPSS, Armonk, NY, version 25.0). Descriptive data on the amount and location of NBF around all contacts are reported. Tetrachoric correlations were used to determine the inter-observer reliability for detecting NBF and were calculated for all intracochlear electrode contacts. Two groups were formed based on the presence of NBF. Associations between NBF groups and categorical variables were tested using chi-square test, and between NBF and continuous variables using a student's t-test. A *p*-value of <0.05 was considered statistically significant.

5

Results

Patient characteristics

123 patients (62 ± 13 years, 63 women) were included and unilaterally implanted at the Radboudumc CI center, Nijmegen. Other demographic and etiologic characteristics can be found in table 1. All participants were implanted with a CI system of Cochlear Ltd.: 80 participants were implanted with a pre-curved electrode (Nucleus® Contour Advanced or CI512/CI24RE), and 43 participants were implanted with a straight electrode (Nucleus® Slim Straight or CI422/522). The pre-curved electrode was inserted via an antero-inferiorly drilled cochleostomy (CS, n=80), whilst the straight electrode was inserted through the round window (RW, n=34). When the round window could not be identified, the straight electrode was inserted via a cochleostomy approach (n=9).

Table 1: Demographic data and hearing characteristics	
Characteristic	Value
No. of participants	129
Sex	
Male	63 (49)
Female	66 (51)
Mean age at implantation (y)*	62.6 ± 12.7 (27-85)
Implant side	
Right	66 (51)
Left	63 (49)
Electrode type	
Pre-curved	85 (66)
Straight	44 (34)
Surgical approach	
Round window	35 (27)
Cochleostomy	94 (73)
Scalar position of electrode†	
All contacts within scala tympani	58 (48)
All contacts within scala vestibuli	27 (22)
Translocation	37 (30)
Aetiology of hearing loss	
DFNA-9	13 (10.2)
Sudden deafness	8 (6.3)
Otosclerosis	5 (3.9)
Usher Syndrome	4 (3.1)
Trauma	3 (2.4)
Meniere's disease	2 (1.6)
Ototoxic medication	2 (1.6)
Maternal Rubella	2 (1.6)
Mumps infection	1 (0.8)
DFNA-22	1 (0.8)
DFNB-3	1 (0.8)
Hereditary, unspecified	25 (20)
Unknown	60 (47)

Note.- Except where indicated, data are numbers of patients, with percentages in parenthesis.
* Data are mean ± standard deviations, with range in parenthesis.
† The quality of 6 UHRCT scans was too poor (due to movement artefacts) to score scalar position

New Bone Formation evaluation

The mean interobserver agreement was 86% (2297/2683 intracochlear contacts). The interobserver agreement per electrode contact is shown in Table 2.

Discrepancies between observers were mainly due to different cut-off points when scoring contacts in the transition zone from evident ossification to fluid-filled cochlear lumen, due to differences in scoring ossification medial to the electrode at basal contacts and due to differences in scoring extracochlear contacts at the level of the round window. After consensus between the two radiologists, 68% (84/123) of the participants showed one or more electrode contacts with adjacent NBF. Examples of intracochlear NBF with varying densities surrounding the electrode contacts are shown in figure 4.

Table 2: Interobserver agreement per electrode contact		
Electrode	Polychoric correlation	% agreement
E1	0.7831	57.7%
E2	0.7235	63.4%
E3	0.6173	61.8%
E4	0.7078	64.2%
E5	0.6828	62.6%
E6	0.5309	65.9%
E7	0.747	76.4%
E8	0.6398	79.7%
E9	0.9973	90.2%
E10	0.7902	93.5%
E11	0.9167	96.7%
E12	0.9622	97.6%
E13	0.8926	95.1%
E14	0.9965	95.1%
E15	0.9965	95.1%
E16	0.9977	95.1%
E17	0.9951	95.9%
E18	0.9972	97.6%
E19	0.9999	100%
E20	0.9999	100%
E21	0.9999	100%
E22	0.9999	100%
Mean	**0.862**	**85.62%**

The overall prevalence of NBF around all electrode contacts was 17% (466/2683 contacts). The distribution of NBF is shown in figure 5A: 92% (428/466) of the contacts with NBF were located around the 10 most basal electrode contacts. On average, contact 10 was located at an angular depth of insertion of 141° (SD 27°; 95% CI: 136– 146). 79 of the 123 participants (64.2%) had NBF around one of the three first contacts. None of the participants had NBF at the most apical electrode contacts 21 or 22. To

5

analyse a possible association between NBF and clinical parameters two groups were formed: 1) the "NBF+ group" and 2) the "NBF-" group. Basal NBF was defined as NBF around one or more of the contacts between an angular insertion depth of 0° to 90°. The "NBF+ group" consisted of eighty-three participants (67.5%) with basal NBF, and the "NBF- group" consisted of 40 participants without basal NBF. The associations between basal NBF, and surgical parameters, tCI, and residual hearing, were evaluated.

Surgical parameters and time between cochlear implantation and the SVOE (tCI)
The associations between electrode type and basal NBF, and between surgical approach and basal NBF, were significant (58/79 with NBF in precurved group vs. 24/43 with NBF in straight group, p=0.04 and 64/88 with NBF in cochleostomy group vs. 18/34 in the round window group, p = 0.03, respectively), but not independent of each other. There were three groups of participants based on electrode type and surgical approach, participants with: (1) pre-curved electrode and CS approach (PC-CS; n=80), (2) straight electrode and RW approach (S-RW; n=34), and (3) straight electrode with CS approach (S-CS; n=9). Basal NBF was found in 74% (59/80) of the PC-CS participants, 53% (18/34) of the S-RW participants and in 68% (6/9) of the S-CS participants. In figure 5B, the number of participants with NBF per *intracochlear* electrode contact is compared between the groups. For E1, E2 and E4 the number of participants with NBF in the PC-CS groups was significantly higher compared to the S-RW group, respectively 70% (56/80) vs. 41.2% (14/34) *p*=0.004, 68.8% (55/80) vs. 41.2% (14/34) *p*=0.006 and 61.3% (49/80) vs. 32.4% (11/34) *p*=0.005. The differences between the PC-CS and S-CS were not significant (*p*>0.05) as can also be observed in figure 5B.

Regarding scalar position, 59% (34/58) of the participants with complete ST position had NBF, whilst 78% (21/27) and 73% (27/37) of participants with complete SV position or translocation had NBF, respectively. This association was not significant (p=0.15).

The associations between surgical factors and NBF should be interpreted in light of the associations between NBF and tCI (i.e., the time between implantation and the measurement of NBF at the SVOE), and the surgical factors and tCI. The tCI in NBF+ group was 4.14 (SD 1.8) years and in the NBF- group 3.24 (SD 1.4) years (p=0.003). The tCI was significantly higher in participants with pre-curved electrode (p<0.001), cochleostomy (p<0.001) and in participants with scala vestibuli position of the electrode (p=0.045).

5
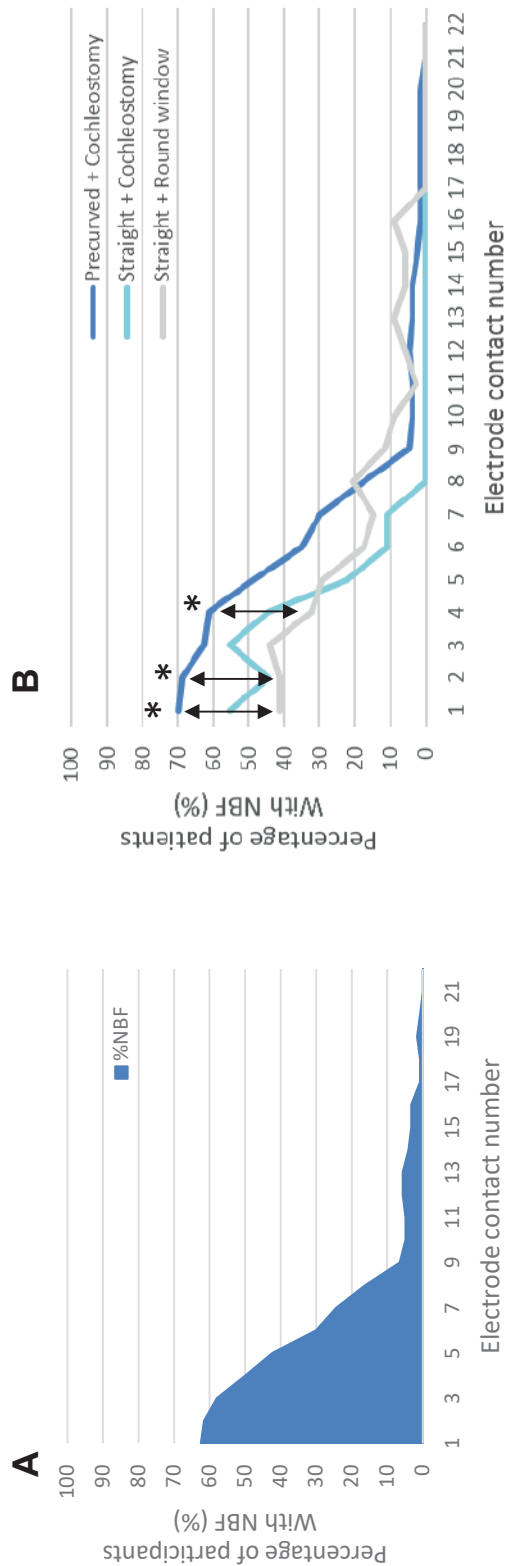
Figure 5: (A) Location of NBF per electrode contact and (B) location of NBF for the three surgical combinations. * = $p < 0.05$.

Residual hearing

Participants with a PTA3 higher than 90dB at first fitting were excluded from residual hearing analysis as these were defined as not having functional residual acoustic hearing. In the residual hearing analysis (n=24), the time since CI was not different between the NBF+ and NBF- group (p>0.05).

Figure 6 shows the mean threshold of PTA3 in the two NBF groups for the CI-ear, at the two time points during follow-up after cochlear implantation. In the contralateral ear, the mean PTA3 was 54.2 dB (SD 13.7) at first-fitting and 60.5 dB (SD 18.7) at long-term follow-up resulting in a PTA3Diff of 6.3dB in the contralateral ear. Compared to this, a higher decrease of PTA3 threshold is seen in the cochlear implant (CI) ear especially in the NBF+ group. The PTA3Diff in the CI ear was significantly larger in the NBF+ group compared to the NBF- group (n=24; p=0.04). This long-term residual HL was 22.9dB (SD 14) in the NBF+ group and 8.6dB (SD 18) in the NBF- group. The relative long-term hearing preservation (RHP%) between first fitting and long-term follow-up, respectively for the NBF+ group and the NBF- group, was 48.0% and 78.6%, this difference was not significant (p=0.06; n=24).
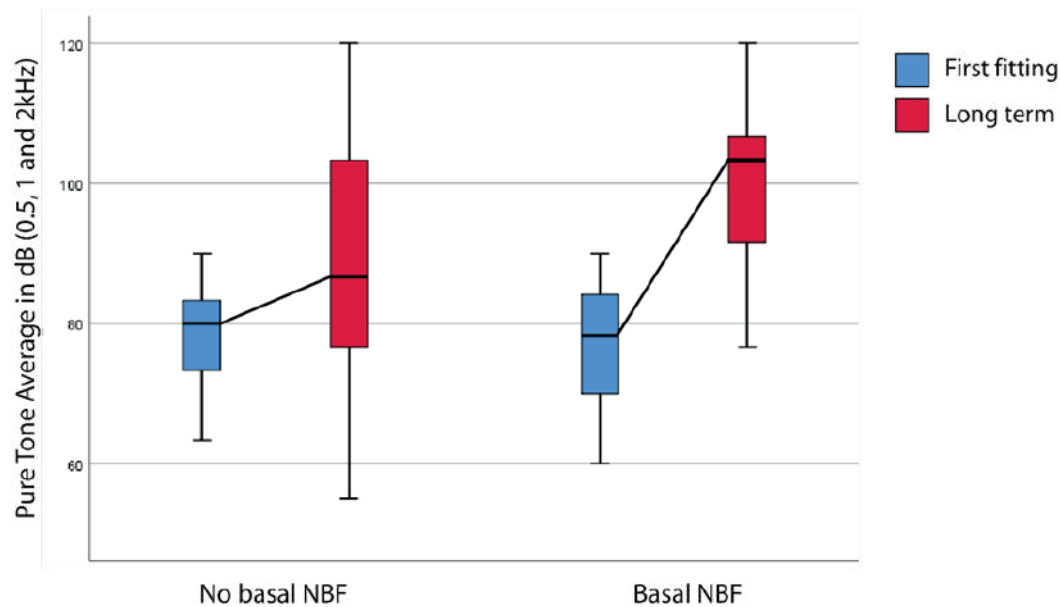
5

Figure 6: Boxplot indicating change in residual acoustic hearing threshold in the implanted ear between first-fitting at 4-6 weeks post-implantation and long-term follow-up at SVOE for participants with and without new bone formation. NBF = new bone formation.

Discussion

Several histopathological post-mortem studies reported NBF after CI and its potential adverse effect on intracochlear electrophysiology and hearing outcome. Our study showed that *in vivo* detection of NBF after CI is feasible with UHRCT. UHRCT doubles the in-plane resolution of MDCT systems as a result of smaller detectors (0.25mm), smaller spot size (0.4-0.5mm) and larger matrix (up to 2048 x 2048). A low noise level can be maintained with limited increase of dose thanks to detector properties and reconstruction algorithms. The method for *in vivo* detection of NBF presented in our study was highly reliable with an interobserver reliability of 86% (2297/2683 intracochlear electrodes).[24] NBF was common (68% (84/123) of participants, 17% (466/2683) of all electrode contacts) and mostly located around the 10 most basal contacts (92% (428/466) of the found NBF). This mostly basal NBF was associated with a negative effect on long-term residual hearing loss (22.9dB (SD 14) in the NBF+ group and 8.6dB (SD 18) in the NBF- group (p=0.04; n=24)).

     The interobserver reliability between the two radiologists was highest in apical regions with minimal or no NBF, implying best agreement on the absence of NBF. NBF is a gradual process from slight fibrosis to dense bone, reflected in different tissue attenuations on CT, while the method described in this paper uses a binary score. During the consensus meeting between the two radiologists, most discrepancies were indeed found at the contacts lying in the gradual transition zone from evident bone formation to a fluid-filled cochlear lumen.

    In three histopathological studies investigating NBF in CI patients, all 39 temporal bones studied showed some degree of NBF.[5, 6, 9] Compared to this, our study showed a lower prevalence of NBF. There may be several

5

possible reasons for this. First, our method is less precise compared to histopathological evaluation. The development of NBF is a gradual transition from mild fibrosis to dense bone.[5, 6, 9-13] Richard et al. [25] showed that the density of intracochlear tissue may range from translucent (areolar) fibrosis to dense fibrosis to neo-ossification. This is reflected in variable densities of NBF on UHRCT. Low-attenuation new tissue formation may not be detected by UHRCT. Second, the follow-up period in years since implantation in our study was shorter than in histopathological studies. Although the time needed for NBF to develop is unclear, a *delayed* inflammatory reaction may continue for several years post-implantation. Finally, developments in surgical technique may have decreased the risk of traumatic insertion and NBF. Considering the publication dates and duration of CI-use reported in the histopathological studies, the time frame of implantation seems to be between 1995 and 2005. In this period, the soft-surgery technique used in the present study was uncommon.

Whilst the amount of NBF differs, the predominantly basal location of NBF is in accordance with previous publications. This suggests an association with trauma due to opening of the cochlea. However, associations found between the surgical factors investigated in this study and NBF were not strong, and covaried strongly with tCI. Although trends were found indicating more NBF in patients with a pre-curved electrode, and partially or completely translocated implants, findings should be interpreted cautiously given the longer follow-up time and potential other factors contributing to intralabyrinthine new tissue formation.

We found a negative effect of NBF on long-term residual hearing. The loss of residual hearing was found in the low frequencies, whereas one might expect basal NBF to cause high frequency HL, considering the

cochlear tonotopic organization. This mismatch indicates that the effect of NBF on residual hearing is likely to be a cochlea-wide process. While this might be the result of a direct negative influence of NBF on residual hearing due to inflammation, oxidative stress and apoptosis of hair cells throughout the cochlea, it is also possible that it is caused by an inner ear conductive HL, due to NBF impeding sound transduction through the cochlea, affecting hearing across all frequencies.
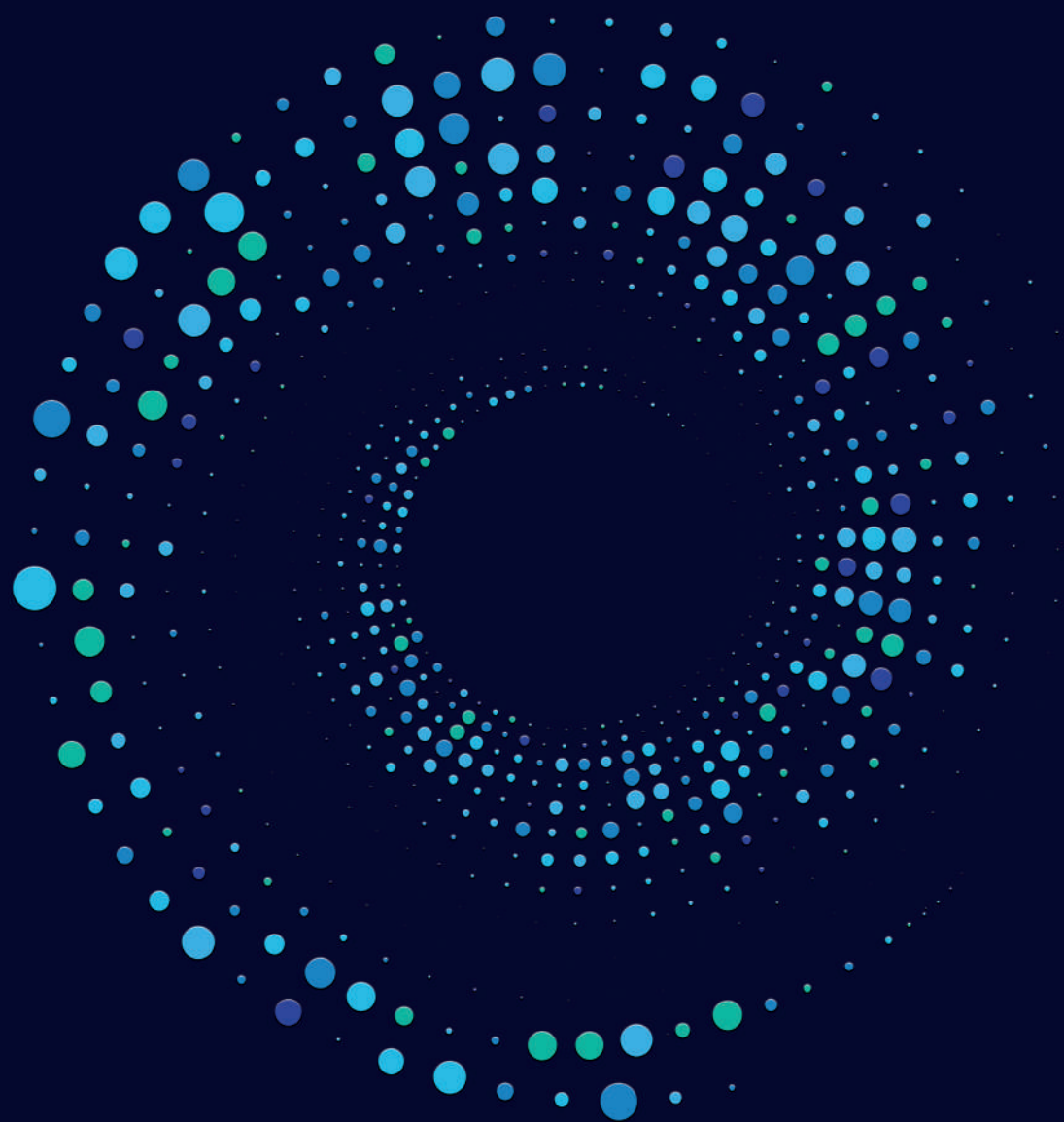
Our study has several limitations. First, there was no reference standard to confirm the presence of NBF. Second, while CT parameters were optimized for artifact and noise reduction, but further improvement may be possible with the use of hybrid-iterative reconstruction (AIDR 3D Enhanced). Third, the time interval between implantation and UHRCT-scanning varied between participants. This may have led to underestimation of NBF as it is unclear how long it takes for NBF to develop. In the residual hearing analysis (n=24), differences in tCI were not significant between the group with and without NBF (*p*>0.05), but the sample size was small (n=24).

In conclusion, the present study indicates that *in vivo* detection of new bone formation using ultra high spatial resolution CT is possible, and that the majority of cochlear implant recipients is likely to develop new bone formation after cochlear implantation. This neo-ossification was predominately located at the base of the cochlea and seems to be associated with surgical parameters that are considered more traumatic. Long-term residual hearing loss was more pronounced in patients with intracochlear bone formation.

5

References

1.   Banakis Hartl, R.M., et al., *Intracochlear Pressure Transients During Cochlear Implant Electrode Insertion: Effect of Micro-mechanical Control on Limiting Pressure Trauma.* Otol Neurotol, 2019. **40**(6): p. 736-744.

2.   Friedland, D.R. and C. Runge-Samuelson, *Soft cochlear implantation: rationale for the surgical approach.* Trends Amplif, 2009. **13**(2): p. 124-38.

3.   Foggia, M.J., R.V. Quevedo, and M.R. Hansen, *Intracochlear fibrosis and the foreign body response to cochlear implant biomaterials.* Laryngoscope Investig Otolaryngol, 2019. **4**(6): p. 678-683.

4.   Ishai, R., et al., *The pattern and degree of capsular fibrous sheaths surrounding cochlear electrode arrays.* Hear Res, 2017. **348**: p. 44-53.

5.   Kamakura, T. and J.B. Nadol, Jr., *Correlation between word recognition score and intracochlear new bone and fibrous tissue after cochlear implantation in the human.* Hear Res, 2016. **339**: p. 132-41.

6.   Li, P.M., et al., *Analysis of intracochlear new bone and fibrous tissue formation in human subjects with cochlear implants.* Ann Otol Rhinol Laryngol, 2007. **116**(10): p. 731-8.

7.   Anderson, J.M., A. Rodriguez, and D.T. Chang, *Foreign body reaction to biomaterials.* Semin Immunol, 2008. **20**(2): p. 86-100.

8.   Sheikh, Z., et al., *Macrophages, Foreign Body Giant Cells and Their Response to Implantable Biomaterials.* Materials (Basel), 2015. **8**(9): p. 5671-5701.

9.   Fayad, J.N., A.O. Makarem, and F.H. Linthicum, Jr., *Histopathologic assessment of fibrosis and new bone formation in implanted human temporal bones using 3D reconstruction.* Otolaryngol Head Neck Surg, 2009. **141**(2): p. 247-52.

10.   Somdas, M.A., et al., *Quantitative evaluation of new bone and fibrous tissue in the cochlea following cochlear implantation in the human.* Audiol Neurootol, 2007. **12**(5): p. 277-84.

11.   O'Leary, S.J., et al., *Relations between cochlear histopathology and hearing loss in experimental cochlear implantation.* Hear Res, 2013. **298**: p. 27-35.

12.   Marsh, M.A., H.A. Jenkins, and N.J. Coker, *Histopathology of the temporal bone following multichannel cochlear implantation.* Arch Otolaryngol Head Neck Surg, 1992. **118**(11): p. 1257-65.

13. Nadol, J.B., Jr., et al., *Histopathology of cochlear implants in humans.* Ann Otol Rhinol Laryngol, 2001. **110**(9): p. 883-91.

14. Clark, G.M., et al., *Cochlear implantation: osteoneogenesis, electrode-tissue impedance, and residual hearing.* Ann Otol Rhinol Laryngol Suppl, 1995. **166**: p. 40-2.

15. Shaul, C., et al., *Electrical Impedance as a Biomarker for Inner Ear Pathology Following Lateral Wall and Peri-modiolar Cochlear Implantation.* Otol Neurotol, 2019. **40**(5): p. e518-e526.

16. Wilk, M., et al., *Impedance Changes and Fibrous Tissue Growth after Cochlear Implantation Are Correlated and Can Be Reduced Using a Dexamethasone Eluting Electrode.* PLoS One, 2016. **11**(2): p. e0147552.

17. Ohara, A., et al., *Improved image quality of temporal bone CT with an ultrahigh-resolution CT scanner: clinical pilot studies.* Jpn J Radiol, 2020. **38**(9): p. 878-883.

18. Yamashita, K., et al., *Ultrahigh-resolution CT scan of the temporal bone.* Eur Arch Otorhinolaryngol, 2018. **275**(11): p. 2797-2803.

19. Oostveen, L.J., et al., *Physical evaluation of an ultra-high-resolution CT scanner.* Eur Radiol, 2020. **30**(5): p. 2552-2560.

20. Heutink, F., et al., *Factors Influencing Speech Perception in Adults With a Cochlear Implant.* Ear Hear, 2021. **42**(4): p. 949-960.

21. Verbist, B.M., et al., *Cochlear coordinates in regard to cochlear implantation: a clinically individually applicable 3 dimensional CT-based method.* Otol Neurotol, 2010. **31**(5): p. 738-44.

22. Verbist, B.M., et al., *Consensus panel on a cochlear coordinate system applicable in histologic, physiologic, and radiologic studies of the human cochlea.* Otol Neurotol, 2010. **31**(5): p. 722-30.

23. Skarzynski, H., et al., *Towards a consensus on a hearing preservation classification system.* Acta Otolaryngol Suppl, 2013(564): p. 3-13.

24. McHugh, M.L., *Interrater reliability: the kappa statistic.* Biochem Med (Zagreb), 2012. **22**(3): p. 276-82.

25. Richard, C., et al., *Round window versus cochleostomy technique in cochlear implantation: histologic findings.* Otol Neurotol, 2012. **33**(7): p. 1181-7.

5

6

Multi-Scale Deep Learning Framework for Cochlea Localization, Segmentation and Analysis on Clinical Ultra-High-Resolution CT Images.

Floris Heutink, Valentin Koch, Berit M. Verbist, Willem Jan van der Woude,
Emmanuel A.M. Mylanus, Wendy J. Huinck, Ioannis Sechopoulos,
Marco Caballo

Abstract

Background and Objective: Performing patient-specific, pre-operative cochlea CT-based measurements could be helpful to positively affect the outcome of cochlear surgery in terms of intracochlear trauma and loss of residual hearing. Therefore, we propose a method to automatically segment and measure the human cochlea in clinical ultra-high-resolution (UHR) CT images, and investigate differences in cochlea size for personalized implant planning.

Methods: 123 temporal bone CT scans were acquired with two UHR-CT scanners, and used to develop and validate a deep learning-based system for automated cochlea segmentation and measurement. The segmentation algorithm is composed of two major steps (detection and pixel-wise classification) in cascade, and aims at combining the results of a multi-scale computer-aided detection scheme with a U-Net-like architecture for pixelwise classification. The segmentation results were used as an input to the measurement algorithm, which provides automatic cochlear measurements (volume, basal diameter, and cochlear duct length (CDL)) through the combined use of convolutional neural networks and thinning algorithms. Automatic segmentation was validated against manual annotation, by the means of Dice similarity, Boundary-F1 (BF) score, and maximum and average Hausdorff distances, while measurement errors were calculated between the automatic results and the corresponding manually obtained ground truth on a per-patient basis. Finally, the developed system was used to investigate the differences in cochlea size within our patient cohort, to relate the measurement errors to the actual variation in cochlear size across different patients.

Results: Automatic segmentation resulted in a Dice of 0.90±0.03, BF score of 0.95±0.03, and maximum and average Hausdorff distance of 3.05±0.39 and 0.32±0.07 against manual annotation. Automatic cochlear measurements resulted in errors of 8.4% (volume), 5.5% (CDL), 7.8% (basal diameter). The cochlea size varied broadly, ranging between 0.10ml - 0.28ml (volume), 1.3mm - 2.5mm (basal diameter), and 27.7mm - 40.1mm (CDL).

Conclusions: The proposed algorithm could successfully segment and analyze the cochlea on UHR-CT images, resulting in accurate measurements of cochlear anatomy. Given the wide variation in cochlear size found in our patient cohort, it may find application as a pre-operative tool in cochlear implant surgery, potentially helping elaborate personalized treatment strategies based on patient-specific, image-based anatomical measurements.

1. INTRODUCTION

A cochlear implant (CI) is a surgically implanted electronic device that
provides a sense of sound to a patient with severe to profound hearing loss.
To date, large variability exists in preservation of residual hearing and speech
understanding abilities after cochlear implantation [1-2]. Among other
factors, a major cause of residual hearing loss (RHL) is traumatic electrode
insertion [3]. The potential occurrence of intracochlear trauma during
electrode insertion may be related to the fact that most current electrodes
are chosen and inserted independently from each specific patient's inner ear
anatomy [4]. Since, currently, electrodes have a fixed size and a standard
insertion length, patients with smaller cochlea may be at higher risk of
trauma and, potentially, of a larger RHL.

   If accurate image-based segmentation and measurements of the
cochlea could be performed pre-operatively, this could potentially allow for
the adaptation of size, shape and depth of insertion of the CI electrode to
each single patient, possibly improving the surgical outcome by reducing risk
of intracochlear trauma and RHL.

   In medical images, simple measurements of regular anatomical parts
are usually performed manually. However, for highly complex and irregular
structures (such as the human cochlea), dedicated computerized methods
are needed to first segment the structure of interest, and then provide
automatic measurements which would otherwise be challenging (if not
impossible) to perform by human readers.

   To address the goal of segmenting and measuring the human
cochlea, previous studies proposed semi-automatic segmentation methods
[5] that require a high degree of human interaction to separate the cochlea
from the connected internal auditory canal and vestibular structures. Other

studies aimed at using segmentation frameworks based on anatomical information of the inner ear, obtained a priori using mathematical modelling or some high-resolution, high-dose cadaver scans [6-11].

These previously developed methods reported high segmentation performance, thanks to their considerable computational and mathematical complexity. However, most methods were developed based on micro-CT scans of a few cadaveric human cochleae, which were used as constraints and as *a priori* information to guide the segmentation model. The extrapolation of information from small datasets could potentially limit the application of such methods in the clinical realm, and potentially account for limited inter-patient variability and validation.

With the advancements in medical imaging technology and analysis algorithms, new solutions can be investigated, thanks both to the improved spatial resolution of the most recently developed CT scanners, and by replacing traditional model-based segmentation with new deep learning approaches.

From the imaging side, advances in computed tomography technology have been proposed over the past few years, with wider detectors being introduced [12], novel electronics with lower noise being designed [13] and, more recently, smaller detector elements being developed [14]. In this respect, ultra-high-resolution (UHR) CT (Aquilion Proteus and Precision, Canon Medical Systems Corporation) was brought to market, with a detector element size of 0.25 mm at isocenter, and with an MTF twice as high as that of current-generation multi-detector CT systems [15].

From the image analysis perspective, deep learning has become one of the major methodologies used for analyzing medical images, including

image segmentation. When a sufficiently large training set is available, deep learning demonstrated high performance in the segmentation of structures with large inter-patient anatomical variability [16]-[17], with limited programming effort, given the ability of learning the segmentation task directly and automatically from the images, i.e. without user-selectable parameters to be tuned in a testing phase.

Among deep learning algorithms, convolutional neural networks (CNNs) have repeatedly demonstrated their high performance in many computer vision tasks [18-23], often outperforming traditional methods based on deterministic or handcrafted approaches [24]. However, they carry the drawback of the dataset size, which has to be large enough for the network to learn sufficient patterns in the input images to correctly replicate them in an independent testing phase [25]. This can be a critical issue in tomographic, high-resolution cochlea imaging, where the dataset sizes are usually limited and, therefore, can potentially limit the application of state-of-the-art Artificial Intelligence techniques.

To address this issue, in this study we developed and validated a deep learning system for cochlea segmentation and measurements that takes advantage of both extensive data augmentation, and a modular structure that localizes the segmentation task in small image regions around the cochlea, allowing to achieve good performance using a small training set. After validation, the developed system was used on clinical ultra-high-resolution (UHR) CT patient images for cochlear measurement extraction, to investigate the differences in cochlea size within a large patient cohort and relate the measurement errors to the actual variation in cochlear size across different patients.

6

2. MATERIALS AND METHODS

The proposed approach is composed of two main blocks: one for cochlea segmentation, followed by one for cochlea measurements. The cochlea segmentation block combines a computer-aided detection system based on multiscale residual CNNs with an encoder-decoder network for pixel-wise classification. The former aims at localizing the cochlea on the input temporal bone CT scans, to reduce the search space of the subsequent pixel-wise classification model, while the latter is aimed at providing automatic cochlea segmentation. The models were trained on 2D image patches extracted with a sliding-window-based approach from the cochlea scans of the training set (as explained in Sections 2.C and 2.D), and then applied in a region-based fashion on the full test set scans (as described in Section 2.E). After segmentation, the cochlea measurement block provides automatic measurements from the segmented cochlea by using a combination of CNNs and morphological thinning algorithms. All main steps of the proposed method are reported in Figure 1.

All steps of the pipeline, along with data collection and preparation, are described in the following sections. Finally, patient-based cochlear size measurements are performed using the proposed approach on all scans of the dataset, and are analyzed to investigate the differences in cochlea size within our patient cohort.
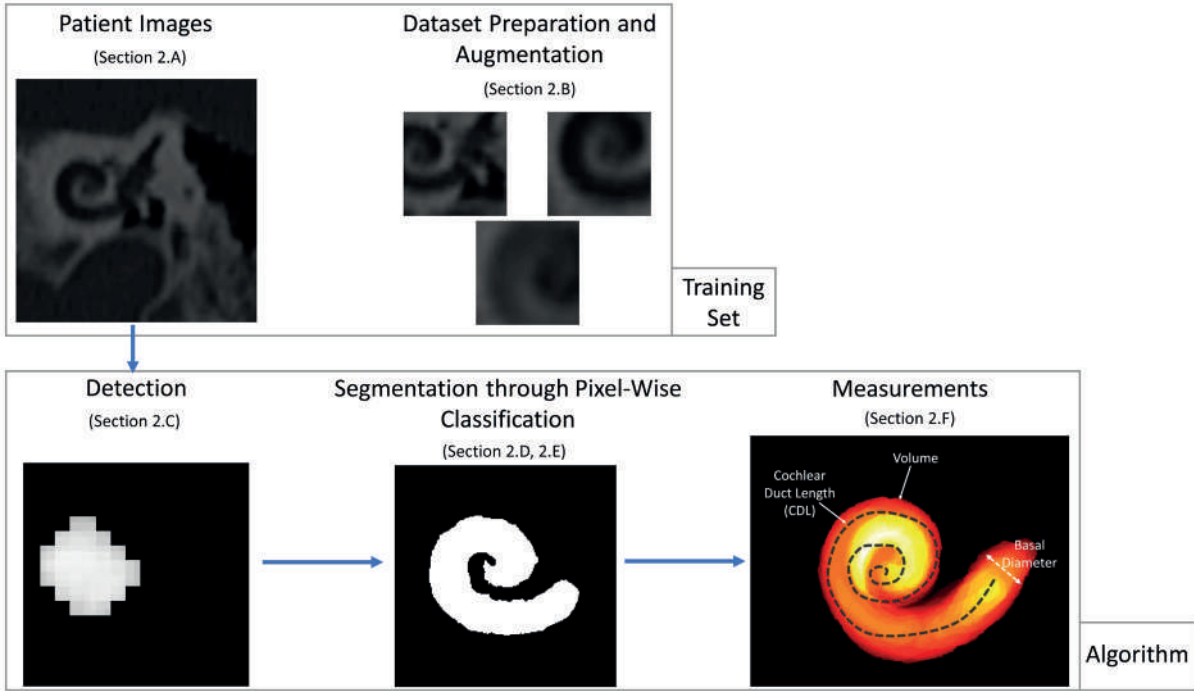
Figure 1. Main steps of the proposed cochlea segmentation and analysis approach. The input scans are first processed by a detection module to localize the cochlea, and by a pixel-wise classification module for segmentation. The detection module aims at reducing the search space of the pixel-wise classification module, serving as pre-processing to speed up the algorithm and for false positive reduction. Both modules were trained on an image patch-basis, to increase the training set size by obtaining multiple examples from each scan. The segmented cochlear structure then undergoes a final module to extract patient-based anatomical measurements through the combination of deep learning and thinning algorithms. Deep learning was adopted in each step for its ability of learning directly from the input data, and provide automatic results without user-selectable parameters to be tuned in a testing phase

2.A. Image Acquisition

123 UHR-CT temporal bone scans were acquired and used to develop our algorithm. Images were acquired with one of two UHR-CT scanners (Aquilion Proteus and Precision, Canon Medical Systems, Otawara, Japan), both composed of a 160 multi-row detector, with an effective detector element size of 0.25 mm x 0.25 mm at the iso-center, 1,792 detector channels, and a nominal focal spot of 0.4 mm x 0.5 mm (Precision) and 0.6 mm x 0.6 mm (Proteus) [26]. For this study, helical acquisitions were acquired using tube voltages of 140 kVp (Precision) and 135 kVp (Proteus), exposure time of 1.5 s, and tube currents of 100 mA (Precision) and 80 mA (Proteus), with a gantry rotation time of up to 0.35 s, and a pitch factor 0.569. The CTDI$_{vol}$ was approximately 31 mGy, measured with a 16 cm phantom (140 kVp, 150 mAs).

CT scans were performed by a trained radiographer over a cross-section of the patient head of approximately 4 cm (including the whole inner ear anatomy). That is, only a 4 cm-thick cross-section of the patient head was imaged (along the craniocaudal direction), so as to reduce the exposure by avoiding to deliver radiation dose in other regions of the patient head.

The scans were then reconstructed using filtered back projection with the reconstruction kernel FC81 (a high-resolution bone kernel) along image planes parallel to the cochlear basal turn (oblique multi-plane reconstruction), with a matrix size of 1,024 x 1,024 and a slice thickness of 0.25 mm. An example of the cochlear basal turn in the axial view is shown in Figure 2. The in-plane reconstructed voxel size was 0.045 mm for the Proteus scanner, and 0.05 mm for the Precision scanner. The reconstructed,

in-plane voxel size was set automatically by the system, based on the reconstruction mode.

The dataset was collected within a prospective, cross-sectional study conducted between December 2016 and January 2018 at our institution, and approved by the local and regional medical ethics committee Arnhem-Nijmegen (METC; NL510071.091.14).

All participants of the study (average age: 64±12 years for males (n=59), and 61±14 years for females (n=64)) agreed to participate and signed informed consent. Adult patients that had undergone CI surgery between January 2010 and July 2016, after being diagnosed with post-lingual hearing loss onset (defined as an onset of severe-to-profound deafness after the age of 5 years), were eligible for this study. The inclusion criteria were patients who could provide written informed consent, and with at least one year of experience with CI after surgery. Exclusion criteria were (i) cognitive dysfunction, and (ii) congenital or acquired anomalies of vestibulo-cochlear system.

For all patients, the cochlear structure on the image was manually annotated, and used to develop and validate our algorithms. Manual annotation was performed slice-by-slice in the reconstructed images using the ImageJ (LOCI, University of Wisconsin, NIH) polyline toolbox by a medical image analysis scientist with 3 years of experience in analysis and segmentation of CT images, under the supervision of a cochlear implant surgeon and a board-certified head-and-neck radiologist.
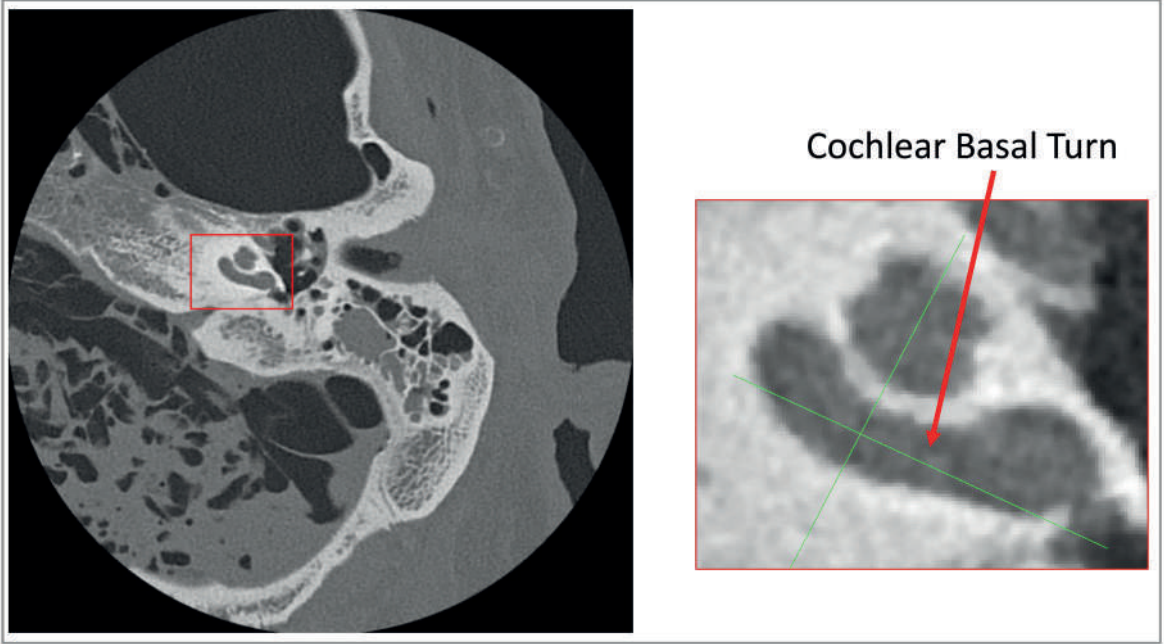
6

Figure. 2. Example of a temporal bone scan (axial view) showing the cochlear basal turn. Crosshairs are aligned parallel and perpendicular to the long axis of the cochlear basal turn.

2.B. Data Preparation and Augmentation

Of the acquired scans, 40 were used to train our models, 8 for validation, while the remaining 75 were kept into an independent test set. Extensive data augmentation was performed on the training scans, in order to maximize the performance by reducing risk of overfitting while keeping most scans for final testing.

Both developed models (detection and pixel-wise classification) were trained on a patch basis. Patches were collected through a sliding window approach from each scan (and respective manual annotation) within a volume of 512x512x50 voxels (approximately corresponding to

2.5x2.5x1.25 cm) including the whole cochlear anatomy. For each cochlea scan, patches were collected in two dimensions on a slice-basis. The allowed overlay of contiguous patches was kept high (stride 10 voxels) to increase the dataset size, and the process was repeated for three different squared window sizes: 150, 100, and 70 voxel side. This multi-scale patch extraction was performed to capture the image information at different dimensions, approximately spanning from the full length of the cochlea, to the size of smaller details such as the different cochlea turns and the cochlear apex. Additional data augmentation was then performed on all extracted patches through four rotations (-20º, -10º, 10º, 20º) and vertical mirroring. These augmentation methods (and their respective parameter values) were chosen to simulate potential realistic variations in image acquisition, while avoiding generating training examples that are too different from real cases. In fact, with the imaging protocol adopted, the cochlea is always imaged at approximately the same in-plane angular orientation for all patients, justifying the use of a limited angular range (between -20º and 20º) to generate new, realistic cases.

 As a result, the number of collected patches was 326,940 (150x150 window), 556,600 (100x100 window), and 904,120 (70x70 window). Some examples are shown in Figure 3.
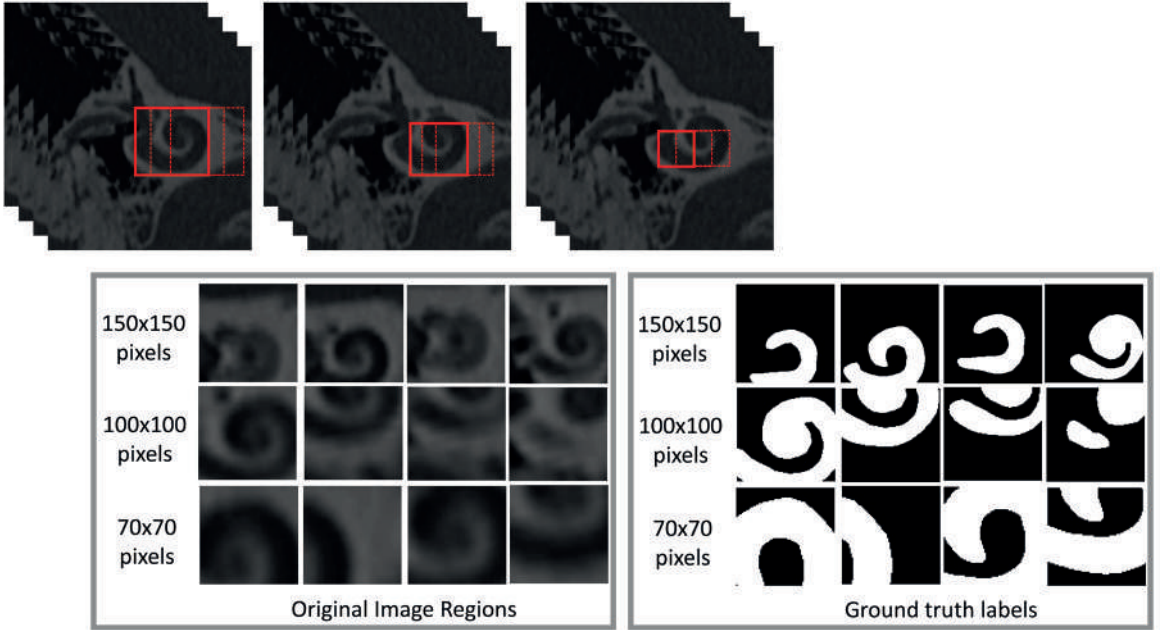
6

Figure. 3. Examples of training image patches for the proposed deep learning system. The patches were extracted through a sliding window approach, with the window size varying for three different sizes (150, 100, and 70 voxel side). The patches were extracted on a 2D-basis from each slice of the reconstructed cochlea scan, resulting in approximately the same number of patches extracted from each scan.

2.C. Cochlea Detection Model

Before segmentation, a detection model was implemented to localize the cochlear structure within the CT scan. This model outputs a probability map of the same size as the input image, with values close to 1 in those image locations where the cochlea is more likely to be present. As a detection task, it was trained with pairs of examples composed by the input image patch, and a discrete label indicating whether that patch contained cochlea voxels (1) or not (0). A training patch was assigned a label of 1 if at least a

given percentage of the respective manually annotated region was composed of cochlea voxels. Given that, for a detection task, bigger field of views are more sensitive, but less specific, we set these percentages to 10%, 20%, and 25% for the 150, 100, and 70-voxel patches, respectively. The model is composed of three residual CNNs [27-28], trained separately for the three image patch sizes, with blocks of 3x3 convolutional kernels plus batch normalization. The number of filters increases with the network depth (as shown in Figure 4), and dropout regularization [29] (probability 0.5) was used before the fully connected layer for regularization. All the weights of the network were normally initialized [30], and biases set to zero. Training was performed on mini-batches [31] of 64 elements using gradient descent with a momentum of 0.9 and a weight decay of 10^{-4}. The starting learning rate was set to 0.01, and decayed exponentially every 10 epochs (over a maximum of 60 epochs). During training, accuracy was calculated on the validation set to prevent overfitting, and the loss function used was binary cross-entropy:

$$Loss = -[y \log(p) + (1 - y) \log(1 - p)] \tag{1}$$

where y is the ground truth label, and p the predicted detection probability. In a testing phase, all image patches are collected from the CT scan using a sliding-window approach (10 voxels stride); the model performs the detection task for the three image patches separately, and then provides a final probability map by averaging the three outputs (Figure 5). This results in a multi-scale probability map that evaluates the image information in a high-to-low level fashion. High-level information is restricted by the two CNNs with smaller patches, allowing to keep the sensitivity high (large

6

patch) while devoting the specificity to the CNNs with smaller receptive fields.
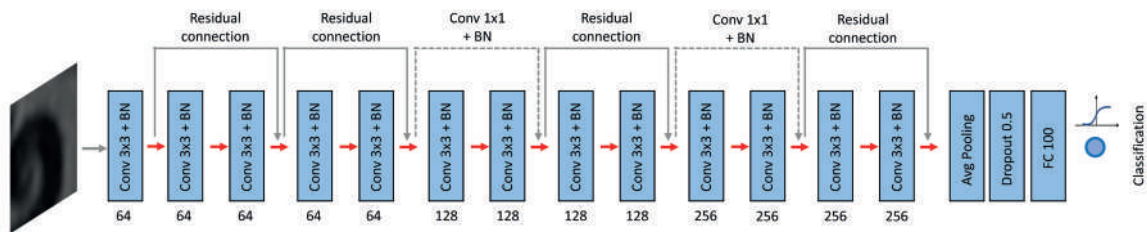

Figure. 4. Residual network architecture used for the cochlea detection model.
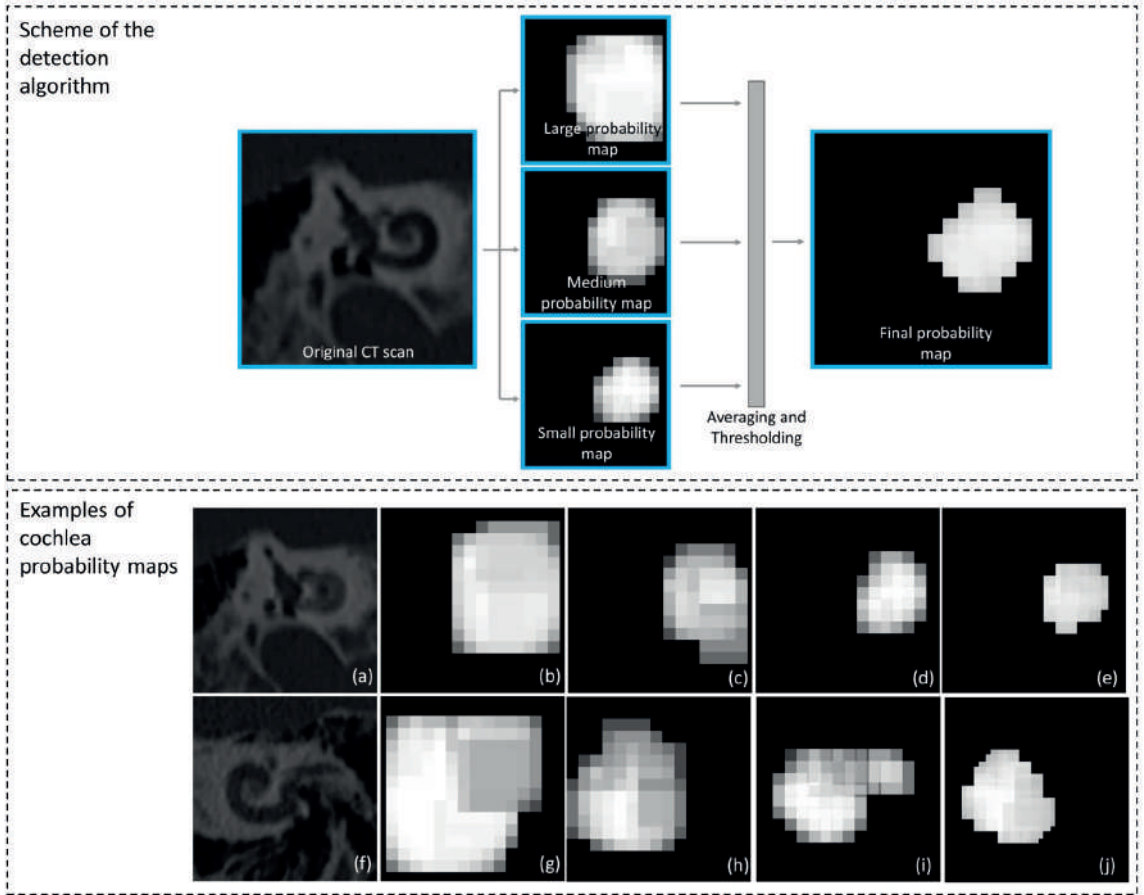
Figure. 5. (top) Schematic representation of the detection algorithm, which outputs a final probability map by averaging the results of the three CNNs (window size 150, 100, and 70 voxel side, stride equal to 10 voxels); (bottom) two examples of automatic cochlea detection showing all generated probability maps (b, g: 150x150 window; c, h: 100x100 window; d, i: 70x70 window; e, j: final map). The two examples show how the cochlea detection task can benefit from the proposed multi-scale approach. Especially, the second example shows how false positives (i.e. the connected auditory canal incorrectly detected by the 70 voxel-side CNN, panel (i)) are reduced and corrected in the final probability mask (panel (j)).

2.D. Cochlea Pixel-Wise Classification Model

A second model was developed for cochlea segmentation through pixel-wise classification. For this, a U-net-like architecture [32-34] composed of an encoder-decoder structure was implemented. This model learns the segmentation task in a supervised manner, by performing a pixel-wise mapping between the original image and the manually annotated mask. It is composed of an encoder-decoder structure as shown in Figure 6; the encoder part vectorizes the input bidimensional feature space via 3x3 convolutions and max pooling [35] operations (kernel size 2x2, stride equal to 2 voxels), while the decoder part recovers the information via 2x2 nearest-neighbour up-sampling followed by two 3x3 convolutional kernels. The outputs of the convolutional blocks from the encoding architecture are concatenated with each corresponding decoding step, leading to a high detail preservation of the original input image. In the last layer, a 1x1 convolution followed by a sigmoid activation function outputs the segmentation result in the form of a pixel-wise probability.

The network was trained on the largest image patches (150x150 voxels) using mini-batches of 4 examples and the Adam (adaptive moment estimation) optimization method [36], an algorithm that adapts the learning rate for each network weight by using first and second moments of the gradient. The initial learning rate was set to 10^{-3}, with an exponential decay every 10 epochs (over a maximum of 50 epochs). The energy function was computed by a pixel-wise softmax (equation 2) over the final feature map combined with the cross-entropy loss function (equation 3):

$$p_i(\boldsymbol{x}) = \frac{e^{x_i}}{\sum_{j=1}^{2} e^{x_j}}$$

(2)

$$Loss = -\sum_{i=1}^{2} t_i \log(p_i(\boldsymbol{x}))$$

(3)

In equation (2), the non-normalized output of the network is mapped to a probability distribution over the predicted output class, where the network output is encoded by the activation values x_i of each pixel i, resulting in the pixelwise network prediction $p_i(\boldsymbol{x})$.

In equation (3), the learning of the network is performed by penalizing (i.e. increasing) the loss in case of wrong predictions (compared to the ground truth labels t_i).

As for the detection model, accuracy during training was calculated on the validation set to prevent overfitting.
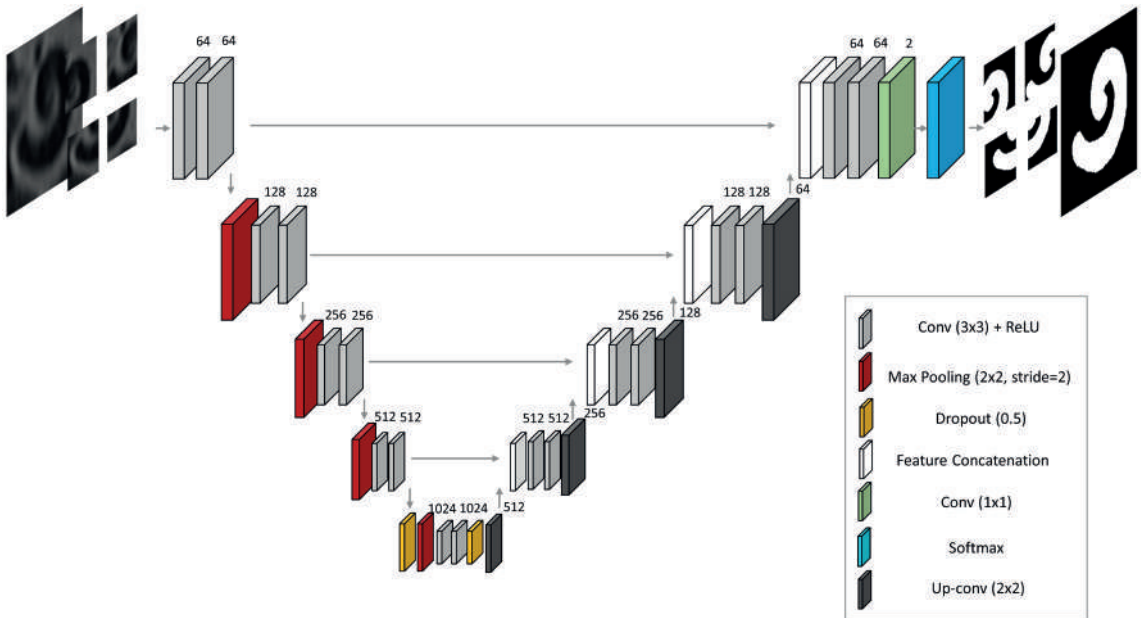
6

Figure. 6. Encoder-decoder network used in the pixel-wise classification model.

2.E. Main Algorithm for Cochlea Segmentation

The whole algorithm for cochlea detection and segmentation (Figure 7.a) combines the two previously described models (detection and pixel-wise classification).

The algorithm requires a single starting seed point to be defined at any location within the part of the image occupied by the cochlear volume. Given that the cochlea (or part of it) is always located approximately in the central area of each scan, this point was selected as the central pixel of each image. After this initialization, a square window (150x150 voxels) is generated around the seed, and processed by the detection model. A probability score is assigned to the window, with a probability higher than 0.5 associated with a positively predicted outcome. Then, an 8-connected

macro-region is grown starting from the seed point, with the macro-region containing 8 squared regions obtained by radially translating the first window along 8 different directions (0º, 45º, 90º, 135º, 180º, 225º, 270º, 315º), with a stride of 10 voxels. Translations of 45º, 135º, 225º, 315º were obtained by moving the region of interest by ±10 voxels in each direction in the (x,y) plane. These regions, translated diagonally, in addition to those translated by 0º, 90º, 180º, and 270º, were included to increase the algorithm sensitivity in this first step.

Each region is processed by the detection model, and the output probability of overlaying region parts is averaged. The process is iterated from each new positively predicted region, resulting in the macro-region to grow and cover the whole cochlear structure, and stops when no further areas fulfilling the detection criterion (probability ≥0.5) are found. The process is repeated for contiguous slices (always starting from the same seed point location) until positive regions are found, resulting in a 3D local probability map which displays the probability of voxels being cochlea. The same process is then applied for the other two window sizes (100 and 70 voxels side), and a final map is generated by averaging the three outputs.

After this step, the pixel-wise classification model is applied in the same manner as for the detection model (for partially overlaying regions, logical *or* operation is applied), and the result is then multiplied on a voxel-by-voxel level with the final probability map derived from the detection model. Voxels are then rounded to obtain the final segmentation.

6

2.F. Algorithm for Automatic Cochlea Measurements

After segmentation, the extracted cochlear structure undergoes an automatic analysis (Figure 7.b) to compute three different measurements: volume, cochlear duct length (CDL), and basal diameter of the cochlear basal turn. Cochlear volume is automatically measured by counting the number of cochlea voxels identified by the segmentation. The CDL was calculated from a previously proposed equation, which reliably estimates the distance from the middle of the round window to the helicotrema starting from the cochlear length [37], obtained as the longest dimension of the 3D bounding box enclosing the segmented cochlea. To automatically measure the basal diameter, the centerline was extracted from the 2D image slice containing the largest amount of cochlea voxels through a well-established iterative thinning algorithm [38], and the diameter was calculated as twice the distance between the basal endpoint of the centerline and the outer cochlear wall. The basal endpoint was automatically identified and distinguished from the apex endpoint through an additional CNN, which was simply trained to recognize the inner ear laterality given an input CT image slice. The CNN has the same architecture and hyperparameters as the ones used for the detection model, and was trained on 1,163 examples (427 left, 536 right cochleae), where each example was a single CT slice displaying the full inner ear anatomy. The network was then tested on an additional 200 slices (100 left, 100 right) and achieved 100% accuracy.
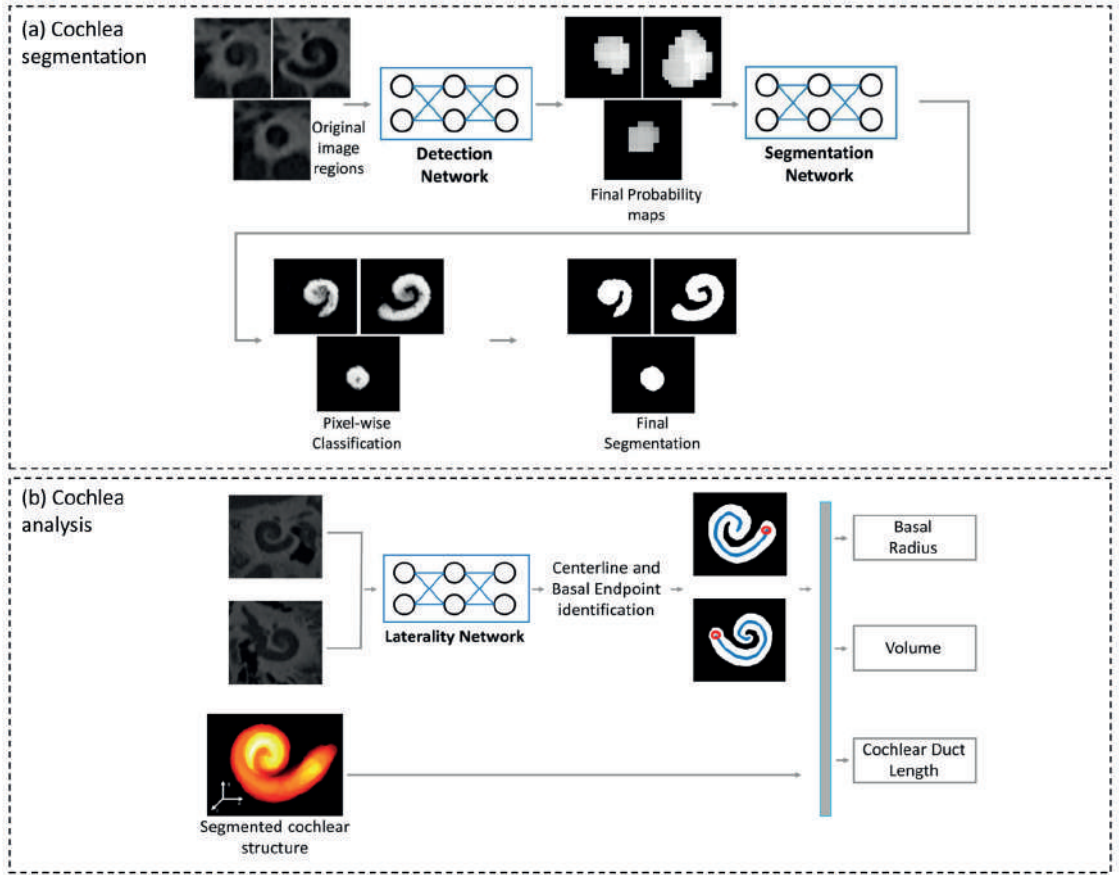
Figure. 7. Schemes for the (a) segmentation and (b) analysis algorithm.

2.G. Algorithm Performance Evaluation

The proposed pipeline was tested on 75 cochlea scans. The results of automatic cochlea segmentation were compared with the manually annotated scans using the four following metrics [39-41].

6

- Dice similarity, which measures the intersection between the two samples A and B over their union, ranging between 0 (no overlap) and 1 (perfect overlap)

$$Dice = \frac{2 \cdot |A \cap B|}{|A| + |B|} \tag{4}$$

- Boundary F1 (BF) score: defined as the harmonic mean of the precision (P) and sensitivity (S), it measures how close the boundary of the segmented object matches the ground truth contour

$$BF\ score = 2 \cdot \frac{P \cdot S}{P + S} \tag{5}$$

- Hausdorff distance, which calculates the highest distance (d) between the contours of the two compared samples (the lower is the value, the better is the segmentation result)

$$HD = max \left\{ \begin{array}{l} max_{a \in A} min_{b \in B}[d(a,b)], \\ max_{b \in B} min_{a \in A}[d(a,b)] \end{array} \right\} \tag{6}$$

- Averaged Hausdorff distance, which replaces the maximum operator in previous equation by averaging all distances, resulting in a more robust metric less sensitive to outliers.

For the automatic cochlea measurements, basal diameter, volume, and CDL were validated against the same measurements performed on the manually

annotated ground truth scans. All ground truth measurements were compared with the automatic measurements on a per patient basis. After validation, automatic measurements were extracted from all patient scans, to investigate the differences in cochlea size in the full cohort.

3. RESULTS

Some examples of automatic segmentation are reported in Figure 8. The testing of the segmentation algorithm (Table 1) against the manually annotated ground truth resulted in a Dice of 0.90±0.03, BF score of 0.95±0.03, Hausdorff distance of 3.05±0.39 voxels, and averaged Hausdorff distance of 0.32±0.07 voxels.

Automatic measurements (Table 2) resulted in absolute errors of 0.01 ml ± 0.008 ml (8.4%, volume), 1.69 mm ± 1.1 mm (5.5%, CDL), and 0.13 mm ± 0.10 mm (7.8%, basal diameter).

The size of the cochlea varied broadly among the patients in our dataset, ranging between 0.10 ml - 0.28 ml (volume), 1.3 mm - 2.5 mm (basal diameter), and 27.7 mm – 40.1 mm (CDL) (Figure 9 and Table 3).

6

Table 1. Results of automatic cochlea segmentation, compared to ground truth manual annotation

	Dice	BF-Score	Max Hausdorff Distance (voxel)	Average Hausdorff Distance (voxel)
Mean	0.90	0.95	3.05	0.32
Maximum	0.99	0.99	4.03	0.52
Minimum	0.87	0.92	1.62	0.11
Median	0.89	0.94	3.10	0.33
Standard deviation	0.03	0.02	0.39	0.07

Table 2. Errors between automatic and manual cochlear measurements

	Volume Error [ml]	Basal Diameter Error [mm]	CDL Error [mm]
Mean	0.013	0.134	1.693
Maximum	0.036	0.429	4.182
Minimum	0.0004	0	0.007
Median	0.011	0.115	1.657
Standard deviation	0.008	0.100	1.130

Table 3. Mean, maximum, minimum, median and standard deviation values for the cochlea measurements, for all patients in our cohort.

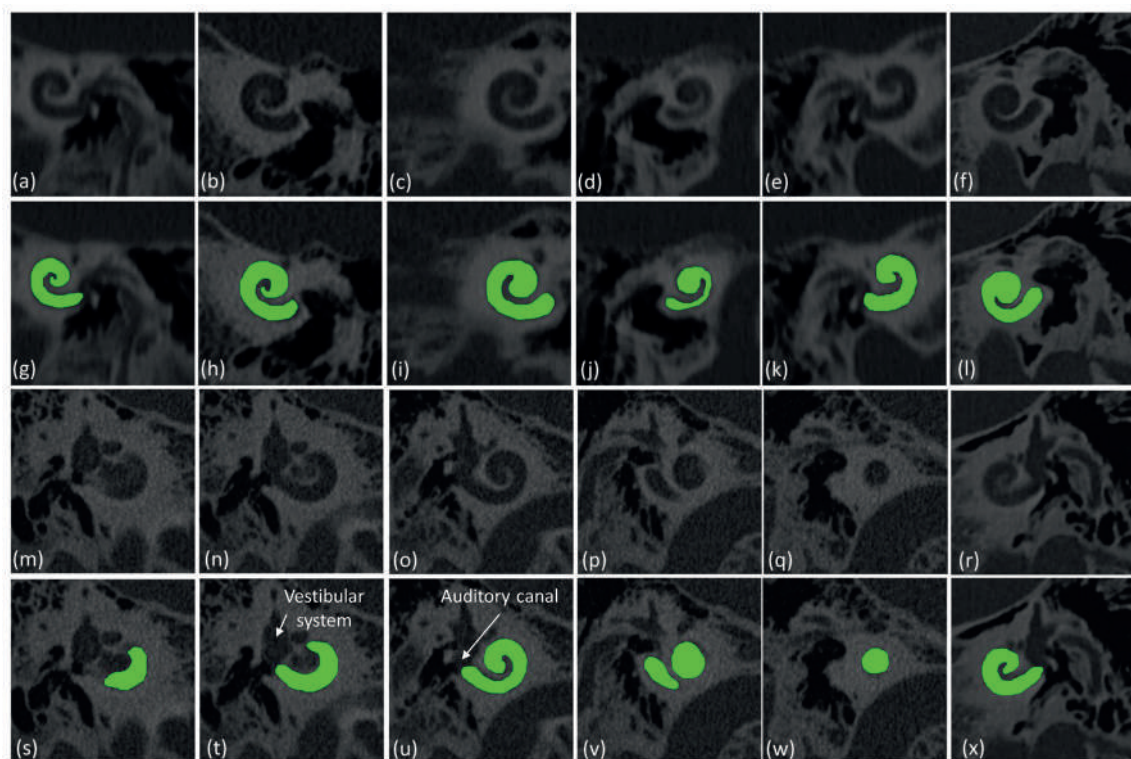|	Volume [ml]	Basal Diameter [mm]	Cochlear Duct Length [mm]
Mean	0.165	1.879	33.519
Maximum	0.280	2.531	40.127
Minimum	0.100	1.299	27.727
Median	0.161	1.877	33.620
Standard deviation	0.031	0.184	1.805
Mean			
Male (n=59)	0.171 ± 0.031	1.912 ± 0.184	33.815 ± 1.884
Female (n=64)	0.161 ± 0.030	1.849 ± 0.181	33.246 ± 1.697

Figure 8. Examples of original cochlea image slices (a-f, m-r), and respective segmentation results (g-l, s-x). The algorithm could correctly avoid the other structures connected to the cochlea, especially the vestibular system (t) and the external auditory canal (s, t, u). Images in panels (a), (c) - (f), (r) were acquired with the Precision UHR-CT scanner, while images in panels (b), (m) – (q) were acquired by the Proteus UHR-CT scanner.
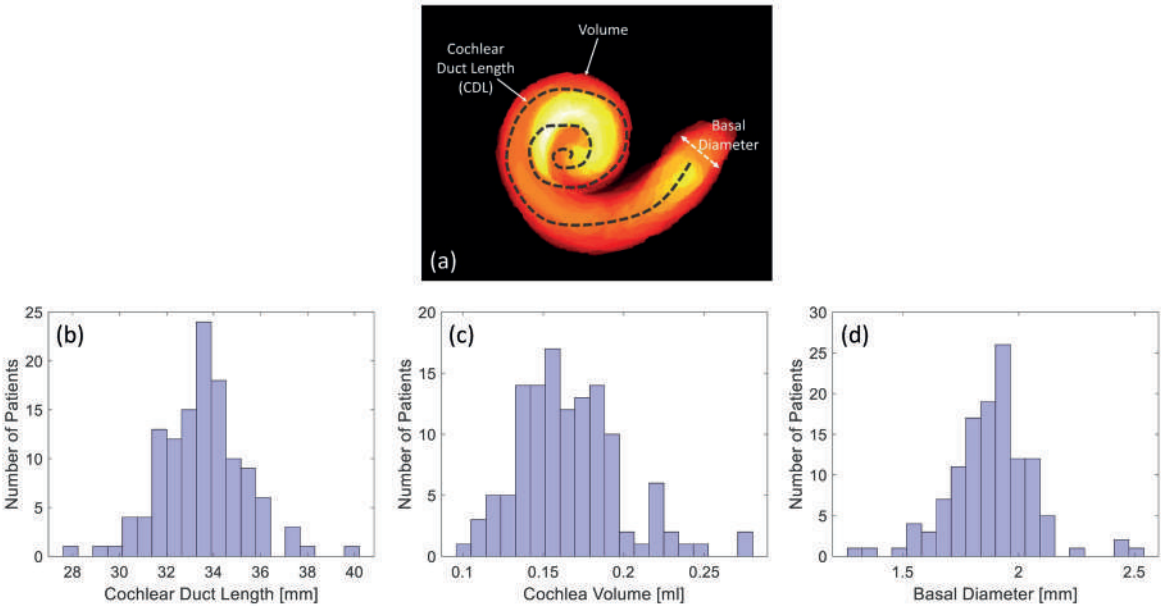
6

Figure 9. (a) Scheme of the extracted cochlear size measurements; (b)-(d) Histograms of the cochlear measurements for the evaluated patient cohort.

4. DISCUSSION

In this study, a deep learning-based system capable of segmenting and measuring the human cochlea on UHR-CT images was developed and validated, and used to investigate the differences in cochlea size in a large patient cohort.

The proposed system resulted in accurate cochlea segmentation and measurements, thanks to an extensive training data augmentation and the combination of different deep learning techniques.

The region-based, modular approach presented in this work achieved high performance by overcoming the issue of a limited dataset size (due to UHR-CT being made available in clinics only very recently). In fact, as opposed to full image-based approaches (that usually require much larger training sets), working on a multi-scale patch basis allowed to obtain a massive dataset from few scans, helping avoid the common issues related to deep learning and dataset size (such as overfitting and class imbalance) and leave the majority of the images for independent testing.

Incorporating a detection model into the encoder-decoder network allowed to reduce the search space of the segmentation network, decreasing the risk of false positives (examples shown in Figure 5) and the computational time (about 10 minutes for segmenting and analyzing a full cochlea on a 2.7GHz CPU, 8GB RAM workstation). Furthermore, the multi-scale approach for cochlea detection helped keep the specificity high, by localizing the segmentation only around cochlea regions, and therefore by avoiding anatomical parts which may be fully connected to the cochlea and that present the same intensity, such as the internal auditory canal, blood vessels or the vestibular system (Figure 8), without losing in sensitivity thanks to the averaging process of different window sizes. Finally,

6

restricting the segmentation only around regions showing the object of interest helped reduce the feature space processed by the subsequently applied U-Net, making the training process of the pixel-wise classification model easier and less prone to overfitting as opposed to working on a full image-basis.

The segmentation algorithm resulted in an average error of 10% (Dice), and the automatic measurements resulted in the highest error for the volume measurement (8%). Although these errors could limit the accuracy of our methods when measuring the human cochlea, their impact is implicitly lowered by the large variability in cochlea size across different patients highlighted by our results. This strengthens the reliability of the proposed approach in detecting the differences in cochlea size among different patients, holding the potential of being incorporated, in future and after additional extensive validation, into the cochlear imaging pipeline as a decision-making tool for cochlear implant surgery.

The main limitation of the proposed methods is the difficulty to objectively validate the measurements extracted from the segmented cochlea. For all comparisons, we considered manual annotation and measurements as the ground truth, due to the sparsity (or unavailability) of other validation methods. A more accurate approach could be performed using measurements with high-resolution, high-dose micro-CT scans acquired from cadavers, and comparing these results with the ones extracted from the same cochlea acquired in a clinical setting. However, a limited number of cadaver images is available, which would limit the validation process to too few cases. Furthermore, it would still be a completely image-based validation process, therefore potentially biased by specific image characteristics. This could be solved if the measurements

were physically performed on cochlea samples, but this approach carries the additional limitations of a very low number of available specimens, along with the difficulty to accurately drill the surrounding temporal bone for sample preparation.

Prior to moving to personalized cochlear implant modelling, several technical issues need to be overcome. Specifically, before implementing the proposed measurement approach on a clinical routine-basis, prospective clinical trials need to be performed to investigate whether the size of the cochlea correlates with the surgical and clinical outcome of cochlear implantation, currently performed with fixed-size electrodes. Especially, correlation between cochlear size and post-operative loss of residual hearing should be investigated, to test the hypothesis that smaller cochleae could be at higher risk of traumatic electrode insertion which, in turn, would lead to a higher loss residual hearing. Furthermore, since UHR-CT is not yet commonly used in clinical practice, the possibility of obtaining similar cochlear measurement performance with conventional CT should be investigated. While previous studies showed encouraging results in cochlear segmentation obtained from conventional CT [6]-[8], much larger datasets are needed for testing. Since such datasets are currently unavailable, we can only hypothesize that UHR-CT helps reduce measurement errors compared to conventional CT (given the small size of the human cochlea), and consequently potentially leads to an improved surgical outcome in personalized cochlear implant surgery. Therefore, while UHR-CT and Artificial Intelligence seem to have promising applications for personalized surgical planning, future studies are needed to confirm their effective performance, quantify their effect on the surgical outcome, and evaluate the potential advantages over normal resolution CT.

6

In addition to this, future work includes the collection of additional patient scans to further assess the appropriateness of our methods, and potentially the development of other computational strategies to further improve the segmentation performance (for example, 3D-based methods that take advantage of weakly-supervised learning to address the issue of annotating a large dataset). Finally, the extracted cochlea measurements will be related to the loss of residual hearing after cochlear implant surgery, to investigate the effect of cochlear size on speech recognition abilities after cochlear implantation.

5. CONCLUSIONS

The developed computerized system was successfully applied to extract automatic and accurate cochlear measurements based on UHR-CT images, thanks to the combination of multiple deep learning approaches and extensive data augmentation. The system highlighted a large variability in cochlea size in a large patient cohort, suggesting that the proposed approach could therefore potentially be useful as a pre-operative tool for future personalized cochlear implant surgery.
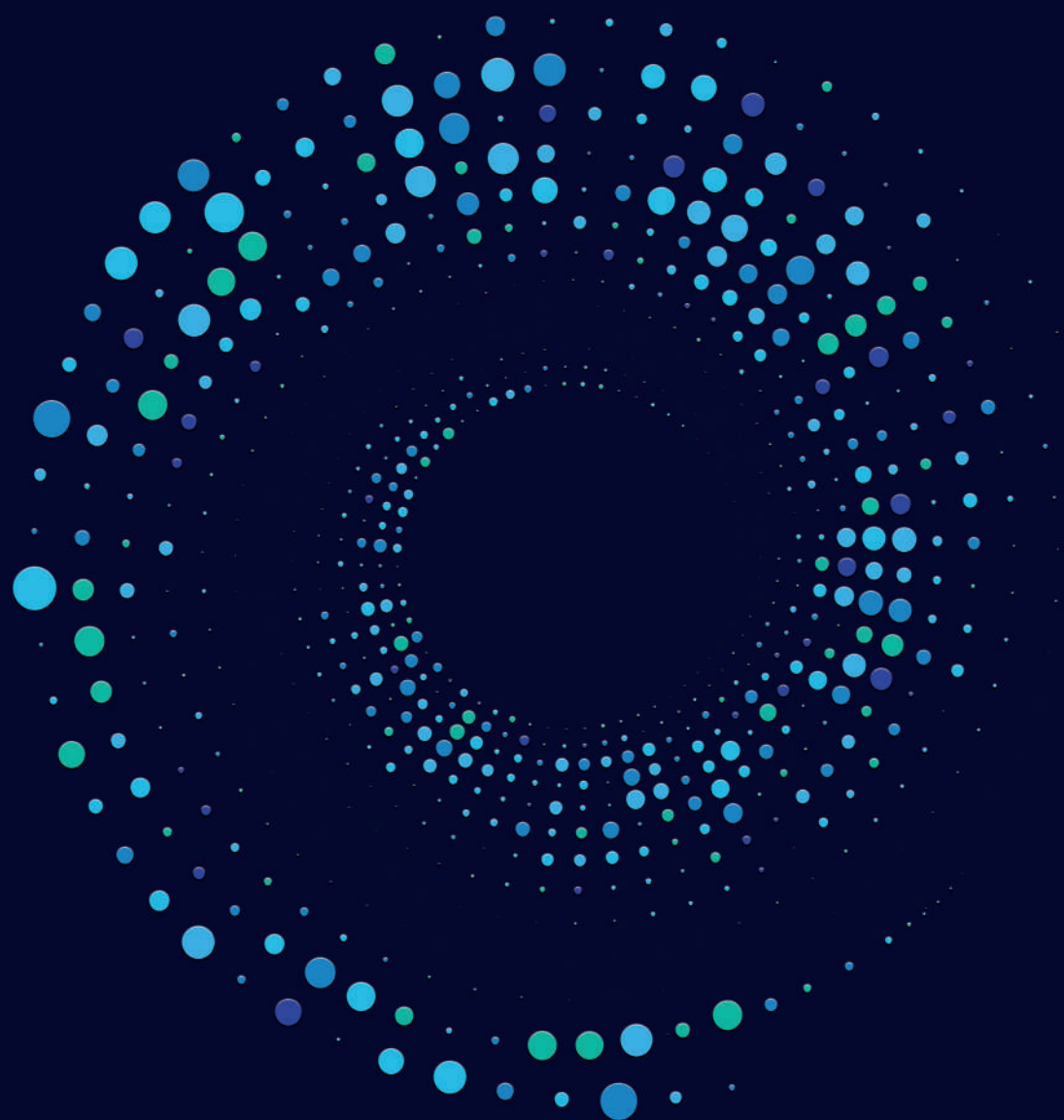
References

1. Peterson NR, Pisoni DB, Miyamoto RT. Cochlear implants and spoken language processing abilities: review and assessment of the literature. Restor Neurol Neurosci. 2010;28(2):237-50.

2. Whiting BR, Bae KT, Skinner MW. Cochlear Implants: Three-dimensional Localization by Means of Coregistration of CT and Conventional Radiographs. Radiology 2001; 221:543–549.

3. Turner CW, Gantz BJ, Vidal C, Behrens A, Henry BA. Speech recognition in noise for cochlear implant listeners: benefits of residual acoustic hearing. J Acoust Soc Am. 2004 Apr;115(4):1729-35.

4. Dorman MF, Loizou PC, Rainey D. Simulating the effect of cochlear-implant electrode insertion depth on speech understanding. J Acoust Soc Am. 1997 Nov;102(5 Pt 1):2993-6.

5. Xianfen D, Siping C, Changhong L, Yuanmei W. 3D semi-automatic segmentation of the cochlea and inner ear. Conf Proc IEEE Eng Med Biol Soc. 2005;6:6285-8.

6. Noble JH, Rutherford BR, Labadie RF, Majdani O, Dawant BM. Modeling and segmentation of intra-cochlear anatomy in conventional CT. Conf Proc SPIE Med Im. 2010;7623,762302.

7. Noble JH, Labadie RF, Majdani O, Dawant BM. Automatic segmentation of intracochlear anatomy in conventional CT. IEEE Trans Biomed Eng. 2011 Sep;58(9):2625-32.

8. Reda FA, Dawant BM, McRackan TR, Labadie RF, Noble JH. Automatic segmentation of intra-cochlear anatomy in post-implantation CT. Conf Proc SPIE Med Im. 2013;8671,867101.

6

9. Reda FA, McRackan TR, Labadie RF, Dawant BM, Noble JH.
    Automatic segmentation of intra-cochlear anatomy in post-
    implantation CT of unilateral cochlear implant recipients. Med
    Image Anal. 2014 Apr;18(3):605-15.

10. Pujadas ER, Kjer HM, Vera S, Ceresa M, Ballester MAG. Cochlea
    segmentation using iterated random walks with shape prior. Conf
    Proc SPIE Med Im. 2016;9784,97842U.

11. Verbist BM, Ferrarini L, Briaire JJ, Zarowski A, Admiraal-Behloul F,
    Olofsen H, Reiber JH, Frijns JH. Anatomic considerations of cochlear
    morphology and its implications for insertion trauma in cochlear
    implant surgery. Otol Neurotol. 2009;30(4):471-7.

12. Rybicki FJ, et al. Initial evaluation of coronary images from 320-
    detector row computed tomography. Int J Cardiovasc Imaging
    2008;24;535–546.

13. Duan X, et al. Electronic Noise in CT Detectors: Impact on Image
    Noise and Artifacts. AJR 2013;201:626-632.

14. Hata A, et al. Effect of Matrix Size on the Image Quality of Ultra-
    high-resolution CT of the Lung: Comparison of 512 × 512,
    1024 × 1024, and 2048 × 2048. Acad Radiol. 2018;25(7):869-876.

15. Oostveen L, et al. Physical evaluation of an ultra-high-resolution CT
    scanner. European Radiology, In Press.

16. Dalmış MU, et al. Using deep learning to segment breast and
    fibroglandular tissue in MRI volumes. Med Phys. 2017;44(2):533-
    546.

17. Sun W, Huang X, Tseng T-LB; Qian W. Automatic lung nodule graph
    cuts segmentation with deep learning false positive reduction. SPIE
    Proc. Med. Im. 2017;10134. https://doi.org/10.1117/12.2251302

18. Russakovsky O, et al. ImageNet Large Scale Visual Recognition
    Challenge. arXiv:1409.0575, 2015.

19. Ganesan K, et al. Computer-Aided Breast Cancer Detection Using
    Mammograms: A Review. IEEE Reviews on Biomedical Engineering
    2013, 6:77-97.

20. Oakden-Rayner L, et al. Precision Radiology: Predicting longevity
    using feature engineering and deep learning methods in a radiomics
    framework. Sci Rep. 2017, 10;7(1):1648.

21. Litjens G, A survey on deep learning in medical image analysis.
    Medical Image Analysis 2017, 42:60-88.

22. Al-antari MA, et al. A fully integrated computer-aided diagnosis
    system for digital X-ray mammograms via deep learning detection,
    segmentation, and classification. International Journal of Medical
    Informatics 2018, 117:44-54.

23. Cheng JZ, et al. Computer-Aided Diagnosis with Deep Learning
    Architecture: Applications to Breast Lesions in US Images and
    Pulmonary Nodules in CT Scans. Sci Rep. 2016, 15;6:24454.

24. Truhn D, et al. Radiomic versus Convolutional Neural Networks
    Analysis for Classification of Contrast-enhancing Lesions at
    Multiparametric Breast MRI. Radiology 2019, 290(2):290-297.

25. Kooi T, et al. Large scale deep learning for computer aided
    detection of mammographic lesions. Med Image Anal. 2017,
    35:303-312.

26. Tanaka R, Yoshioka K, Takagi H, Schuijf JD, Arakita K. Novel
    developments in non-invasive imaging of peripheral arterial disease
    with CT: experience with state-of-the-art, ultra-high-resolution CT
    and subtraction imaging. Clin Radiol. 2019 Jan;74(1):51-58.

6

27. He K, Zhang X, Ren S, Sun J. Deep Residual Learning for Image Recognition. IEEE Conf on Comp Vis and Patt Recogn 2016. arXiv:1512.03385.

28. Peng J, Kang S, Ning Z, et al. Residual convolutional neural network for predicting response of transarterial chemoembolization in hepatocellular carcinoma from CT imaging. Eur. Radiol. 2019; doi: 10.1007/s00330-019-06318-1.

29. Srivastava N, Hinton G, Krizhevsky A, Sutskever I, Salakhutdinov R. Dropout: A Simple Way to Prevent Neural Networks from Overfitting. J of Machine Learning Research 2014;15;1929-1958.

30. Glorot X, Bengio Y. Understanding the difficulty of training deep feedforward neural networks. PMLR 2010;9:249-256.

31. Li M, Zhang T, Chen Y, Smola AJ. Efficient mini-batch training for stochastic optimization. KDD 2014;661-670.

32. Ronneberger O, Fischer P, Brox T. U-Net: Convolutional Networks for Biomedical Image Segmentation. MICCAI 2015. arXiv:1505.04597.

33. Weston AD, Korfiatis P, Kline TL, Philbrick KA, Kostandy P, Sakinis T, Sugimoto M, Takahashi N, Erickson BJ. Automated Abdominal Segmentation of CT Scans for Body Composition Analysis Using Deep Learning. Radiology. 2019 Mar;290(3):669-679.

34. Norman B, Pedoia V, Majumdar S. Use of 2D U-Net Convolutional Neural Networks for Automated Cartilage and Meniscus Segmentation of Knee MR Imaging Data to Determine Relaxometry and Morphometry. Radiology 2018 Jul; 288(1):177-185.

35. Nagi J, Ducatelle F, Di Caro GA. Max-pooling convolutional neural networks for vision-based hand gesture recognition. Conf Proc IEEE ICSIPA 2011; 10.1109/ICSIPA.2011.6144164.

36. Kingma DP, Ba J. Adam: A Method for Stochastic Optimization. Conf Proc Int Conf for Learning Representations 2015;arXiv:1412.6980.

37. Alexiades G, Dhanasingh A, Jolly C. Method to estimate the complete and two-turn cochlear duct length. Otol Neurotol. 2015 Jun;36(5):904-7.

38. Lam L, Lee SW, Suen CY. Thinning methodologies-a comprehensive survey. IEEE Trans Pattern Analysis and Machine Intelligence 1992;14(9): 869-85.

39. Taha AA, Hanbury A. An efficient algorithm for calculating the exact Hausdorff distance. IEEE Trans Pattern Anal Mach Intell. 2015 Nov;37(11):2153-63.

40. Csurka G, Larlus D, Perronnin F. What is a good evaluation measure for semantic segmentation? BMVC 2013. 10.5244/C.27.32.

41. Dubuisson MP, Jain AK. A modified Hausdorff distance for object matching. Proceedings of 12th International Conference on Pattern Recognition (ICPR '94). 1994;566–568. DOI: 10.1109/ICPR.1994.576361

6

7

General discussion

General discussion

With improved technical, surgical and audiological knowledge about cochlear implantation, complexity in this path of care has increased. Besides the generally known patient specific biographic and audiometric factors of influence (e.g. age at implantation, cognitive function, duration of deafness, and pre-operative state of hearing and speech recognition), factors related to the electrode design have become more important in terms of performance outcome for the recipients. The last three decades, CI manufacturers have developed an own philosophy on design-related factors responsible for the best speech perception result for the patient. This resulted in a broad range of electrode types to select from. However, to choose the right electrode type, knowledge regarding the effect of electrode type, electrode position, insertion behavior of a specific electrode type in an individual patient and tissue reaction following the surgical introduction of a specific 'foreign body' into the cochlea, is needed. Moreover, it is a task for the CI clinician to critically review electrode related factors and provide manufacturers with information to further improve the electrode design.

In this thesis, ultra-high-resolution computed tomography (UHR-CT) imaging was used as a tool to visualize the cochlea, and in particular, electrode position and tissue reaction within the implanted cochlea. The thesis consists of two parts. In the first part, surgical technique and cochlear implant electrode positional factors were investigated in relation to clinical outcome for the CI patient. Electrode positional factors investigated were electrode type, angular insertion depth, scalar location, and wrapping factor. In the second part, the UHR-CT imaging was used to develop two

7

new methods to measure factors potentially associated with CI performance: I) a method to post-operatively assess the presence of new bone formation around the cochlear implant electrode, and II) a method to automatically segment and measure the human cochlea dimensions, to investigate differences in cochlea size and to substantiate electrode selection for individual patients.

Key findings and clinical implications

The aim in part 1 of this thesis was to find possible effects of electrode type, angular insertion depth, scalar location, wrapping factor and surgical approach on speech perception with CI. We found that implantation with a precurved electrode gives the best speech perception in quiet and in noisy conditions. As expected by design the wrapping factor of the precurved electrode was smaller compared to the straight electrode. Based on the results of our study (Chapter 2) and studies in literature [1] we believe that the superior speech perception outcome of the precurved electrode is best explained by the close position to the modiolus of this electrode. Close proximity to the modiolus gives lower thresholds [2], improved pitch discrimination [3], and improved channel separation [4], potentially all contributing to improved speech perception of the precurved electrode. We found no effect of insertion depth of the electrode on speech perception; not in the clinical trial (Chapter 2), nor in a systematic review (Chapter 1). Interestingly, at the start of my thesis in 2017, it was generally accepted to use straight electrodes for the purpose of residual hearing preservation, as these were assumed to be less traumatic compared to precurved electrodes available at that time. We showed that this assumption was incorrect for two reasons (Chapter 2). First, as described

above, the precurved electrode outperformed the straight electrode on speech perception, and second, the participants implanted with a straight electrode completely lost their residual hearing during the follow-up of this study (mean follow-up time 3.8 years; SD 1.7; range 1.2–7.7 years).

Clinical Implication(s) I: In our clinic (Radboudumc, Nijmegen, The Netherlands), patients with a normal cochlear anatomy, regardless of the pre-operative hearing threshold, are now preferably implanted with a precurved electrode (if produced by the manufacturer of choice).

In another clinical study (Chapter 3) we investigated the slim perimodiolar electrode (SPE), a precurved electrode, which was introduced in 2016, implanted via a cochleostomy approach. This electrode was developed to combine two electrode properties (hypotraumatic and modiolus hugging), which in older generation electrodes have shown to be contradictory [5]. Our study showed that the SPE, once correctly positioned in the scala tympani, provides good preservation of residual hearing. However, in over one-third of the participants (36%) a translocation was found. In these participants the entire electrode was located in the scala vestibuli suggesting the translocation occurred at or directly after the cochleostomy. These cochleostomy associated translocations showed to be detrimental for the residual hearing, as the loss was 4 times higher compared to participants with scala tympani position. In literature the number of translocations using the round window or extended round window technique were significantly lower compared to our study [6-9]. This study also brought the important insight that a SPE carries a risk of tip-fold over, underscoring the need for intra-operative control of the position for this electrode (Chapter 3).

7

Clinical implication(s) II: First, the slim, precurved electrode is preferred invpatients with residual hearing. Speech perception results are registered in a prospective follow-up study to confirm the hypothesis that the SPE provides equal or superior results compared to the previous generation precurved electrode (which were shown to be superior compared to the straight electrode in chapter 2). Second, in our clinic, if the anatomical situation allows it, it is preferred to insert the slim perimodiolar electrode through a round window or extended round window approach, rather than making a cochleostomy. Third, when implanting a SPE, intra-operative control for potential tip-fold over is standard in all patients.

In part 2 of this thesis we studied how two new imaging measuring methods could improve current or future CI care. First, using Ultra-High Resolution CT imaging (UHR-CT), we showed that in vivo detection of tissue reaction in proximity of the cochlear implant electrode, in particular, new bone formation (NBF), is possible. There was a strong reliability between two radiologists (85%) scoring NBF and it appeared that the majority of CI patients (68%) is likely to develop NBF after cochlear implantation. This NBF was predominantly located at the basal area of the cochlea (92% of the NBF located next to the 10 most basal electrodes contacts), which was in accordance with histopathological studies [10-15]. NBF was seen more often in patients with a longer follow-up time, and patients with surgical parameters that are considered more traumatic (Scala Vestibuli position / Translocation, Precurved electrode (previous generation, not the SPE), and Cochleostomy) seem to be associated with increased risk of developing NBF. However, these surgical factors were also correlated with longer follow-up time and therefore an evidence based conclusion on which surgical factors increase the risk on NBF could not be drawn. We did show a negative effect of NBF on residual hearing, as participants with NBF had

higher loss of long term residual hearing loss (mean absolute pre- and post-operative difference in PTA of 22.9dB) compared to participant without NBF (mean absolute pre- and post-operative difference in PTA of 8.6dB). In this analysis follow-up time was not different between groups, and higher than the natural hearing loss of the contralateral ear.

The second imaging method, described in part 2 of this thesis, showed that automatic and successful segmentation and analysis of the cochlea using UHR-CT images results in accurate automated measurements of cochlear anatomical dimensions. Given the wide variation in cochlear size found in our patient cohort (ranging between 0.10 and 0.28 ml (volume), 1.3 and 2.5 mm (basal diameter), and 27.7 and 40.1 mm (Cochlear Duct Length), this automated method might, after further development, find its application as a pre-operative tool in future cochlear implant surgery. This potentially improves personalized treatment strategies based on patient-specific, image-based anatomical measurements.

Research implication(s) I: Based on Part II of this thesis a new prospective UHR-CT imaging study has been initiated with five consecutive UHR-CT's in 2 years per participant. A preoperative UHR-CT will be used for automated cochlear size measurements to investigate the clinical influence of cochlear size. In the first and second year after implantation 4 scans will be obtained to evaluate the occurrence and development of tissue fibrosis, in particular new bone formation, the associated surgical and electrode positional factors, and the clinical influence of the formation / presence of NBF.

7

The future of the cochlear implant electrode position

The basic principle of cochlear implants is relatively straightforward. Basically, cochlear implantation is about organized electric stimulation of tonotopically-structured afferent hearing nerve fibers. The interface between these two elements is formed by the electrode contacts on the array of the cochlear implant on one side, and neuronal elements like dendrites and ganglion cells of the cochlear nerve with Rosenthal's canal on the other side. It is therefore easy to imagine that the position of the cochlear implant electrode could be critical. However, one has to take into mind that the electrical current used in clinical practice implicates a wide spread of excitation within the cochlea. As a result, while at most a CI has 22 electrode contacts in consecutive channels, only 4-7 channels stimulate the spiral ganglion cells independently. In normal hearing subjects this is assessed at 30-50 channels [16]. Larger spread of excitation causes more channel interaction. It is believed that a larger number of independent channels may improve selective stimulation and therefore the listening experience of patients [4]. Improving the electrode position might allow for more selective stimulation. This thesis showed that precurved electrodes with close proximity to the spiral ganglion cells (- i.e. modiolus) gives high speech perception, which we believe is a result of a more selective stimulation.

Feasible steps in further improvement of the electrode – cochlea interface could be done by innovations on: further improvement of the electrode position, the prevention of neural damage and degeneration, or the prevention of tissue formation compromising the electrode to neuron interface.

Improving electrode position

Since the most recent precurved electrodes are capable to combine a hypotraumatic insertion and a perimodiolar position, future development of electrodes and surgical techniques could focus on even closer proximity to the modiolus without compromising cochlear structure due to trauma. Current perimodiolar electrodes curve around the modiolus in a passive way using the precurved properties and an insertion tool. Future designs could include robotic insertion [17]. A robotic arm could control pressure and direction in a perfect manner. Moreover, in near future it is possible to use intra-operative control systems which can warn a CI surgeon (or robotic systems) if structure is (about to be) damaged permanently. Electrocochleographic (ECochG) signals captured by the tip of the electrode array during insertion have shown to function as a measure of cochlear health [18], and clinical application is currently investigated in several research trials globally. Considering the above current developments, one can "imagine" future techniques working towards a cochlear implant electrode which contains an automated system that can actively position itself in the cochlea in the closest perimodiolar position possible, without damaging or even touching any cochlear structure.

Preventing neural degeneration or damage

Improvement in electrode design goes hand in hand with prevention of neural damage as it is clear the world of CI has moved towards structure preservation. In this thesis it was shown that in our clinic translocation to the scala vestibuli was less likely when using the round window approach compared to the cochleostomy approach (Chapter 3). In addition,

7

molecular and cellular damage, not directly visible on imaging, could result in the loss of neural tissue [19]. There are several advantages of structure preservation by minimizing trauma, as it offers: (1) the possibility for electric – acoustic stimulation (EAS) in patients with significant levels of pre-operative low frequency hearing [20], (2) limitation of the amount of intracochlear tissue fibrosis or new bone formation (see the next paragraph *"Preventing tissue formation blocking electrode – interface")*, and (3) any direct effect of preservation of cochlear structure on CI performance when using electric only stimulation [21]. Moreover, structure preservation might be important for the purpose of future increased and advanced stimulation techniques, as these will require more healthy neural tissue compared to the current electrode arrays and stimulation strategies [22].

Preventing tissue formation blocking CI electrode interface

As shown in this thesis tissue formation in the proximity of the cochlear implant electrode array is common (Chapter 4). New bone formation is correlated with loss of long-term residual hearing (Chapter 4). Follow-up studies are currently investigating any direct effect of tissue formation on speech perception on our clinic (Radboudumc, The Netherlands). Preventing such tissue is a feasible option for future CI improvement. Besides reducing insertion trauma, tissue formation due to a foreign body response on the presence of the inserted electrode might be reduced or prevented by anti-inflammatory drugs. A future opportunity are electrode integrated drug delivery systems, allowing for a steady infusion of the anti-inflammatory drugs [23, 24].

CI electrode position studies; key findings

Conducting this research has made me realize that there are three key points to consider in CI research when investigating cochlear implants in general, and CI electrode design and position in particular. These issues may be considered either a methodological flaw or strength in CI research, and are discussed separately below.

First, most CI literature consists of observational studies. When a study is not randomized, the study contains a higher risk of bias. I believe one element of observational research that can be easily overlooked is the fact that observational CI research automatically includes a wide variety of clinical choices which might, besides the investigated factors, also influence the performance with CI. One example is related to the pre-operative factors that are used to select an electrode type. Two studies in the systematic review of chapter 1 included more than five electrode types of different manufacturers without mentioning the criteria on which the electrodes were selected. As it is likely that the choice of the electrode in clinics is not random, it is inevitable that there is a thus selection bias. The factors used for selection (e.g. pre-operative state of hearing) are related to the characteristics of the electrode types. The study design of Chapter 2 of this thesis is an example of this type of selection which we acknowledged and accounted for it in our analysis. Correlations between factors of interest and other factors which also potentially influence the outcome go beyond selection of electrode type. Age at implantation and cognition is another example of factors that have been shown to be related in literature [25]. Therefore, all studies in literature not investigating both factors, or not considering that this relationship might have influenced results, could have

7

drawn false conclusions on one of those factors. Clinical cochlear implantation is a complex matrix of factors with correlations between these factors. Future observational studies should, as a minimal standard, always consider and address these types of selection and confounding bias and if possible statistically correct for them.

The second issue is both challenging as it is exciting for future research. All CI researchers should realize that cochlear implantation, as a whole, is moving "forward" quickly. This means that factors that deemed important 10 years ago, may not have (equal) influence in current times. One example, is 'duration of deafness' [26, 27]. It was one of the most acknowledged factors to influence speech perception with a cochlear implant for a long time, but in current CI practice it might not be so relevant for the largest group of patients. The physiological explanation for the negative effect of long duration of deafness is that a long-term unstimulated auditory nerve (- e.g. 30 years or more) may not be stimulated properly with a CI due to neural degeneration. This factor was of considerable importance when CI was still an unknown new technique. In those times a large group of patients had not used any adequate form of hearing for many years. However, in present day high-power hearing aids are standard and CI is more common, especially in western civilization, and if a patient fails at recognizing speech with optimally fitted hearing aids he / she will be referred to a CI clinic. Therefore, it might be better to state, the absolute influence of duration of deafness on speech perception has decreased because of the contemporary options with hearing aids for severe hearing loss and the fact that long duration of deafness is not as common as it used to be. Changing influence over time for other factors,

potentially influencing speech perception, with a less obvious physiology might also be realistic, especially with the changes in indication criteria and rapid development of CI designs [28].

The third and final issue is especially important for researchers investigating electrode position. The electrode position that is measured is largely dependent on the electrode type that is implanted. There is a limited number of manufacturers with a limited number of electrode types. A researcher should always consider an electrode position measurement in line with the implanted electrode type, as these factors (electrode type and position) are highly dependent. For example, a measured insertion depth, is the relative depth as a result of a specific electrode (with a pre-defined length and certain tendency to curve around the modiolus) inserted to a particular depth by a surgeon in a patient which has an individual cochlear size and shape. All of these factors could influence the final depth of insertion, and therefore insertion depth cannot be seen independently from these factors. A specific example, the straight electrode used in the study in chapter 2 can be inserted to two markers labeled by the manufacturer on the electrode, the markers are 5mm apart. If in the one patient the electrode is inserted to the first marker, and in a second patient to the second marker, the absolute difference is 5mm, the latter will likely result in a deeper insertion, however the difference in measured insertion depth might be different than the 5mm depending on the position relative to the modiolus and the anatomical dimensions of the cochlea in each of the individual patients. Moreover, the 5mm deeper insertion means similar coverage of the cochlea but the coverage shifted to a deeper area. This means that in the basal area, an area of 5mm is not directly covered. Thus,

7

in literature many electrode positional factors appear to be measured objectively and independently, but are largely dependent on the electrode type, other positional factors, surgical technique, and individual cochlear dimensions. In CI electrode position research, these details should therefore always be reported and taken into account, or if possible standardize for all patients.

Conclusion

Because of its multifactorial determination, research in cochlear implantation is complex yet rewarding as eventually outcome of research may lead to improvement of speech perception for individual patients. In terms of the choice of electrodes, our findings have currently led to a preference for a precurved electrode in adult patients with a normal anatomy of the cochlea and possible residual hearing.

References

1.   Holder, J.T., et al., *Matched Cohort Comparison Indicates Superiority of Precurved Electrode Arrays.* Otol Neurotol, 2019. **40**(9): p. 1160-1166.

2.   Perenyi, A., et al., *Electrophysiological measurements with electrode types of different perimodiolar properties and the same cochlear implant electronics - a retrospective comparison study.* J Otolaryngol Head Neck Surg, 2019. **48**(1): p. 46.

3.   Ramos Macias, A., et al., *Importance of Perimodiolar Electrode Position for Psychoacoustic Discrimination in Cochlear Implantation.* Otol Neurotol, 2017. **38**(10): p. e429-e437.

4.   Berg, K.A., et al., *Speech recognition as a function of the number of channels in perimodiolar electrode recipients.* J Acoust Soc Am, 2019. **145**(3): p. 1556.

5.   Wanna, G.B., et al., *Impact of electrode design and surgical approach on scalar location and cochlear implant outcomes.* Laryngoscope, 2014. **124 Suppl 6**: p. S1-7.

6.   Hey, M., et al., *Objective, audiological and quality of life measures with the CI532 slim modiolar electrode.* Cochlear Implants Int, 2019. **20**(2): p. 80-90.

7.   McJunkin, J.L., et al., *Early Outcomes With a Slim, Modiolar Cochlear Implant Electrode Array.* Otol Neurotol, 2018. **39**(1): p. e28-e33.

8.   Ramos-Macias, A., et al., *Hearing Preservation with the Slim Modiolar Electrode Nucleus CI532(R) Cochlear Implant: A Preliminary Experience.* Audiol Neurootol, 2017. **22**(6): p. 317-325.

9.   Shaul, C., et al., *Scalar localisation of peri-modiolar electrodes and speech perception outcomes.* J Laryngol Otol, 2018. **132**(11): p. 1000-1006.

10.   Fayad, J.N., A.O. Makarem, and F.H. Linthicum, Jr., *Histopathologic assessment of fibrosis and new bone formation in implanted human temporal bones using 3D reconstruction.* Otolaryngol Head Neck Surg, 2009. **141**(2): p. 247-52.

11.   Ishai, R., et al., *The pattern and degree of capsular fibrous sheaths surrounding cochlear electrode arrays.* Hear Res, 2017. **348**: p. 44-53.

12.   Kamakura, T. and J.B. Nadol, Jr., *Correlation between word recognition score and intracochlear new bone and fibrous tissue*

7

after cochlear implantation in the human. Hear Res, 2016. **339**: p. 132-41.

13. O'Leary, S.J., et al., *Relations between cochlear histopathology and hearing loss in experimental cochlear implantation.* Hear Res, 2013. **298**: p. 27-35.

14. Sheikh, Z., et al., *Macrophages, Foreign Body Giant Cells and Their Response to Implantable Biomaterials.* Materials (Basel), 2015. **8**(9): p. 5671-5701.

15. Somdas, M.A., et al., *Quantitative evaluation of new bone and fibrous tissue in the cochlea following cochlear implantation in the human.* Audiol Neurootol, 2007. **12**(5): p. 277-84.

16. Richter, C.P., S. Rajguru, and M. Bendett, *Infrared neural stimulation in the cochlea.* Proc SPIE Int Soc Opt Eng, 2013. **8565**: p. 85651Y.

17. Schneider, D., et al., *Robotic cochlear implantation: feasibility of a multiport approach in an ex vivo model.* Eur Arch Otorhinolaryngol, 2019. **276**(5): p. 1283-1289.

18. Bester, C.W., et al., *Characterizing Electrocochleography in Cochlear Implant Recipients with Residual Low-Frequency Hearing.* Front Neurosci, 2017. **11**: p. 141.

19. Eshraghi, A.A., et al., *Molecular mechanisms involved in cochlear implantation trauma and the protection of hearing and auditory sensory cells by inhibition of c-Jun-N-terminal kinase signaling.* Laryngoscope, 2013. **123 Suppl 1**: p. S1-14.

20. Gantz, B.J., et al., *Preservation of hearing in cochlear implant surgery: advantages of combined electrical and acoustical speech processing.* Laryngoscope, 2005. **115**(5): p. 796-802.

21. Carlson, M., R. Gifford, and N. Tombers, *Hearing Conservation with Conventional Cochlear Implantation [Abstract].* Otolaryngol Head Neck Surg (https://journals.sagepub.com/doi/full/10.1016/j.otohns.2010.06.156), 2017.

22. Roehm, P.C. and M.R. Hansen, *Strategies to preserve or regenerate spiral ganglion neurons.* Curr Opin Otolaryngol Head Neck Surg, 2005. **13**(5): p. 294-300.

23. Sternberg, K., et al., *Implant-associated local drug delivery systems based on biodegradable polymers: customized designs for different medical applications.* Biomed Tech (Berl), 2013. **58**(5): p. 417-27.

24. Tan, F., et al., *Recent advances in the implant-based drug delivery in otorhinolaryngology.* Acta Biomater, 2020. **108**: p. 46-55.

25.   Holden, L.K., et al., *Factors affecting open-set word recognition in adults with cochlear implants.* Ear Hear, 2013. **34**(3): p. 342-60.
26.   Blamey, P., et al., *Factors affecting auditory performance of postlinguistically deaf adults using cochlear implants.* Audiol Neurootol, 1996. **1**(5): p. 293-306.
27.   Blamey, P., et al., *Factors affecting auditory performance of postlinguistically deaf adults using cochlear implants: an update with 2251 patients.* Audiol Neurootol, 2013. **18**(1): p. 36-47.
28.   Huinck, W.J., E.A.M. Mylanus, and A.F.M. Snik, *Expanding unilateral cochlear implantation criteria for adults with bilateral acquired severe sensorineural hearing loss.* Eur Arch Otorhinolaryngol, 2019. **276**(5): p. 1313-1320.

7
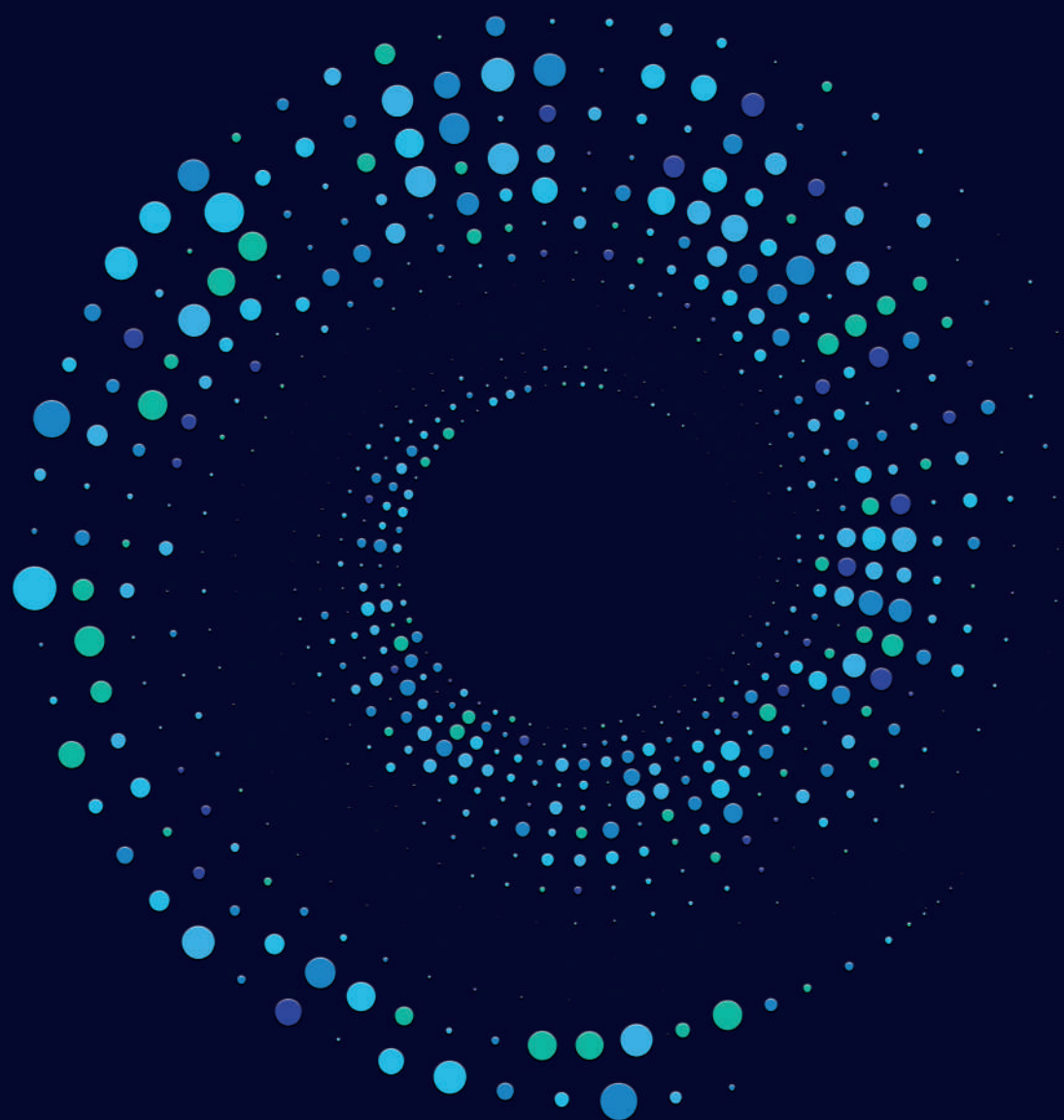
8

Summary in English

Summary in Dutch / Samenvatting in het Nederlands

Summary in English

Since its introduction, cochlear implantation (CI) knowledge has rapidly increased, leading to improved outcomes and subsequently expanded indication criteria for patients with hearing loss. Moreover, decisions within the CI care path trajectory about the type of electrode, surgical approach, and types of intra-operative measurements in relation to intracochlear processes have become more complex. In this thesis: Imaging the cochlear implant electrode position and related performance, ultra-high-resolution computed tomography (UHR-CT) imaging was used as a tool to measure the cochlea and the electrode position and tissue reaction within the implanted cochlea. Measurements were related to clinical outcomes that are most important for CI patients as a base for further hearing improvement with a CI.

The thesis is divided into two parts. In the first part, surgical techniques and cochlear implant electrode positional factors were investigated in relation to patients' CI performance. Electrode positional factors investigated were electrode type, angular insertion depth, scalar location, and wrapping factor (average electrode – to – modiolus distance). In the second part, the UHR-CT imaging was used to develop two new methods to assess factors potentially associated with CI performance: I) a method to post-operatively measure the presence of new bone formation around the cochlear implant electrode, and II) a method to automatically segment and measure the human cochlea dimensions, to investigate differences in cochlea size and to substantiate electrode selection for individual patients.

8

In part I, we found that the best speech perception in quiet and noisy
conditions was obtained when implanting a precurved electrode. The
design of the precurved electrode has made the wrapping factor smaller
than the wrapping factor of the straight electrode. The superior speech
perception outcomes with the precurved electrode seem to be best
explained by the close position to the modiolus of this electrode. We found
no effect of insertion depth of the electrode on speech perception, not in
the clinical trial **(Chapter 3)**, nor in a systematic review **(Chapter 2)**.
At the start of my thesis in 2017, it was generally accepted to use straight
electrodes for residual hearing preservation, as these were assumed to be
less traumatic than precurved electrodes available at that time. The study
described in Chapter 3 shows that, in hindsight, this choice might not be the
right one for two reasons: 1) In our data, the precurved electrode
outperformed the straight electrode on speech perception, and 2)
participants implanted with a straight electrode lost their near to all
residual hearing during the follow-up of our study (mean follow-up time 3.8
years; SD 1.7; range 1.2–7.7 years). The results of these studies have led us
at the Radboudumc to place pre-curved electrodes in all patients regardless
of their residual hearing, as these seem to give the best results.

In **Chapter 4,** the study investigating the slim perimodiolar electrode (SPE)
is described. The slim perimodiolar electrode (SPE) is a thin precurved
electrode introduced in 2016 and was initially implanted via a cochleostomy
approach. This electrode was developed to combine two electrode
properties (hypotraumatic and modiolus hugging), which in older
generation electrodes have shown to be contradictory. Our study showed
that the SPE, once correctly positioned in the scala tympani, provides good

preservation of residual hearing. However, in more than one-third of the participants (36%) a translocation was found on CT images. In these participants, the entire electrode was located in the scala vestibuli suggesting the translocation occurred at or directly after the cochleostomy. These cochleostomy-associated translocations were detrimental for the residual hearing, as the loss was four times higher than participants with a scala tympani position. Due to the results of this study, we at the Radboudumc decided to place all the pre-curved electrodes via a round window approach instead of the cochleostomy. Furthermore, this study revealed the insight that a SPE carries a risk of tip-fold over, underscoring the need for intra-operative control of the position for this electrode.

In part 2 of this thesis we studied how two new applications of Ultra-High Resolution CT imaging (UHR-CT) might further improve CI care. First, we showed that in vivo detection of tissue reaction in the proximity of the cochlear implant electrode, particularly new bone formation (NBF), is possible **(Chapter 5)**. There was strong reliability between two radiologists (86%) scoring NBF, and it appeared that most CI patients (68%) are likely to develop NBF after cochlear implantation. This NBF was predominantly located at the basal area of the cochlea (92% of the NBF located next to the ten most basal electrodes contacts). NBF was more often observed in patients with a longer follow-up time. Surgical parameters considered more traumatic (Scala Vestibuli position / Translocation, Precurved electrode (previous generation, not the SPE) Cochleostomy) seem to be associated with increased risk of developing NBF. However, these surgical factors were also correlated with longer follow-up time. Therefore, an evidence-based conclusion on which surgical factors increase the risk on NBF could not be

8

drawn. There was a negative effect of NBF on residual hearing, as participants with NBF had higher loss of long term residual hearing loss (mean absolute pre- and post-operative difference in PTA of 22.9dB) compared to participant without NBF (mean absolute pre- and post-operative difference in PTA of 8.6dB). In this analysis, follow-up time was not different between groups and was higher than the natural hearing loss of the contralateral ear, indicating the development of NBF is unfavorable for the preservation of long-term residual hearing. The second application of UHR-CT imaging showed that automatic and successful segmentation and analysis of the cochlea using UHR-CT images results in accurate automated measurements of cochlear anatomical dimensions **(Chapter 6)**. Given the wide variation in cochlear size found in our patient cohort (ranging between 0.10 and 0.28 ml (volume), 1.3 and 2.5 mm (basal diameter), and 27.7 and 40.1 mm (Cochlear Duct Length), this automated method might, after further development, find its application as a pre-operative tool in future cochlear implant surgery. This potentially improves personalized treatment strategies based on patient-specific, image-based anatomical measurements.

Conclusion

Due to the multifactorial nature of current CI systems, CI clinics, and the variation in CI patients, research in cochlear implantation is complex yet rewarding. The outcome of research eventually may lead to the immediate improvement of speech perception in individual patients. In terms of the choice of electrodes, our findings have led to a preference for a precurved electrode in adult patients with a normal anatomy of the cochlea and possible residual hearing.

Summary in Dutch

Sinds de introductie is de kennis over cochleaire implantatie (CI) snel toegenomen, hetgeen heeft geleid tot verbeterde uitkomsten en vervolgens uitgebreidere indicatie criteria voor patiënten met gehoorverlies. Bovendien zijn beslissingen binnen het CI zorgpad over het type elektrode, chirurgische benadering, en soorten intra-operatieve metingen in relatie tot intra-cochleaire processen complexer geworden. In dit proefschrift: Imaging the cochlear Implant electrode position and related performance, werd ultra-high-resolution computed tomography (UHR-CT) gebruikt als een instrument om het slakkenhuis, de elektrode positie en weefselreactie binnen het geïmplanteerde slakkenhuis te meten. Metingen werden gerelateerd aan klinische uitkomsten die het belangrijkst zijn voor CI patiënten als basis voor verdere gehoorverbetering met een CI.

Het proefschrift heeft twee delen. In het eerste deel werden chirurgische technieken en cochleair implantaat elektrode positie geassocieerde factoren onderzocht in relatie tot de prestaties van patiënten met een CI. Onderzochte elektrode positie factoren waren het type elektrode, de angulaire insertiediepte, de scalaire positie en de ""wrapping factor" (gemiddelde afstand van elektrode tot modiolus). In het tweede deel werd de UHR-CT gebruikt om twee nieuwe methoden te ontwikkelen om factoren te beoordelen die mogelijk geassocieerd zijn met de CI prestaties: I) een methode om postoperatief de aanwezigheid van nieuw bot te meten rond de cochleaire implantaat elektrode, en II) een methode om automatisch de afmetingen van de menselijke cochlea te segmenteren en te meten, om de verschillen in slakkenhuis dimensies te onderzoeken en om zo elektrode selectie voor individuele patiënten te onderbouwen.

In deel I vonden we dat de beste spraakperceptie in rustige en rumoerige omstandigheden werd verkregen bij implantatie van een voorgebogen elektrode. Het ontwerp van de voorgebogen elektrode zorgt voor een kleinere wrapping factor dan die van de rechte elektrode. De gevonden superieure spraakperceptie met de voorgebogen elektrode lijken het best verklaard te kunnen worden door deze dichte positie bij de modiolus van de voorgebogen elektrode. We vonden geen effect van insertiediepte van de elektrode op de spraakperceptie, niet in de klinische trial (hoofdstuk 3), noch in een systematische review met dit als onderwerp (hoofdstuk 2). Bij de start van mijn proefschrift in 2017 was het algemeen geaccepteerd om rechte elektroden te gebruiken voor restgehoorbehoud, omdat werd aangenomen dat deze minder traumatisch waren dan voorgebogen elektroden die op dat moment beschikbaar waren. De studie beschreven in hoofdstuk 3 laat zien dat, achteraf gezien, deze keuze niet de juiste was om twee redenen: 1) In onze gegevens presteerde de voorgebogen elektrode beter dan de rechte elektrode op het gebied van spraakperceptie, en 2) de meeste deelnemers die geïmplanteerd waren met een rechte elektrode verloren tijdens de follow-up van onze studie ook hun restgehoor (gemiddelde follow-up tijd 3,8 jaar; SD 1,7; range 1,2-7,7 jaar). Door de uitkomsten van deze studies zijn we in het Radboudumc, ook bij patiënten met restgehoor voornamelijk voorgebogen elektrodes gaan plaatsen omdat deze de beste resultaten geven.

In hoofdstuk 4 wordt de studie naar de smalle perimodiolaire elektrode (SPE) beschreven. De PE is een dunne voorgevormde elektrode die in 2016 werd geïntroduceerd en aanvankelijk werd geïmplanteerd via een cochleostomie benadering. Deze elektrode is ontwikkeld om twee

elektrode-eigenschappen, namelijk hypotraumatisch en voorgebogen, te combineren. Twee factoren die bij oudere generatie elektroden niet met elkaar verenigbaar bleken te zijn. Onze studie toonde aan dat de SPE, eenmaal correct gepositioneerd in de scala tympani, een goed behoud van het restgehoor biedt. Echter, bij meer dan een derde van de deelnemers (36%) werd een translocatie gevonden op CT beelden. Bij deze deelnemers bevond de gehele elektrode zich in de scala vestibuli, wat suggereert dat de translocatie plaatsvond bij of direct na de cochleostomie. Deze cochleostomie-geassocieerde translocaties waren nadelig voor het restgehoor, aangezien het verlies vier keer hoger was dan bij deelnemers met een scala tympani positie. Door de uitkomsten van deze studie zijn we in het Radboudumc, de voorgebogen elektrodes gaan plaatsen via een ronde venster benadering in plaats van de cochleostomie. Bovendien versterkte deze studie het inzicht dat een SPE een risico van tip-fold over met zich meebrengt, wat de noodzaak onderstreept van intra-operatieve controle van de positie voor deze elektrode.

In deel 2 van dit proefschrift hebben we onderzocht hoe twee nieuwe toepassingen van Ultra-Hoge Resolutie CT beeldvorming (UHR-CT) de CI zorg verder zouden kunnen verbeteren. Ten eerste toonden we aan dat in vivo detectie van weefselreactie in de nabijheid van de cochleaire implant elektrode, in het bijzonder nieuwe botvorming (NBF), mogelijk is (Hoofdstuk 5). Er was een sterke betrouwbaarheid tussen twee radiologen (86%) bij het scoren van NBF, en het bleek dat de meeste CI patiënten (68%) NBF zullen ontwikkelen na cochleaire implantatie. Deze NBF was overwegend gelokaliseerd in het basale gebied van het slakkenhuis (92% van de NBF gelokaliseerd naast de tien meest basale elektroden contacten).

8

NBF werd vaker waargenomen bij patiënten met een langere follow-up tijd. Chirurgische parameters die als traumatischer worden beschouwd (Scala Vestibuli positie / Translocatie, voorgevormde elektrode (vorige generatie ten opzichte van de SPE), en Cochleostomie) lijken geassocieerd te zijn met een verhoogd risico op het ontwikkelen van NBF. Deze chirurgische factoren waren echter ook gecorreleerd met een langere follow-up tijd door de opzet van de studie. Daarom kon geen op statistisch bewijs gebaseerde conclusie worden getrokken over welke chirurgische factoren het risico op NBF verhogen. Er was een negatief effect van NBF op restgehoor, aangezien deelnemers met NBF een groter verlies van restgehoor op lange termijn hadden (gemiddeld absoluut verschil in PTA vóór en na de operatie van 22,9dB) vergeleken met deelnemers zonder NBF (gemiddeld absoluut verschil in PTA vóór en na de operatie van 8,6dB). In deze analyse was de follow-up tijd niet verschillend tussen de groepen en was het verlies in de NBF groep ook significant hoger dan het natuurlijke gehoorverlies van het contralaterale oor. Dit betekent dat het de ontwikkeling van NBF ongunstig is voor het behoud van het restgehoor op lange termijn.

De tweede toepassing van UHR-CT beeldvorming toonde aan dat automatische en succesvolle segmentatie en analyse van het slakkenhuis met behulp van UHR-CT beelden resulteert in nauwkeurige geautomatiseerde metingen van de anatomische dimensies van het slakkenhuis (Hoofdstuk 6). Gezien de grote variatie in cochleaire grootte gevonden in ons patiënten cohort (variërend tussen 0,10 en 0,28 ml (volume), 1,3 en 2,5 mm (basale diameter), en 27,7 en 40,1 mm (Cochlear Duct Length), kan deze geautomatiseerde methode, na verdere

ontwikkeling, zijn toepassing vinden als een pre-operatief hulpmiddel in de toekomst cochleaire implantaat chirurgie. Dit verbetert mogelijk gepersonaliseerde implantatiestrategieën.

Conclusie

Door de multifactoriële aard van de huidige CI systemen, CI klinieken, en de variatie in CI patiënten, is onderzoek naar cochleaire implantatie complex maar ook lonend. Het implementeren van onderzoeksresultaten kan namelijk leiden tot een onmiddellijke verbetering van de spraakperceptie bij individuele patiënten. Wat de keuze van de elektroden betreft, hebben onze bevindingen in deze thesis geleid tot een voorkeur voor voorgebogen elektrodes bij volwassen patiënten met een normale anatomie van het slakkenhuis en bij mogelijk restgehoor.

8
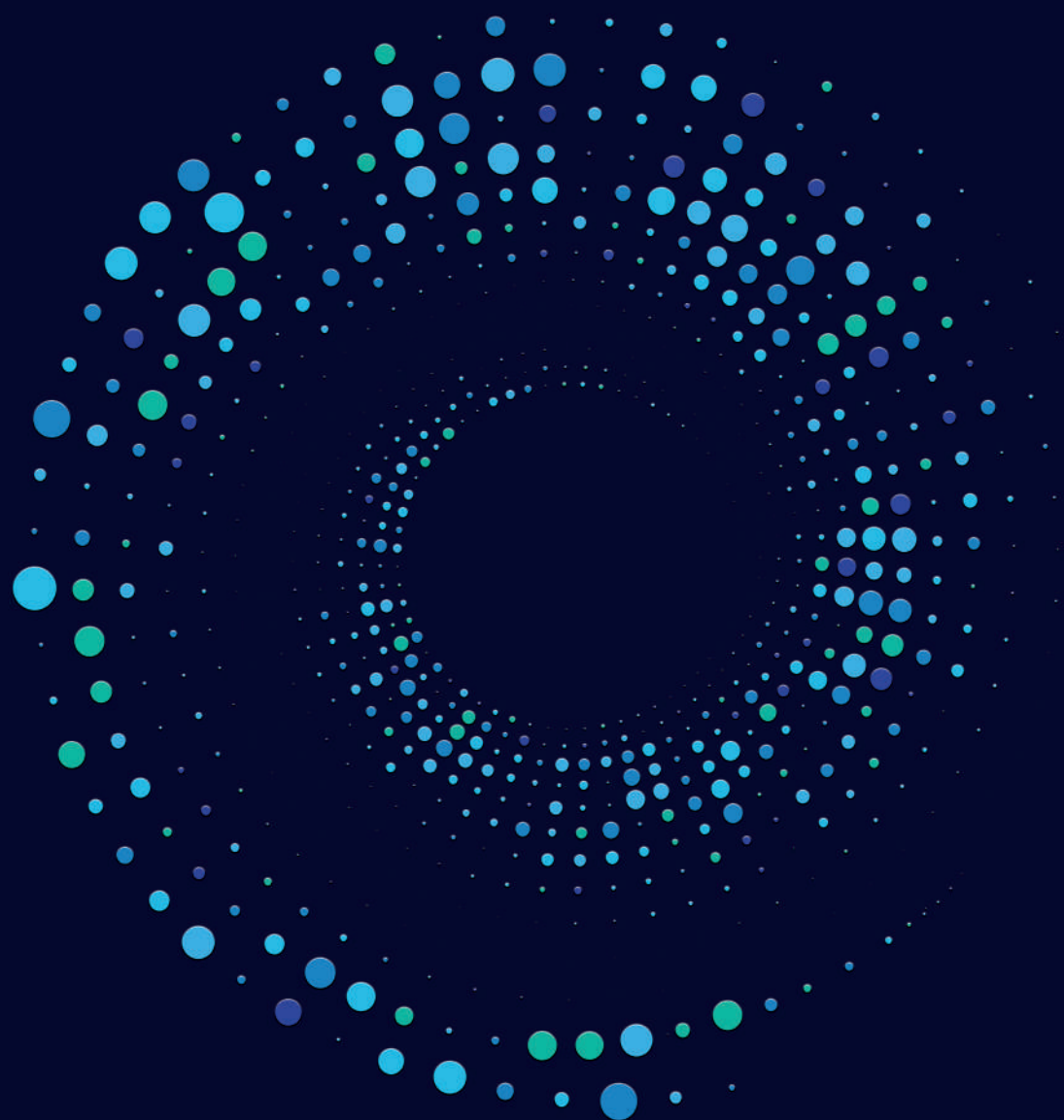
9

Acknowledgements in Dutch

Curriculum Vitae in Dutch

List of Publications

Acknowledgements in Dutch

Dit proefschrift is de inspanning van mijzelf in samenwerking met vele anderen. Iedereen die direct of indirect heeft geholpen met het tot stand brengen van dit proefschrift wil ik hartelijk danken. In het bijzonder de onderstaande mensen die een enorme bijdrage hebben geleverd:

Emmanuel, Wendy en Berit, zonder jullie geen proefschrift. **Emmanuel**, je liet mij als onderzoeker erg vrij. De rode lijn was wel duidelijk maar ik was vrij om allerlei ideeën te onderzoeken. Je bent ontzettend laagdrempelig en gezellig, en dat combineer je gelukkig ook nog met adviezen die het onderzoek naar een hoger niveau brengen. **Wendy**, je hebt altijd zorggedragen voor het onderzoek, maar daarnaast ook voor mij als persoon. Het was zo makkelijk samenwerken en zonder jou was het nooit zo snel gegaan en succesvol verlopen. Heel tof hoe je dit hebt aangepakt. **Berit**, superviseren op afstand is niet altijd makkelijk maar laten we jouw bijdragen niet onderschatten. Je was er altijd en ik heb je ervaren als een warm en toegankelijk persoon. Ik ben voor het radiologische deel afhankelijk geweest van je kennis en kunde, en zonder jou was de kwaliteit niet zo hoog geweest. Het is uiteindelijk een resultaat van synergie tussen twee vakken.

Frank, zonder jou geen AIOS. Als jonkie met ambitie echter zonder enige vorm van noemenswaardige KNO-gerichte ervaring klopte ik bij je aan. De klik was er direct. Via een seniorcoschap volgde een ANIOS plek, gevolgd door een opleidingsplek. Zonder je motiverende coaching was dat nooit gelukt. Ik hoop daar nog vele jaren gebruik van te kunnen maken.

De **staf** en **AIOS KNO** van het Radboudumc, wat een team. Genieten hoe we met elkaar omgaan. Op de werkvloer, maar ook daarbuiten. Laten we dat vasthouden; want dat maakt het werken zo heerlijk. Work hard, play hard!

Mijn vrienden en familie: Bedankt voor de ondersteuning en ontspanning die de energie gaven dit te presteren. In het bijzonder mijn broers **Renso, Reinout en Pepijn**. "The Band of Brothers" zoals we dat wel eens noemen,

9

waar ik altijd op kan terugvallen voelt als een baken van rust. Ik realiseer me steeds meer hoe bijzonder onze band is.

Mijn ouders, **Papa en Mama**, wat een reis tot nu toe. Vier zonen en ieder volgt zijn eigen pad. Het is zo bijzonder hoeveel energie jullie stoppen in het vooruit kunnen bewegen van ons als kinderen. Geen probleem is te groot, en alles is relatief. Jullie tomeloze inzet en persisterende bijdrage aan mijn leven is geweldig. De liefde voel ik elke dag en ik hoop dat dit altijd zo mag blijven. Op het gebied van onderwijs en carrière nog een extra bijzonder bedankje voor jou mam; je motiverende woorden en no-nonsense instelling is geweldig om te ervaren. Je weet mijn motivatie altijd weer hard aan te zwengelen als dit even nodig is!

Doutse, mijn schatje. Geweldig wie je nu al bent! Heel veel zin om je te zien opgroeien.

Lieve **Juul**, bedankt voor wie je bent. Je stimuleert en remt mij precies op de juiste manieren. Je opent mijn ogen wanneer dat even nodig is. Onze band is niet te beschrijven in woorden en ik geniet dagelijks van ons heerlijke leven met elkaar en met Doutje. Love you!

Curriculum Vitae in Dutch

Floris Heutink werd geboren op 14 juli 1989 in Tilburg. Opgegroeid vanaf zijn 5^e levensjaar in Overasselt is hij niet onbekend in de regio Nijmegen. Na de basisschool in Malden (Tovercirkel) en de Middelbare school in Nijmegen (VWO; Nijmeegse Scholengemeenschap (NSG)) is hij geneeskunde gaan studeren, ook in Nijmegen. Na een levendige studententijd en coschappen KNO in Tanzania en Nijmegen is hij vanaf december 2016 tot november 2017 gaan werken als ANIOS KNO in het Radboudumc. Hierna volgde dit promotietraject als fulltime onderzoeker tot maart 2019. Vervolgens is zijn opleiding tot KNO-arts begonnen vanaf april 2019 in het Radboudumc onder begeleiding van Henri Marres en Frank van den Hoogen. Sindsdien heeft hij zijdelings dit promotietraject afgerond dat in oktober 2021 is goedgekeurd. In 2020 is hij voor een deel van zijn opleiding 12 maanden in het Rijnstate ziekenhuis in Arnhem geweest, onder begeleiding van Anja Meulenbroeks. Sinds mei 2021 werkt hij weer in het Radboudumc voor het vervolg van zijn opleiding tot KNO-arts die hij in 2024 zal afronden.

9

List of Publications

Ultra-High-Resolution CT to Detect Intracochlear New Bone Formation after Cochlear Implantation. Heutink F, Klabbers TM, Huinck WJ, Lucev F, van der Woude WJ, Mylanus EAM, Verbist BM. Radiology. 2022. PMID: 35196178 2.

Intracochlear electrode array position and cochlear implant outcomes using the nucleus slim modiolar electrode and the extended round window approach: a follow-up study. Klabbers TM, Heutink F, Huinck WJ, van der Woude WJ, Verbist BM, Mylanus EAM. Eur Arch Otorhinolaryngol. 2022 PMID: 35041067

Ultra-High-Resolution CT to Detect Intracochlear New Bone Formation after Cochlear Implantation. Heutink F, Klabbers TM, Huinck WJ, Lucev F, van der Woude WJ, Mylanus EAM, Verbist BM.Radiology. 2022 PMID: 34874202

Factors Influencing Speech Perception in Adults With a Cochlear Implant. Heutink F, Verbist BM, van der Woude WJ, Meulman TJ, Briaire JJ, Frijns JHM, Vart P, Mylanus EAM, Huinck WJ. Ear Hear. 2021 PMID: 33480623

Transimpedance Matrix (TIM) Measurement for the Detection of Intraoperative Electrode Tip Foldover Using the Slim Modiolar Electrode: A Proof of Concept Study. Klabbers TM, Huinck WJ, Heutink F, Verbist BM, Mylanus EAM. Otol Neurotol. 2021. PMID: 32941298

Multi-Scale deep learning framework for cochlea localization, segmentation and analysis on clinical ultra-high-resolution CT images. Heutink F, Koch V, Verbist B, van der Woude WJ, Mylanus E, Huinck W, Sechopoulos I, Caballo M.Comput Methods Programs Biomed. 2020 PMID: 32109685

Impact of Time to Diagnosis and Treatment in Head and Neck Cancer: A Systematic Review. Schutte HW, Heutink F, Wellenstein DJ, van den Broek GB, van den Hoogen FJA, Marres HAM, van Herpen CML, Kaanders JHAM, Merkx TMAW, Takes RP. Otolaryngol Head Neck Surg. 2020 PMID: 32093572

Optimizing Settings for Office-Based Endoscopic CO_2 Laser Surgery Using an Experimental Vocal Cord Model. Schimberg AS, Klabbers TM, Wellenstein DJ, Heutink F, Honings J, van Engen-Van Grunsven I, Verdaasdonk RM, Takes RP, van den Broek GB.Laryngoscope. 2020 PMID:

The evaluation of a slim perimodiolar electrode: surgical technique in relation to intracochlear position and cochlear implant outcomes. Heutink F, Verbist BM, Mens LHM, Huinck WJ, Mylanus EAM. Eur Arch Otorhinolaryngol. 2020 PMID: 31650350

Angular Electrode Insertion Depth and Speech Perception in Adults With a Cochlear Implant: A Systematic Review. Heutink F, de Rijk SR, Verbist BM, Huinck WJ, Mylanus EAM.Otol Neurotol. 2019 PMID: 31135680

9